การตั้งตำรับซีไลมารินไมโครอิมัลชันสำหรับการนำส่งทางผิวหนัง

นางสาวสาวิตรี เจริญศรี

วิทยานิพนธ์นี้เป็นส่วนหนึ่งของการศึกษาตามหลักสูตรปริญญาเภสัชศาสตรมหาบัณฑิต
สาขาวิชาเภสัชกรรม ภาควิชาวิทยาการเภสัชกรรมและเภสัชอุตสาหกรรม
คณะเภสัชศาสตร์ จุฬาลงกรณ์มหาวิทยาลัย
ปีการศึกษา 2552

FORMULATION OF SILYMARIN MICROEMULSION FOR DERMAL DELIVERY

Miss Sawitree Charoensri

A Thesis Submitted in Partial Fulfillment of the Requirements

for the Degree of Master of Science in Pharmacy Program in Pharmaceutics

Department of Pharmaceutics and Industrial Pharmacy

Faculty of Pharmaceutical Sciences

Chulalongkorn University

Academic Year 2009

Thesis Title	FOMULATION OF SILYMARIN MICROEMULSION FOR DERMAL DELIVERY
By	Sawitree Charoensri
Field of Study	Pharmaceutics
Thesis Advisor	Vipaporn Panapisal, Ph.D.
Thesis Co-Advisor	Assistant Professor Angkana Tantituvanont, Ph.D.

Accepted by the Faculty of Pharmaceutical Sciences, Chulalongkorn University in Partial Fulfillment of the Requirements for the Master's Degree

…….. Dean of the Faculty of Pharmaceutical Sciences

(Associate Professor Pintip Pongpetch, Ph.D.)

THESIS COMMITTEE

…….. Chairman

(Associate Professor Uthai Suvanakoot, Ph.D.)

……. Thesis Advisor

(Vipaporn Panapisal, Ph.D.)

…….. Thesis Co-Advisor

(Assistant Professor Angkana Tantituvanont, Ph.D.)

…….Examiner

(Associate Professor Waraporn Suwakul, Ph.D.)

…….. External Examiner

(Napasinee Aksornkoae, Ph.D.)

สาวิตรี เจริญศรี : การตั้งตำรับซิไลมารินไมโครอิมัลชันสำหรับการนำส่งทางผิวหนัง (FORMULATION OF SILYMARIN MICROEMULSION FOR DERMAL DELIVERY). อ. ที่ปรึกษาวิทยานิพนธ์หลัก : อ.ดร.วิภาพร พนาพิศาล, อ. ที่ปรึกษาวิทยานิพนธ์ร่วม : ผศ.ดร.อังคณา ตันติธุวานนท์, 100 หน้า.

ซิไลมารินเป็นสารสกัดมาตรฐานจากเมล็ดของ *Silybum marianum* ซึ่งจากการมีคุณสมบัติต้านออกซิเดชัน ต้านการอักเสบ และกระตุ้นภูมิคุ้มกัน ซิไลมารินจึงน่าจะป้องกันความผิดปกติของผิวหนังจากรังสีอัลตราไวโอเล็ต เช่น ผื่นแดง บวม การสร้างเซลล์ที่ผิดปกติ การเสื่อมของผิวหนัง และมะเร็งผิวหนังได้ การศึกษานี้มีวัตถุประสงค์เพื่อเตรียมไมโครอิมัลชันของซิไลมารินสำหรับนำส่งทางผิวหนัง และประเมินคุณสมบัติการปลดปล่อย ความคงตัว รวมถึงการซึมผ่านผิวหนังของซิไลมารินไมโครอิมัลชัน โดยเลือกกลีเซอริล โมโนโอลีเอท กรดโอเลอิก เอทิล โอลีเอท และไอโซโพรพิล ไมริสเตท เป็นวัฏภาคน้ำมัน เลือกสารผสมของ Tween 20® กับ HCO-40® (1:1) หรือ Labrasol® กับ HCO-40® (1:1) หรือ Span 20® กับ HCO-40® (1:1) เป็นสารลดแรงตึงผิว และใช้ Transcutol® เป็นสารลดแรงตึงผิวร่วมในการสร้างซูโด-เทอนารีเฟสไดอะแกรม จากนั้นเลือกไมโครอิมัลชันชนิดน้ำมันในน้ำของแต่ละซูโด-เทอนารีเฟสไดอะแกรมที่มีสารลดแรงตึงผิวต่ำมาใช้ในการนำส่งซิไลมารินทางผิวหนัง เพื่อหลีกเลี่ยงการระคายเคืองผิวจากสารลดแรงตึงผิวและน้ำมันในสูตรตำรับ ไมโครอิมัลชันที่บรรจุซิไลมาริน 2% โดยน้ำหนัก มีความคงตัวดีทางกายภาพ กล่าวคือไมโครอิมัลชันยังคงความใส ไม่พบการแยกชั้นหรือการตกตะกอนของซิไลมาริน หลังจากการเก็บที่อุณหภูมิเย็นสลับร้อนจำนวน 6 รอบ แต่อย่างไรก็ตามซิไลบินซึ่งเป็นสารออกฤทธิ์สำคัญของซิไลมารินมีการสลายตัวระหว่างการเก็บซิไลมารินไมโครอิมัลชันที่ 40°C เป็นเวลา 6 เดือน เปอร์เซ็นต์ซิไลบินที่คงอยู่ในสูตรตำรับเรียงลำดับตามชนิดของสารลดแรงตึงผิวที่ใช้ได้ ดังนี้ Labrasol® > Tween 20® > Span 20® (เมื่อ HCO-40® เป็นส่วนประกอบในทุกสูตรตำรับ) การปลดปล่อยซิไลมารินจากไมโครอิมัลชันเป็นการปลดปล่อยแบบช้าๆ เมื่อเทียบกับการปลดปล่อยซิไลมารินจากสารละลาย (40% เอทานอลในสารละลายเกลือฟอสเฟต พีเอช 7.4) รูปแบบการปลดปล่อยมีความสัมพันธ์อย่างดีกับสมการของฮิกูชิ และพบว่าอัตราการปลดปล่อยซิไลมารินจากไมโครอิมัลชันไม่มีความแตกต่างกันอย่างมีนัยสำคัญ การศึกษาการซึมผ่านผิวหนังพบว่าซิไลบินไม่สามารถตรวจวัดได้ในสารละลายตัวรับ เปอร์เซ็นต์ซิไลบินที่อยู่ในสารสกัดผิวหนังไม่มีความแตกต่างอย่างมีนัยสำคัญระหว่างสูตรตำรับซิไลมารินไมโครอิมัลชัน แต่พบว่าสารละลายซิไลมารินจะให้เปอร์เซ็นต์ซิไลบินที่อยู่ในสารสกัดผิวหนังมากกว่าซิไลมารินไมโครอิมัลชันอย่างมีนัยสำคัญ อย่างไรก็ตามสารละลายแอลกอฮอล์นั้นไม่เหมาะสมสำหรับการใช้ทางผิวหนัง เนื่องจากทำให้เกิดการระคายเคือง ในการศึกษาต่อไปควรทำการศึกษาการซึมผ่านผิวหนังในสภาวะปิดเปรียบเทียบกับสภาวะเปิดนี้ และควรทำการทดสอบฤทธิ์และความระคายเคืองต่อผิวหนังของซิไลมารินไมโครอิมัลชัน

ภาควิชา: วิทยาการเภสัชกรรมและเภสัชอุตสาหกรรม ลายมือชื่อนิสิต .....

สาขาวิชา : เภสัชกรรม ลายมือชื่ออ.ที่ปรึกษาวิทยานิพนธ์หลัก .....

ปีการศึกษา : 2552 ลายมือชื่ออ.ที่ปรึกษาวิทยานิพนธ์ร่วม .....

4976601733 : MAJOR PHARMACEUTICS

KEYWORDS : SILYMARIN / SILYBIN / MICROEMULSION / SKIN / ANTIOXIDANT

SAWITREE CHAROENSRI : FORMULATION OF SILYMARIN MICROEMULSION FOR DERMAL DELIVERY. THESIS ADVISOR : VIPAPORN PANAPISAL, Ph.D., THESIS CO-ADVISOR : ASST. PROF. ANGKANA TANTITUVANONT, Ph.D., 100 pp.

Silymarin is a standardized extract from the seeds of *Silybum marianum*. Due to its antioxidant, anti-inflammatory, and immunomodulatory properties, silymarin may prevent UV-induced skin disorders including erythema, edema, sun burn cell formation, photoaging, and skin cancer. The objective of this study is to prepare silymarin-loaded microemulsions for dermal delivery and then evaluate its release properties, stabilities and permeability. Glyceryl monooleate, oleic acid, ethyl oleate, isopropyl myristate were selected as an oil phase, mixture of Tween 20® and HCO-40® (1:1), Labrasol® and HCO-40® (1:1) or Span 20® and HCO-40® (1:1) were selected as surfactants, and Transcutol® was used as a cosurfactant to construct the pseudo-ternary phase diagrams. From each pseudo-ternary phase diagram, o/w microemulsion with low surfactants/cosurfactant mixture (Smix) content was selected for dermal delivery of silymarin and to avoid skin irritation from surfactant and oil. Microemulsions containing 2% w/w silymarin showed a good physical stability; remained transparent and no phase separation or drug precipitation after 6 heating-cooling cycles. However, silybin, the main active component of silymarin, degraded during storage of microemulsions at 40°C for 6 months. The percentages of silybin remainings were sequenced in the order of surfactants: Labrasol® > Tween 20® > Span 20® (as HCO-40® was used in every formulation). In vitro releases of silymarin microemulsions showed the prolong release when compared to its solution (40% ethanol in phosphate buffer saline pH 7.4). All silymarin release profiles showed the best fit with Higuchi kinetics and the release rate constants of silymarin from microemulsions were not significantly different. In vitro skin permeation study found that silybin could not be detected in the concentrated receiver fluid. The percentages of silybin remainings in skin extracts from silymarin microemulsions were not significantly different, except for the solution which significantly higher than microemulsions. However, alcohol solutions are still not suitable for skin delivery due to their skin irritation. For further studies, the permeation study in occlusive condition should be performed comparing to this non-occlusive condition, as well as in vivo studies of efficacy and skin irritation of silymarin microemulsions.

Department : Pharmaceutics and Industrial Pharmacy	Student's Signature .....
Field of Study : Pharmaceutics	Advisor's Signature .....
Academic Year : 2009	Co-Advisor's Signature .....

ACKNOWEDGEMENTS

This thesis would not have been possible to complete without the great supports from a number of people. First of all, I would like to express my greatest thankful to my advisor, Dr. Vipaporn Panapisal for her valuable advice encouragement, and understanding throughout my research study.

I am also deeply thankful to Dr. Angkana Tantituvanont, my co-advisor, for her suggestion and kindness.

I am highly indebted to Associate Professor Dr. Uthai Suvanakoot, chairman of my thesis examination committee, as well as other committee members, Associate Professor Dr. Waraporn Suwakul and Dr. Napasinee Aksornkoae for their valuable comments and helpful discussions.

I am very grateful to Associate Professor Dr. Suchada Chutimaworapan and Assistant Professor Nontima Vardhanabhuti, for allowance of using refrigerated and hot air incubator.

My gratitude is given to the Chulalongkorn University research fund for partially financial support to my thesis work. It is also a pleasure to thank Berlin Pharmaceutical Co., Ltd. for donation of silymarin; Croda Co., Ltd. for contribution of glyceryl monooleate and ethyl oleate; and Kru Somboon farm for giving the dead newborn pigs.

I am appreciated all my friend and staff members of Department of Pharmaceutics and Industrial Pharmacy, Faculty of Pharmaceutical Sciences, Chulalongkorn University for their friendship and kindly helping.

A special thank is dedicated to my family for their love, understanding, and support over the past years.

CONTENTS

LIST OF TABLES

LIST OF FIGURES

FIGURE PAGE

FIGURE PAGE

LIST OF EQUATIONS

LIST OF ABBREVIATIONS

ANOVA	=	analysis of variance
CoS	=	cosurfactant
DNA	=	deoxyribonucleic acid
g	=	gram
H_2O_2	=	hydrogen peroxide
HLB	=	hydrophilic-lipophilic balance
HPLC	=	high performance liquid chromatography
iNOS	=	inducible nitric oxide syntase
mg	=	milligram
mL	=	milliliter
mM	=	milimole
nm	=	nanometer
NO	=	nitric oxide
o/w	=	oil-in-water
R^2	=	coefficient of determination
ROS	=	reactive oxygen species
rpm	=	revolutions per minute
S	=	surfactant
SD	=	standard deviation
Smix	=	surfactants/cosurfactant blend
UV	=	ultraviolet
w/o	=	water-in-oil
w/w	=	weight by weight
µg	=	microgram
µL	=	microliter
µm	=	micrometer
°C	=	degree Celsius
%CV	=	percentage of coefficient of variation
Φ_c	=	critical water volume fraction
Φ_w	=	water volume fraction

CHAPTER I

INTRODUCTION

Nowadays, the larger amount of ultraviolet (UV) radiation reaches the surface of the earth because of ozone layer depletion. UV radiation forms a part of the electromagnetic spectrum with wavelengths between 100 and 400 nm. It is divided into three categories depending on wavelength, long wave UVA (315-400 nm), medium wave UVB (280-315 nm), and short wave UVC (100-280 nm). Although ozone can absorb UV radiation up to about 310 nm (all of the UVC and most of the UVB), a part of the UVB and UVA can induce several skin disorders, including erythema, sunburn, photoaging and skin cancer. Erythema and sunburn occur acutely in response to excessive exposure to the UV, whereas photoaging and skin cancer result from accumulated damage caused by repeated exposures. Skin cancer typically occurs in skin that is photoaged (Fisher et al., 1996; Frank, de Gruijl, and Jan, 2002).

It is well known that skin exposed to UV radiation results in the generation of reactive oxygen species (ROS), which causes oxidative stress when their formation exceeds the antioxidant defense ability of the cellular target. The induction of oxidative stress and subsequent imbalance of the antioxidant defense system have been associated with the onset of the skin diseases.

Although the skin possesses a complex and interlinked antioxidant defense system to protect itself from damage by UV-induced ROS, the capacity of these endogenous antioxidants is limited. Thus, the use of exogenous antioxidants, naturally occurring herbal compounds, is receiving considerable interest to protect skin from adverse biological effects of solar UV radiation (Afaq et al., 2002; Křen and Walterová, 2005).

Silymarin, a mixture of flavonolignans isolated from milk thistle, is known to be an antioxidant compound. Antioxidant and radical scavenging properties of silymarin were demonstrated in many studies. Pre-treatment with silymarin and its flavonolingans, silybin and dehydrosilybin, prevented hydrogen peroxide-induced

oxidative stress in human keratinocyte and mouse fibroblast cell lines (Svobodová, Walterová, and Psotoá, 2006). In UVA exposed human keratinocyte cell line, post-treatment of silymarin, silybin or 2,3 dehydrosilybin resulted in diminution of UVA caused oxidative stress (Svobodová et al., 2007a; Svobodová et al., 2007b). Moreover, silymarin was shown to mitigate oxidative stress and inflammatory responses to benzoyl peroxide, a free radical-generating skin tumor-promoting agent in SENCAR mouse skin (Zhao et al., 2000). Silymarin application to UVB irradiated SKH-1 mouse skin resulted in significantly reduced the number of sunburn cells, skin edema, and the depletion of catalase activity. In long term studies, silymarin reduced UVB induced tumor incidence, tumor multiplicity, and tumor size (Katiyar et al., 1997). In order silymarin to be functional, topical silymarin has to be formulated to deliver silymarin into the skin with the sufficient amount. Since silymarin is poorly soluble in water (3.2 mg/100 mL) (Saller et al., 2007), the formulated silymarin skin delivery should have a capacity to solubilize and incorporate the effective amount silymarin.

Microemulsions, as drug delivery system, have several advantages such as enhanced drug solubility, high stability, and ease of manufacturing. Moreover, it improves percutaneous penetration of drug (Date, Naik and, Nagarsenker, 2006). The potential enhancing effect of microemulsions is typically attributable to the individual constituent rather than the specific microemulsion structure (Kreilgaard, 2002). For example, oleic acid, which was used as an oil phase in many microemulsion systems, can interact with the stratum corneum lipids and increases their fluidity, so drug mobility will then increase (Barry, 1987). Surfactants, which are able to function as enhancers, are believed to penetrate the skin mainly in their monomer form, and it is not likely that the micelle-like microemulsion structures are able to penetrate the skin intact. However, as microemulsions are highly dynamic structures, it is plausible that monomer surfactant (or oil molecules) can diffuse to the skin surface and acts as enhancer, either by disruption the lipid structure of stratum corneum or by increasing the solubility of the drug in the skin, i.e., increasing the partition coefficient of the drug between the skin and the vehicle (Kreilgaard, 2002).

In this study, silymarin was incorporated into microemulsions and then evaluated its release properties, stabilities and permeability to ensure that the prepared silymarin microemulsions are suitable formulations for skin delivery.

The purposes of this present study were as follows:

1. To construct the pseudo-ternary phase diagrams from different oils and surfactants and characterize the microemulsions obtained from each constructed pseudo-ternary phase diagram.
2. To develop silymarin-loaded microemulsions and study its release properties.
3. To evaluate the physical and chemical stabilities of silymarin microemulsions.
4. To investigate the in vitro skin permeation of silymarin microemulsions.

CHAPTER II

LITERATURE REVIEW

Silibum marianum (Linneaus) Gaertner

Common name: Milk thistle, Blessed Milk thistle, Holy thistle, Marian thistle, Our Lady's thistle, Mary thistle, St. Mary's thistle, Wild Artichoke, Mariendistel (Germany), Chardon-Marie (French), Shui Fei Ji (Chinese).

Family: Asteraceae (Compositae).

Distribution: Native of Northern Africa, Western Asia, Southeastern and Southwestern Europe; widely introduced into elsewhere in Europe, British Isles, Topical and Northern Africa, Australia, New Zealand, United States, and Canada (GRIN Taxonomy of Plants, Online).

Figure 1: Photographs of *silybum marianum* (Florabase: the Western Australian Flora, Online)

Description: *Silybum marianum* is described as an annual, winter annual, and biennial herb. The main stem is stout, ridged, and branching. The overall plant size can range from 2 to 6 feet tall. A distinguishing characteristic of milk thistle is the white marbling found along the vein of the dark green leaves.

The branch leaves are deeply lobed, and basal leaves can be 20 inches long and 10 inches wide. The leaf margins are yellow and tipped with woody spines 1/8 to 1/2 inch long. The leaves are alternate, and clasping to the stem.

The stem leaves are smaller and not quite as lobed. Each stem ends in a solitary composite flower head, about 2 inches in diameter, consisting of purple disc flowers. The flower head of milk thistle differs from other thistles with the presence of broad leathery bracts that are also tipped with stiff spines 3/4 inch to 2 inches long.

The seed are heavy, 1/4 inch long, flat, smooth, and shiny. The color rages form black to brown mottled. The seeds do have a tuft of minutely barbed bristles. Which deciduous, and falls off in a ring when the seed mature (Written findings of the state noxious weed control board – class A weed, Online).

Part Used: seeds.

Energetic and traditional indications: the energetic actions of milk thistle have been described as sweet and cooling, but also as pungent, warm, and dry.

Traditional indications are nourishes liver, stomach, intestines, kidney. Used by the eclectics for liver disease, splenic or hepatic congestion, varicose veins, uterine hemorrhage and menstrual problems. It is used by some herbalists to increase lactation (*Silibum marianum*: Milk thistle, Online).

Notes of interest: Milk thistle's name comes for its white, milky sap and from belief in past times that it helped the flow of breast milk in new mother. The plant has long been associates with Mary, the mother of Jesus. It's said, for example, that the white markings on milk thistle's leaves were caused by a drop of Mary's milk (Flora delaterre: the plant detective, Online).

Milk thistle is sometime cultivated as an ornamental, a minor vegetable, or as a medicinal herb. Young shoots can be boiled and eaten like cabbage and young leaves can be added to salads. The seed can be used as a coffee substitute (Flora of North America, Online).

Silymarin

Silymarin is a standardized extract obtained from the seeds of the milk thistle. Silymarin contains approximately 70% - 80% flavonolignans and approximately 20% - 30% chemically undefined fraction, comprising mostly polymeric and oxidized polyphenolic compounds. The main component of silymarin flavonolignans is silybin, synonymous with silibinin, which is a mixture of two diasteriomers A and B in approximately 1:1 proportion. Besides silybin, considerable amounts of other flavonolibnans are isosilybin, dehydrosilybin, silychristin, silydianin and a few flavonoids, mainly taxifolin (Figures 2, 3).

Typical applications, for which milk thistle preparations have been used and prescribed since ancient times, are mostly treatments of liver diseases and gastrointestinal tract problems. Also currently, silymarin and their preparation are advocated for the treatment of cirrhosis, chronic hepatitis, and liver diseases associated with alcohol consumption and environmental toxin exposure.

Recently, both silymarin and silybin received attention due to their alternative beneficial activities that are not directly bound to their hepatoprotective effect. These include mostly anticancer and chemopreventive actions, as well as hypocholesterolemic, cardioprotective, and neuroprotective activities. Silybin seems to be prospective also in treatment of pancreas problems and balancing glycemia, treatment of lung problems and kidney diseases, and last but not least in dermatology and cosmetics (Křen, and Walterová, 2005).

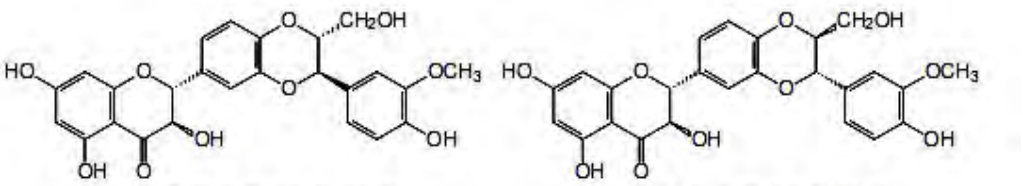

Figure 2: Chemical structures of silybin A and B (Křen, and Walterová, 2005)

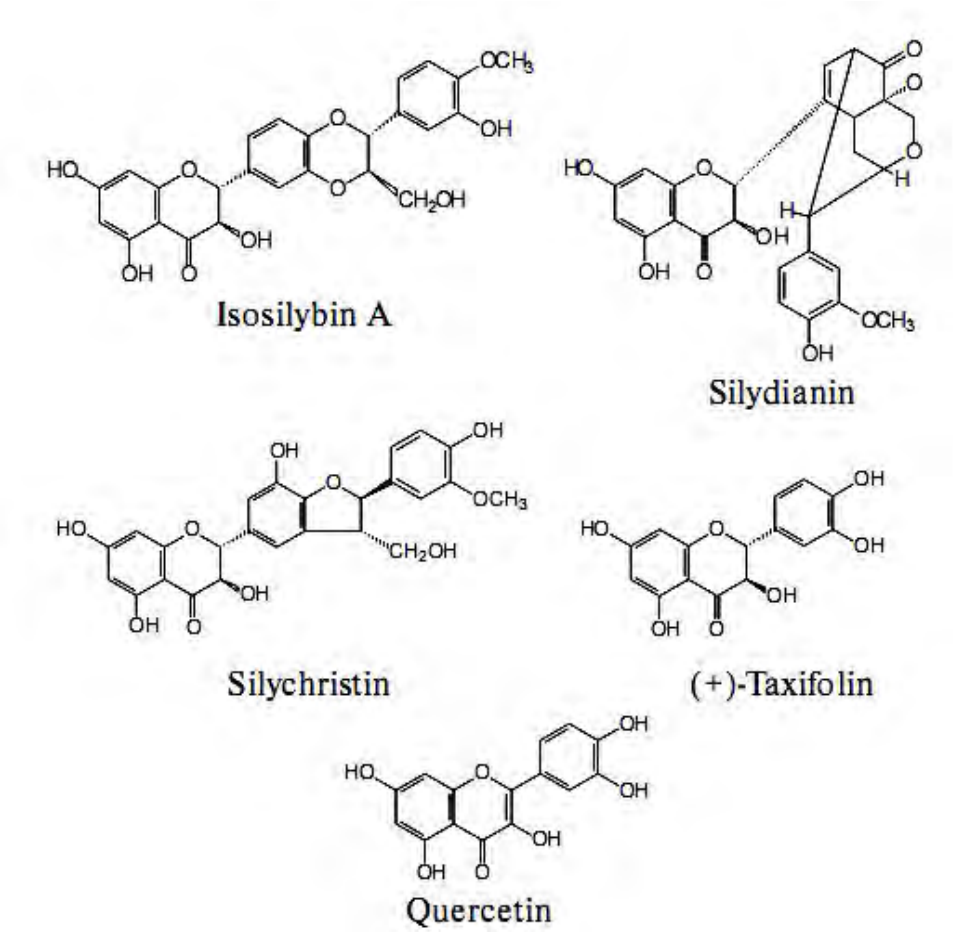

Figure 3: Chemical structures of flavonolignans in silymarin (Křen, and Walterová, 2005)

Skin protection properties of silymarin

Skin is the largest human body organ which provides a major interface between the environment and the body. Skin exposure to solar UV radiation induces a number of skin disorders, including erythema, edema, sunburn cell formation, hyperplasia, immune suppression, DNA damage, photoaging, melanogenesis and skin cancers. It is well documented that UV irradiation, both UVB and UVA components, induces the generation of reactive oxygen species (ROS), where ROS create the oxidative stress in skin cells and play an important role in the initiation, promotion, and progression of skin aging and carcinogenesis (Křen, and Walterová, 2005).

ROS are short-lived entities that are continuously generated at low level during the course of normal aerobic metabolism. ROS include free radicals, such as superoxide ($O_2^{\bullet -}$), peroxyl ($ROO^{\bullet}$), alkoxyl ($RO^{\bullet}$), hydroxyl ($OH^{\bullet}$) and nitric oxide

($NO^{\bullet}$). In addition to these ROS radicals, there are other ROS nonradicals, such as the singlet oxygen ($^1O_2$), hydrogen peroxide (H_2O_2), and hydrochlorous acid (HOCl). ROS can attack lipids in cell membranes, proteins in tissues or enzymes, carbohydrates and DNA, to induce oxidations which cause membrane damage through protein modification (including enzymes) and DNA damage. This oxidative damage is considered to play a causative role in aging and several degenerative diseases associated with it such as heart disease, cataracts, and cancer (Pietta, 2000).

The cell is well equipped to deal with most oxidative damage. Cell integrity is maintained by enzymes including catalase, glutathione reductase, and glutathione peroxides, which collectively destroy hydrogen peroxide and lipid hydroperoxides. In addition, superoxide dismutase destroys superoxide. The extracellular space is protected from superoxide anion by extracellular superoxide dismutase. Non enzymatic antioxidants protecting skin include glutathione and ascorbic acid in the aqueous phase and vitamin E and ubiquinol-10 in the lipid phase, particular membranes. However, in time of increased of oxidative stress; including high metabolic demands and outside forces such as sunlight, smoking, and pollution; protective controls may not adequate and oxidative damage may occur.

Because low molecular weight antioxidants protect skin against oxidative stress, undergoing depletion in the process, it should be desirable to add to the skin reservoir by applying the antioxidants directly to skin. Although antioxidants can be supplied to skin through diet and oral supplementation, physiological process related to absorption, solubility, and transport can limit the amount of antioxidant delivered into skin. Direct application has the added advantage of targeting the antioxidants to the area of skin needing the protection. However, antioxidants need to have photoprotective effects including reduction of erythema, reduction of sunburn cell formation, reduction of DNA changes such as thymine dimmers of oxidized nucleotides, reduction of immunosuppression, reduction of pigment abnormalities, and eventually, reduction of skin cancer and photoaging changes (Pinnell, 2003).

Silymarin possesses antioxidant, anti-inflammatory, and immunomodulatory properties which may prevent UV-induced skin disorders including photocarcinogenesis and photoaging. Topical application of silymarin to mouse skin

(SKH-1 hairless mice) reduced UVB induced tumor incidence, tumor multiplicity, and tumor size compared to those of untreated animals. In short-term experiments, silymarin application results in significant inhibition in UV-caused sunburn and apoptotic cell formation, skin edema, depletion of catalase activity, and induction of cyclooxygenase (COX) and its prostaglandin metabolites, ornithine decarboxylase (ODC) activities and its mRNA expression, a biomarker of tumor promotion (Katiyar et al., 1997). Moreover, topical treatment of silymarin to mouse skin (C3H/HeN mice) prevents UVB induced infiltration of inflammatory leukocytes (MHC^+CD11b^+), which are responsible for the induction of UVB induced suppression of immune responses and oxidative stress (Katiyar, 2002; Katiyar, Meleth, and Sharma, 2008).

In addition, treatment of silymarin to UVB irradiated skin inhibits UVB induced immunosupression by reducing the UVB induced enhancement of the levels of the immunosuppressive cytokine, interleukin (IL)-10, and enhancing the levels of the immunostimulatory cytokine, IL-12. Furthermore, treatment of silymarin resulted in reduction of $H_2O_2^+$ and $iNOS^+$ cells, and also in reduction of intracellular H_2O_2 and NO in epidermis and dermis (Katiyar, 2002; Meeran et al., 2006). In human keratinocyte cell line (HaCaT), treatment with silymarin, silybin or 2,3 dehydrosilybin resulted in diminution of UVA caused oxidative stress; including ROS production, glutathione depletion, and lipid peroxidation. UV-induced DNA single stand break and caspase-3 activity which has a primordial role in apoptosis was also significantly decreased by silymarin (Svobodová et al., 2007a; Svobodová et al., 2007b).

With all attractive skin protective efficacies of silymarin, the need of topical formulation of silymarin is not in doubt. However, in order to allow silymarin to be efficiently protective deeper skin layer, silymarin need to be formulated in a way to deliver into the skin.

Skin and drug delivery

An important function of human skin is to bar the entry of unwanted molecules from outside while controlling the loss of water, electrolyte, and other endogenous constituents. When a molecule reaches intact skin, it contacts cellular debris, microorganism, sebum, and other materials. The diffusant then has three

potential entry routes to the viable tissue: 1) via the sweat ducts; 2) across the continuous stratum corneum between the appendages; or 3) through the hair follicles with hair associated sebaceous glands.

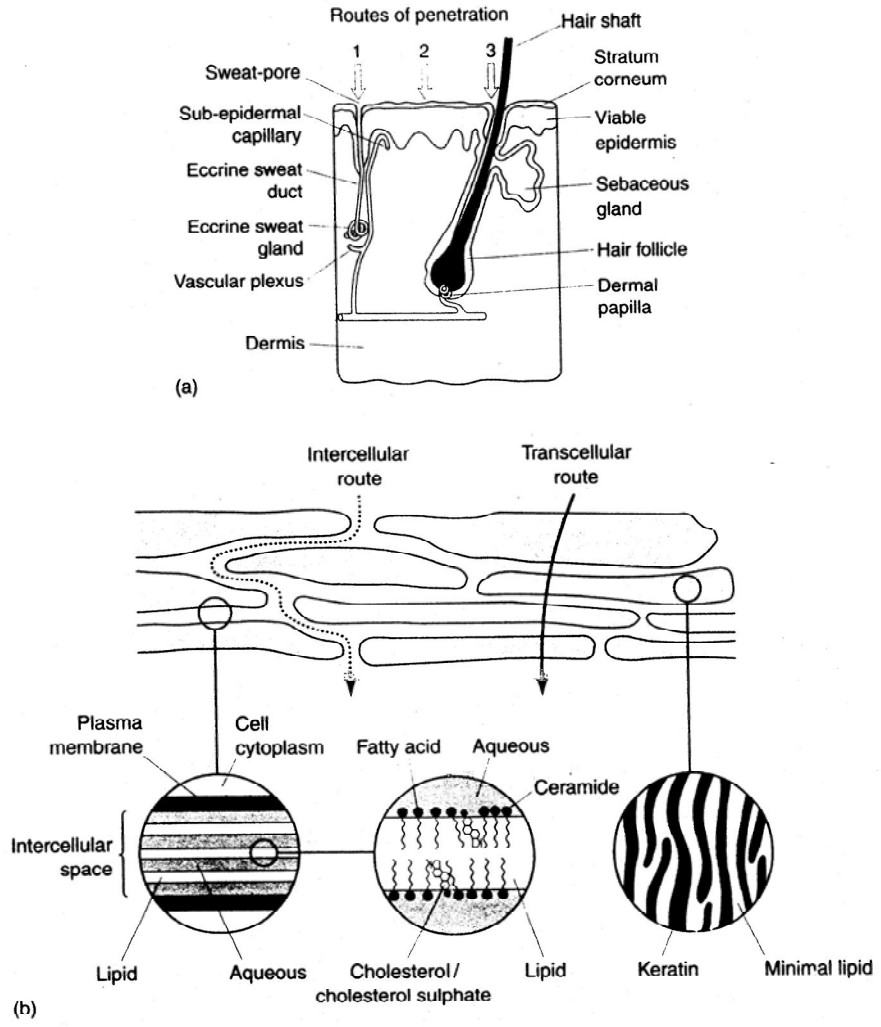

Figure 4: Skin structure and routes of drug penetration (Barry, 2002)

The intact skin is a very effective barricade because the diffusional resistance of the stratum corneum or honey layer is large and the permeable appendageal shunt route provides only a small fractional area. The stratum corneum has a ‘bricks and mortar’ structure, analogous to a wall. The corneocytes, consisting of hydrated keratin, comprise the ‘bricks’. These are embedded in the ‘mortar’, which is

composed of a complex lipid mixture of ceramides, fatty acids, cholesterol and cholesterol esters, formed into multiple bilayers. Because stratum corneum is dead, it is assumed that there are no active transport processes and no fundamental differences between in vivo and in vitro permeation processes. In addition, for in vitro studies, excised skins from mice, rats, and rabbits are frequently used to assess percutaneous absorption, but their skins have more hair follicles than human skin and they lack sweat glands. Comparative studies on skin penetration indicate that, in general, monkey and pig skins are most like that of humans.

Once past the stratum corneum, molecules permeate rapidly through the living tissues and sweep into the systemic circulation. The fraction of the penetrating molecules that penetrates the skin depends on many factors. The biological factors, such as the site and condition of the skin, the skin age, and as previously discussed, the species differences. The physicochemical factors such as the skin hydration, the temperature and pH of the skin, the molecular size and shape of the penetrating molecules; and also the parameters of the diffusion process which expressed as Fick's law of diffusion (Equation 1), diffusion coefficient, diffusant concentration, and partition coefficient.

$$\frac{dm}{dt} = \frac{D C_0 K}{h} \qquad \text{Equation 1}$$

dm/dt is the rate of transfer per unit area (the flux), where m is the mass of diffusant which passes through the skin as a function of time, t. D is the diffusion coefficient, C_0 is the concentration of diffusant in the donor, K is the partition coefficient, and h is the skin thickness.

It was seen that the flux of solute is proportional to the concentration gradient across the skin. Thus, one requirement for maximal flux in a thermodynamically stable situation is that the donor concentration should be saturated. Moreover, while the concentration differential is usually considered to be the driving force for diffusion, the chemical potential gradient or activity gradient is actually the fundamental parameter. It is useful in this context to think of thermodynamic activity as 'escaping tendency', i.e. the drive for the drug to escape from the vehicle and enter

the skin. Thus, the thermodynamic activity of a drug in the donor phase or the skin may radically alter by pH change, complex formation, or the presence of surfactants, micelle or cosurfactant. Such factors also modify the effective partition coefficient. Therefore, an alternative form of equation 1 uses thermodynamic activity is equation 2.

$$\frac{dm}{dt} = \frac{a\,D}{\gamma\,h} \qquad \text{Equation 2}$$

where a is the thermodynamic activity of the drug in its vehicle and γ is the effective activity coefficient in the skin barrier. To obtain the maximum rate of penetration, it should be used with the drug at its highest thermodynamic activity. When the dissolved molecules in a saturated solution are in equilibrium with the pure solid, the solute molecules are at maximum activity and equal to that of the solid. In conclusion, all vehicles that contain a drug as a finely ground suspension should produce the same penetration rate (Barry, 2002).

In general, exceeding the solubility of the drug within the vehicle is unnecessary as no benefit accrues; excess drug powder merely remains in suspension and is ultimately wiped from the skin surface. Rarely, solubility within the vehicle can be so low that rapid depletion of the formulation would occur, whereupon excess drug powder that dissolves to replenish that which has permeated can be of benefit. Thus, optimum drug delivery is provided when the drug is saturated in its vehicle (Williams, 2003). By appropriate formulation, it is thus possible to reduce the amount of drug in a formulation while maintaining its activity by remaining the same thermodynamic activity. In addition to the thermodynamic aspects, there are also possibilities of improving drug delivery while decreasing drug loading through incorporating penetration enhancers. Surfactant-based formulations, which may interact with the lipids in the stratum corneum and alter their structure, offer a way to modify this protective barrier, and specifically to reach an enhanced drug penetration over the stratum corneum (Malmsten, 2002; Williams, 2003).

Microemulsions

Definitions

Microemulsions are thermodynamically stable colloidal dispersions of water and oil stabilized by a surfactant and in many cases, also cosurfactant. Microemulsions are readily distinguished from normal emulsions by their transparency, low viscosity, and more fundamentally their thermodynamic stability (Santos et al., 2008; Swarbrick and Boylan, 1994). The comparison of microemulsions and emulsions is summarized in Table 1.

Hoar and Schulman introduced the term microemulsion in 1943 to define a clear solution obtained by titrating a normal emulsion with medium chain length alcohol. Despite some controversy, the definition of microemulsion suggested by Danielson and Lindman was systems compose of water, oil and amphiphile molecules, which are single optically isotropic and thermodynamically stable liquid solutions and it is widely accepted (Attwood, 1994; Santos et al., 2008; Swarbrick and Boylan, 1994).

Table 1: The comparison of emulsions and microemulsions (Attwood, 1994; Moulik and Paul, 1998; Santos et al., 2008)

Properties	Emulsions	Microemulsions
Droplet size of disperse phase	Typically 0.2-10 μm	5-150 nm
Appearance	Cloudy	Clear or transparent
Preparation	Require energy input	Spontaneous formation
Scale up	Complex	Straightforward
Stability	Kinetically stable	Thermodynamically stable
Interfacial energy	High	Very low

Structure

When the volume fraction of oil is low, the microemulsion is normally a continuous water solution with dispersed oil droplets (oil-in-water microemulsions, o/w), whereas, when the volume fraction of water is low, the microemulsion is a continuous oil solution with dispersed water droplets (water-in-oil microemulsions, w/o). However, when similar amounts of oil and water are used, the structures formed are not well characterized and are assumed to be continuous. In this case, both oil and water domains are separated by an interfacial layer. Some studies have shown that

through the formation of these continuous systems, it is possible to achieve the transition of an o/w to a w/o system (Lawrence and Rees, 2000; Santos et al., 2008).

Microemulsions can also exist in equilibrium with excess water, excess oil, or both. These multiple phase systems can be conveniently described using the Winsor classification (Figure 5). The Winsor type I system consists of a lower phase o/w microemulsion coexisting with excess oil, and the type II system consists of an upper phase w/o microemulsion in equilibrium with excess water. Both phase equilibriums are driven by the bending stress of the interfacial film. The type III system forms when the surfactants are concentrated in surfactant-rich bicontinuous middle phase which coexists with both oil and water. However, in Winsor classification, the one phase microemulsions that are generally explored as drug delivery systems are known as the Winsor type IV (Lawrence and Rees, 2000; Swarbrick and Boylan, 1994, Moulik and Paul, 1998).

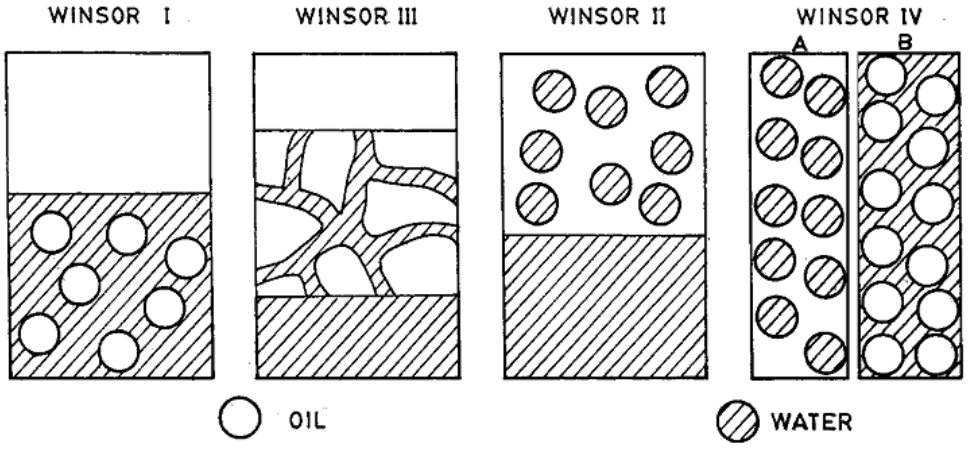

Figure 5: Winsor I, II, III, and IV systems. Type I, o/w microemulsion in equilibrium with excess oil; Type II, w/o microemulsion in equilibrium with excess water; Type III, bicontinuous structure in equilibrium with excess oil and water; Type IV, either o/w or w/o microemulsion not in contact with any other phase (Moulik and Paul, 1998)

Phase diagrams

The most common way to form a microemulsion is to construct a phase diagram of the main ingredients: the oil phase, the aqueous phase, the surfactant and the cosurfactant. Each corner in the phase diagram represents 100% of that particular

component (Garti and Aserin, 2006). Phase diagrams provide the boundaries of the different phases as a function of the component composition. Quaternary phase diagram (Figure 6), a regular tetrahedron composed of four equilateral triangles, can be used to plot the composition of the four component systems, with the pure components represented by each corner of the tetrahedron and the edges representing binary mixtures. In practices it is more usual to investigate planar sections of the tetrahedron by plotting a two-dimensional triangular diagram (pseudo-ternary phase diagram, Figure 7) by either keeping the composition of one component fixed and varying the other three, or by using a constant ratio of two components, generally the surfactant and cosurfactant (Swarbrick and Boylan, 1994).

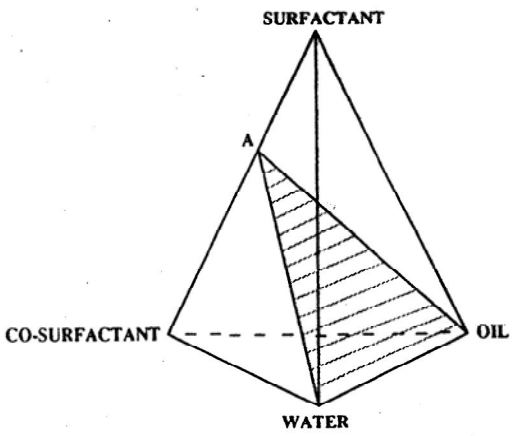

Figure 6: Quaternary phase diagram; the hatched area represents a fixed surfactant/cosurfactant ratio (Swarbrick and Boylan, 1994)

The construction of these phase diagrams is performed often by simple visual inspection or by polarized light microscopy of samples of known compositions. Generally, the surfactant mixture (or other mixture of two components) is selected and fixed for the location of the microemulsion region. At the pre-determined ratios, the oil and the surfactant mixture are blended and slowly titrated with the aqueous phase at constant temperature with constant stirring. After each addition, the container should be stoppered to minimize loss of any volatile composition and the system is inspected for clarity and birefringence, and then the proportion of each component is calculated and noted. The various proportions at which microemulsions can be formed

are then plotted in order to generate a pseudo-ternary phase diagram (Attwood, 1994; Santos et al., 2008).

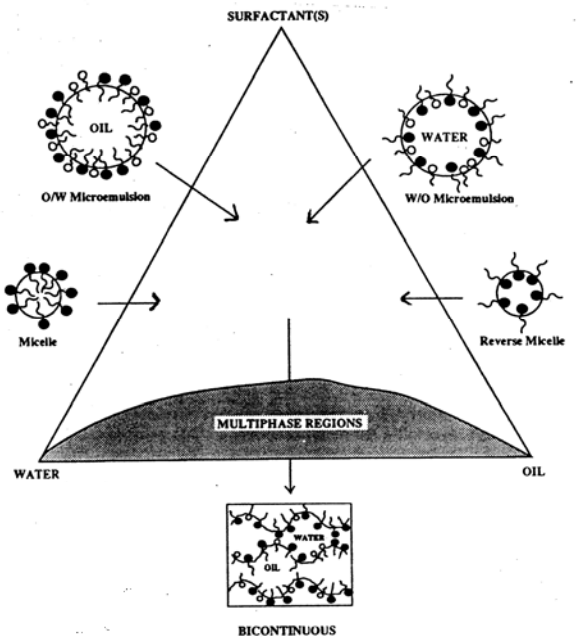

Figure 7: Pseudo-ternary phase diagram, corresponding to the hatched area in figure 6, showing micellar, microemulsion, and multiple phase regions (Swarbrick and Boylan, 1994)

Formation theories

Many approaches have been used to explore the mechanisms of microemulsion formation and stability. Some emphasize on the formation of an interfacial film and the production of ultra-low interfacial tensions (mixed-film theories), others emphasize on the monophasic nature of many microemulsions (solubilization theories). Thermodynamic theories are other approaches which consider the free energy of formation of microemulsions (Swarbrick and Boylan, 1994).

1) Mixed film theories

The spontaneous formation of microemulsion droplets was considered to be due to the formation of a complex film at the oil-water interface by the surfactant and cosurfactant. This caused a reduction in the oil-water interfacial tension to very low values (from close to zero to negative). The mixed interfacial film in equilibrium with

both oil and water was considered to be liquid and duplex in nature with a two-dimensional spreading pressure; π_i, which determined the interfacial tension; γ_i by equation 3.

$$\gamma_i = \gamma_{o/w} - \pi_i \qquad \text{Equation 3}$$

where $\gamma_{o/w}$ represents the oil/water interfacial tension without the film present. When large amounts of surfactant and cosurfactant are adsorbed to form the interface, the spreading pressure; π_i, may become larger than $\gamma_{o/w}$. A negative interfacial tension results, and energy is available to increase the interfacial area, effectively reducing droplet sizes. This interfacial tension produced by mixing the components is a transient phenomenon, and at equilibrium it becomes zero or a very small positive value.

A major drawback to this concept was the high value of the spreading pressure; π_i, necessary to give the transient negative interfacial tension. There are some reports postulated that the negative interfacial tension could be a results of the depression of $\gamma_{o/w}$ by alcohol cosurfactant partitions between the oil and the interface rather than unrealistically high initial pressure in the original model.

The interfacial film must be curved to form small droplets. A flat duplex film would be under stress because of the different tensions and spreading pressures on either side of it. The reduction of this tension gradient by equalizing the two surface pressures and tensions is the driving force for the film curvature (Figure 8). Both sides of the interfacial expand spontaneously with penetration of oil and cosurfactant until the two pressures become equal. The side with the higher tension would be concave and would be envelop the liquid on that side, making the internal phase. Since it is generally easier to expand the oil side of an interphase (by penetration of the oil or cosurfactant into the hydrocarbon chain area) than the water side, w/o are easier to form rather than o/w microemulsions (Swarbrick and Boylan, 1994).

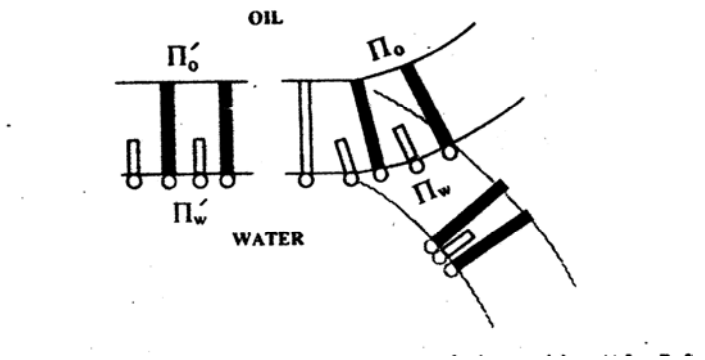

Figrue 8: The mechanism of curvature of a duplex film of microemulsions (Swarbrick and Boylan, 1994)

2) Solubilizing theories

In this concept, microemulsions are considered to be thermodynamically stable monophasic solution of water-swollen (o/w) or oil-swollen (w/o) spherical micelles. The relationship between inverse micelles and w/o microemulsions can be illustrated with the aid of phase diagrams. The quaternary phase diagram constructed on addition of hydrocarbon directly to the inverse micellar phase clearly shows the relationship of these areas to the isotropic inverse micelle region. Since they were an extension of the inverse micelle region, it was proposed that they consist of swollen inverse micelles rather than small emulsion droplets.

The inverse micelle regions of the ternary system; water, pentanol, and sodium dodecyl sulfate (SDS) is shown in Figure 9. The region is composed of water solubilized in reverse micelles of SDS in pentanol. The addition of up to 50% p-xylene gives rise to transparent w/o microemulsion regions containing a maximum of 28% water with 16% pentanol and 6% surfactant.

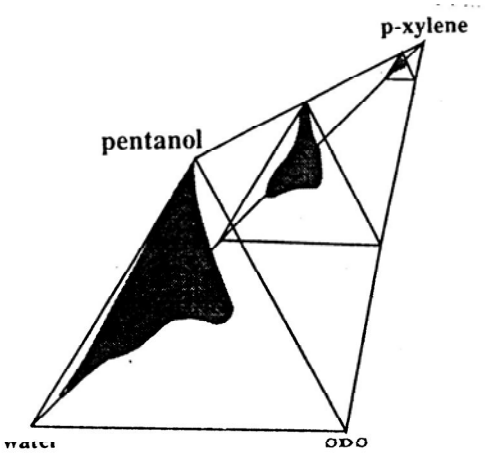

Figure 9: Ternary phase diagram illustrating that the w/o microemulsion p-xylene is a direct continuation of the inverse micellar solution of water, surfactant (SDS), and cosurfactant (pentanol)

However, the relationship between o/w microemulsions and the isotropic aqueous micellar region is less direct. The solubilization of oil in normal micelles is small, and the molecular characteristic and concentration of all the components are critical for an aqueous micelle solubilized large amounts of hydrocarbon and swell directly into an oil droplet without forming a large number of intermediate structures of low curvature (Swarbrick and Boylan, 1994).

3) Thermodynamic treatment

In contrast to emulsions, microemulsions are very stable. Emulsions are kinetically stable, but thermodynamically unstable, the size of the dispersed droplets will increase due to coalescence, then the two phases separate after storage. While the thermodynamic stability of microemulsions means that their droplet size remains unchanged over extended periods of time. This high thermodynamic stability promotes self-emulsification of the system, hence no significant energy input or complex processing equipment are required (Garti and Aserin, 2006; Santos et al., 2008).

For a dispersion to form spontaneously, the free energy of mixing (ΔG) must be negative, i.e. lower than that of the unmixed components. The free energy of mixing is defined in equation 4.

$$\Delta G = \gamma \Delta A - T\Delta S \qquad \text{Equation 4}$$

where γ is the surface tension of the oil-water interfaces, ΔA is the change in interfacial area on emulsification, ΔS is the change in entropy of the system, and T is the temperature.

For the dispersion to be thermodynamically stable, ΔG must show a minimum value (Santos et al., 2008).

The free energy gain is considered to be derived form:

(i) the extent to which surfactant lowers the interfacial tension between the two phases

(ii) the dispersion entropy which arising from the mixing of one phase in the other in the form of large numbers of small droplets and from other dynamic process such as surfactant diffusion in the interfacial layer and monomer-micelle surfactant exchange (Garti and Aserin, 2006; Lawrence and Rees, 2000).

Therefore, the stability is a consequence of the low interfacial tension, which able to compensate for the increase in the entropy of the system (Santos et al., 2008). Furthermore, it is entropically more favorable as the hydrocarbon tails have more directional freedom. As a result, interfacial tension tends to be lower for a w/o microemulsions than o/w microemulsions, thereby making their preparation a more facile process (Lawrence and Rees, 2000).

While micreomulsion formulation depends on the capacity of the surfactant system to decrease the surface tension; in practice, almost all surfactants require the presence of additional cosurfactant, such as short- or long- chain alcohol, or polyglycerol derivatives, in order to achieve such low surface energy (Santos et al., 2008). However, nonionic surfactants do not generally need a cosurfactant for microemulsion formation. With such systems, temperature is generally the most crucial factor because the nonionic surfactants become more lipophilic with increase in temperature (Swarbrick and Boylan, 1994).

Characterization

In contrast to their ease of production, microemulsions are very diffucult to characterize principally because of their wide variety of structures. A variety of techniques have been employed to characterize these systems

1) Microscopy

While polarizing microscopy is used to confirm the optical isotropy of the microemulsion systems, conventional optical microscopy cannot be used for studying microemulsion systems because of their small droplet size diameter. Transmission electron microscopy (TEM) combined with freeze fracture technique has been successfully applied for characterization of microemulsions. However, the senstitivity of microemulsion structure to temperature and the potential introduction of experimental artifacts during manipulation are of some concern with this approach (Santos et al., 2008).

2) Laser light and non-optical scattering techniques

Laser light scattering techniques (static and dynamic light scattering) as well as non-optical methods, such as small-angle X-ray scattering and small-angle neutron scattering, have been employed to characterize the size of the colloidal phase. However, several authors have pointed out that the charged interface between the droplet and the continuous phase may lead to misinterpretation of the diffusion coefficient and hence the estimated droplet size. Furthermore, the common approach for reduction of these interparticle interactions (dilution) may result in changes in the microstructure and even droplet disappearance, especially if cosurfactants are partitioned in both phases. Therefore, when using concentrated systems, it is necessary to use different models in order to take into account non-ideality arising from interparticle interaction. The existence of nonspherical microemulsion structures, such as bicontinuous systems, also limits the use of these scattering techniques for droplet measurement (Santos et al., 2008).

3) NMR

Self-diffusion is the random movement of a molecule in the absence of any concentration gradient, and this movement reflects the environment where the molecule is localized. If a molecule is confined in a close aggregate, such as micelles,

its self-diffusion will be two or three orders of magnitude lower than the expected self-diffusion coefficient from a pure solvent. Therefore, in w/o microemulsions, the self-diffusion of water molecule is slow, where as the diffusion of the oil molecule is high. Conversely, for o/w microemulsions the reverse is found. In bicontinuous structures, both oil and water molecules exhibit high self-diffusion coefficients. Microemulsion structure has been characterized as using self-diffusion measurements of the components, obtained by proton Fourier transform pulse-gradient spin-echo NMR (PGSE NMR) (Santos et al., 2008).

4) Conductivity and Viscosity

The nature of the microemulsions and the detection of phase inversion phenomena can be determined using classical rheological methods and by conductivity measurements. It has been demonstrated that microemulsions may also exhibit percolation transition which signifies the first emergence of an infinite cluster for a critical value of the water volume fraction, called the percolation threshold. This state characterizes bicontinuous structures (Santos et al., 2008; Thevenin, Grossiord, and Poleman, 1996).

Mechanism of percutaneous enhancement

Microemulsions may enhance transdermal drug delivery primarily by the following effects:

1) Microemulsions can exhibit a high solubilization capacity for both lipophilic and hydrophilic drugs; thus, more drug can be loaded into the microemulsions which increases the concentration gradient across the skin without depletion.

2) The reservoir effect of the interfacial phase maintains a constant driving force of drug from the external phase to the skin and prolongs absorption. Since the diffusion of the drug into the skin only occurs from the external phase of microemulsions, the internal phase continually supplies drug to the external phase so that it remains saturated with the drug. By these account, hydrophobic drugs show great flux from w/o microemulsions, whereas o/w systems provide controlled release of the drug that is dependent on the partitioning of drug into the outer phase.

3) The formulation components may affect skin permeability, i.e. surfactants, cosurfactant, and oils, may act as permeation enhancer by disruption the stratum corneum lipid organization, thus increasing drug diffusion, or by increasing the partition of the drug in the skin. On the downside, these results may in a potential risk of skin irritation.

4) Microemulsion formulations have also been suggested to alter the polar pathways via hydration of the stratum corneum because of the presence of a water phase.

5) The very low interfacial tension required for microemulsion formation is also responsible for the excellent wetting properties, which ensures excellent surface contact between the membrane and the vehicle.

6) The small droplet size of microemulsions resulting in large surface area from which the drug can partition and be absorbed or permeate through the skin.
(Garti and Aserin, 2006; Santos et al., 2008; Gupta and Moulik, 2008)

CHAPTER III

MATERIALS AND METHODS

Materials

1. Absolute ethanol (RCI Labscan Limited, Thailand)
2. Caprylocaproyl macrogolglycerides or Labrasol® (PC Intertrade Co., Ltd., Thailand) Lot no. 106157
3. Conductivity calibration solution (Eutech Instrument Pte Ltd., Singapore)
4. Diethylene glycol monoethyl ether or Transcutol CG® (PC Intertrade Co., Ltd., Thailand) Lot no. 450723001
5. Disodium hydrogen phosphate (Merck, Germany)
6. Ethyl oleate (Croda Co., Ltd., Thailand) Lot no. 256950
7. Glyceryl monooleate (Croda Co., Ltd., Thailand) Lot no. 16063
8. Hydrochloric acid (Merck, Germany)
9. Isopropyl myristate (Namsiang Trading Co., Ltd., Thailand)
10. Methanol, AR grade (RCI Labscan Limited, Thailand)
11. Methanol, HPLC grade (RCI Labscan Limited, Thailand)
12. Oleic acid (Srichand United Dispensary Co., Ltd., Thailand) Lot no. 5586320594
13. pH calibration solutions (Thermo Electron Corporation, England)
14. Phosphoric acid (J.T. Baker, USA)
15. Polyoxyethylene 20 sorbitan monolaurate or Tween 20® (Srichand United Dispensary Co., Ltd., Thailand) Lot no. 709557
16. Polyoxyethylene-40 hydrogenated castor oil or HCO-40® (Namsiang Trading Co., Ltd., Thailand) Lot no. 7005
17. Potassium dihydrogen phosphate (APS Finechem, Australia)
18. Silybin (Sigma-Aldrich, Germany) Lot no. 057K1873
19. Silymarin (a gift from Berlin Pharmaceutical Co., Ltd., Thailand)
20. Sorbitan monolaurate or Span 20®(Srichand United Dispensary Co., Ltd., Thailand)
21. Sodium chloride (Merck, Germany)

Apparatus

1. Analytical balance (Model AG285, Mettler Toledo, Switzerland)
2. Conductivity meter (Model C535, Consort, Belgium)
3. High performance liquid chromatography
    a. Liquid chromatograph pump (LC-10AD, Shimadzu, Japan)
    b. Automatic sample injector (SIL-10A, Shimadzu, Japan)
    c. Column (BDS Hypersil C18, 5µm, 250mm x 4.6mm, Thermo Electron Corporation, England)
    d. Column oven (CTO-10A, Shimadzu, Japan)
    e. UV-VIS detector (SPD-10A, Shimadzu, Japan)
    f. Communications bus module (CBM-10A, Shimadzu, Japan)
4. Hot air incubator (Thermo scientific)
5. Magnetic stirrer (Model M6, CAT, Germany)
6. Micropipette (Pipetman, Gilson, Inc., France)
7. Minispin® Centrifuge (Eppendrof, Germany)
8. Modified Franz diffusion apparatus
9. pH meter (Model 420A, Orion Research, Inc., USA)
10. Refrigerated incubator (FOC 225 I, VELP scientifica srl, Itary)
11. Sonicator (Model TP680DH, Elma, Germany)
12. Suspension mixture (Model RSM6, Ratek Instrument Pty Ltd., Australia)
13. Thermostated centrifuge (Sima-302K, Germany)
14. Thermostated water bath (Model 02PT623, Hetofrig, Denmark)
15. UV-Visible spectophotometer (UV-1601, Shimadzu, Japan)
16. Vacuum pump (Model DOA-V130-BN, Waters, USA)
17. Viscometer (Model RVTDCP, Brookfield engineering laboratories, Inc., USA)
18. Vortex mixer (Vortex Ginies-2, Scientific Industries, USA)

Others

1. Injection vial (Tan Soon Huat Products Co., Ltd., Thailand)
2. Membrane filter, polyamide, 0.45 µm (Sartorius AG, Germany)
3. Newborn pig abdominal skin (Kru Somboon Farm, Rajchaburi)
4. Operating tools

5. Parafilm® M (Pechiney Plastic Packaging, Inc., USA)
6. Regenerated cellulose membrane, MWCO 12,000-14,000 (CelluSep T4, Canada)
7. Syringe filter, PVDF, 0.45 μm (Agela technology Inc., USA)
8. Syringe, 5 ml (Nipro Corp., Ltd., Thailand)
9. Scalp vein set (Nipro Corp., Ltd., Thailand)

Methods

A. Construction of pseudo-ternary phase diagrams and selection of microemulsion formulations

The pseudo-ternary phase diagrams were constructed by titration of homogenous liquid mixtures of oil, surfactants, and cosurfactant, with water at room temperature. Oil, surfactants, and cosurfactant were weighed into the same screwed cap test-tube, with varied ratios between oil and surfactants/cosurfactant blend (Smix) from 9:1 to 1:9. Water was added drop-wise and mixed by vortex mixer. Following the addition of each drop of water, the mixture was visually examined for transparency. The changes in the sample appearance from turbid to transparent and vice versa were observed. Transparent, single-phase, low viscous mixtures were designated as microemulsions (Djordjevic et al., 2004).

Oils, surfactants and cosurfactant, which was used in this experiment, are as follows:

Oil : glyceryl monooleate, oleic acid, ethyl oleate, isopropyl myristate

Surfactant : mixture of Tween 20®, Span 20®, or Labrasol® with HCO-40® at the ratio of 1:1

Cosurfactant : Transcutol®

To confirm the boundary between clear and unclear regions, the same compositions on the boundary line were prepared in three replications and allowed to reach equilibration at room temperature for three days. All samples were then visually examined for transparency compared with previous observations.

The Smix percentages were kept at minimum to obtain microemulsions. Among several Smix percentages of each pseudo-ternary phase diagram, 5% above the highest % Smix was chosen to ensure the achievement of microemulsion while the water concentrations were varied in 4% interval.

B. Characterization of microemulsions

For characterization, selected microemulsions from A were prepared and stored at room temperature for 3 days to reach equilibrium before investigations.

1. **Visual inspection**

   Transparency and phase separation were observed.

2. **Viscosity**

   Viscosities of microemulsions were measured using viscometer at 25±2°C in triplicate.

3. **Conductivity**

   Conductivities of microemulsions were measured using conductivity meter at 25±2°C in triplicate.

4. **Dilution test**

   Microemulsions were diluted with water or oil used in the formulations, and then were observed for any phase seperation. If water was easily dispersed in the continuous phase, the microemulsion was defined as oil-in-water. If oil was dispersible in the external phase, the microemulsion was defined as water-in-oil (Ho, Hsiao, and Sheu, 1996). If microemulsion becomes turbid when diluted with oil and water, the microemulsion may be bicontinuous.

After characterization, o/w micoremulsions with oil contents in the range of 5-8% were chosen from each pseudo-ternary phase diagram to prepare silymarin micromeulsion.

C. Preparation of silymarin microemulsions

2% w/w of silymarin was incorporated into the selected o/w microemulsions by adding silymarin into homogeneous mixtures of oil and surfactants/cosurfactant blend then stirred by magnetic stirrer. After silymarin dissolved, water was added into the mixtures and continuously stirred with magnetic stirrer for 10 minutes. Prepared silymarin microemulsions were characterized as described in section B to determine any changes due to the hydrophobicity of drug after incorporation into microemulsions.

D. Stability of silymarin microemulsions

1. Physical stability

Heating-cooling cycle was used for the physical stability study. Silymarin microemulsions were stored in the refrigerator at 4±1°C for 48 hours and in the hot air oven at 45±1°C for 48 hours. This was called as one cycle, and six cycles were carried out (Hire et al., 2007) (n=3).

Transparency, phase separation, and precipitation of silymarin from microemulsions were observed.

2. Chemical stability

Silymarin microemulsions were stored in the hot air oven at 40±1°C for 6 months (ICH topic Q1A (R2), 2003) (n=3). Quantitation assays of active component, silybin, were performed at 0, 1, 2, 3, 4, 5, 6 month(s) by HPLC method (validated in section G1).

E. In vitro release study of silymarin microemulsions

Release studies were performed using modified Franz diffusion cells, with a cellulose membrane (cut-off molecular weight 12,000-14,000). The cellulose membrane was first hydrated in water for 24 hours, then washed by hot water, and soaked in receptor solution for 1 hour before the experiment. Then, the membrane was clamped between the donor and receptor compartments of the cells. The receptor solution was 40% ethanol in phosphate buffer saline pH 7.4, and it was maintained at 37±1°C using a thermostatic water bath and was magnetically stirred at 600 rpm throughout the experiment. The receptor solution and membrane were equilibrated to

the desired temperature for 1 hour before the experiment. After equilibration, 250 µl of the freshly prepared silymarin microemulsion was transferred into the donor compartment, and then covered with paraffin film to prevent evaporation. 5 ml of receptor solution were withdrawn at 0.5, 1, 2, 3, 4, 6, 8, 10, 12, 16, 20, 24 hours from receptor compartment, and then replaced by a fresh solution equal amount taken. The samples were analyzed for silymarin concentration using spectrophotometer at 329 nm (validated in section G2). Three replicates of each experiment were performed.

For permeation study, silymarin microemulsions which have preferred stability and release properties were chosen. Moreover, chosen silymarin microemulsions should include different oils and surfactant mixtures in order to study the influences of these parameters to skin permeation.

F. In vitro skin permeation study of silymarin microemulsions

Permeation studies of selected silymarin microemulsions from section D and E were performed using modified Franz diffusion cells, with a newborn pig abdominal skin. The skin was soaked in receptor solution for 1 hour before the experiment. Then, the skin was clamped between the donor and receptor compartments of the cells. The receptor solution was phosphate buffer saline pH 7.4, and it was maintained at 37±1°C using a thermostatic water bath and was magnetically stirred at 600 rpm throughout the experiment. The receptor solution and the skin were equilibrated to the desired temperature for 1 hour before the experiment. After equilibration, 400 µl of the freshly prepared silymarin microemulsion was transferred into the donor compartment. From the preliminary permeation study, receptor samples were analyzed for silybin but no silybin presented. Therefore, no receptor samples were obtained during 24 hour study period.

At the end of permeation experiment, the formulation remaining on the skin was collected and the donor compartment was rinsed with ethanol. The amount of silybin in remaining formulation was quantified using HPLC (validated in secton G1). The permeation area of the skin was cut into small pieces, and then extracted with methanol by shaking at 100 rpm for 3 hours following by 3 cycles of 30 minute long sonication. The methanolic skin extract was evaporated under N_2 purge until dryness and the residue was then reconstituted with 30% ethanol in phosphate buffer saline

pH 7.4. Receptor solution was collected and evaporated at 40°C using a thermostatic water bath until dryness and the residue was then reconstituted with 30% ethanol in phosphate buffer saline pH 7.4. Reconstituted solutions (e.g., skin extract, receptor compartment) were centrifuged at 10,000 rpm for 10 minutes. The supernatants were analyzed for silybin content using HPLC. Six replicates of each experiment were performed.

G. Verification of analytical method for silymarin

1. High performance liquid chromatographic (HPLC) method

The conditions for HPLC analysis was modified from USP 30, 2007

1.1 Chromatographic conditions

The chromatographic conditions for analysis of active constituent (silybin) from silymarin were as follows:

Mobile phase: Solution A: water : methanol : phosphoric acid (80:20:0.5)
Solution B: methanol : water : phosphoric acid (80:20:0.5)

Gradient systems :

Time (min)	Solution A (%)	Solution B (%)	Elution
0-5	85	15	Isocratic
5-20	85→55	15→45	Linear gradient
20-40	55	45	Isocratic
40-41	55→85	45→15	Linear gradient
41-55	85	15	Equilibration

Flow rate : 1 ml/minute

Detector : UV-Visible spectroscopy at wavelength 288 nm

Column temperature: 40°C

Injection volume : 10 µl

Solution A and B were mixed, filtered through a filtering 0.45 µm membrane and degassed by sonication by 30 minute sonication prior to use.

1.2 Standard solution

Silybin was accurately weighed and dissolved in ethanol. This stock solution was further diluted with 30% ethanol in phosphate buffer pH 7.4 to obtain standard solutions with the final concentrations of silybin in range of 4-20 μg/ml.

1.3 Sample solution

Prepared microemulsion was accurately weighed and dissolved with ethanol. This solution was further diluted with 30% ethanol in phosphate buffer pH 7.4 with the final concentrations of silybin in range of 4-20 μg/ml.

Skin extracts and receptor samples from permeation studies were prepared by the method described in permeation session which final diluted with 30% ethanol in phosphate buffer pH 7.4.

1.4 Verification for HPLC method

HPLC analysis method was validated with typical parameters, which are specificity, linearity, accuracy, and precision (ICH topic Q2 (R1), 2005).

1.4.1 Specificity

The specificity of HPLC method was determined by comparing the assay results of silybin in microemulsions, skin extracts, and receptor samples with the standard solution. The test was aimed to ensure that the peak of silybin was free from interference by other components in the sample.

1.4.2 Linearity

Six concentrations of standard solutions were prepared and analyzed. The relation between peak areas and concentrations were plotted and least square linear regressions were calculated. The linearity was determined from the coefficient of determination (R^2). The test was done for three replications.

1.4.3 Accuracy

Three concentrations of standard solutions (five replicates/concentration), covering the specified linearity range, were prepared and analyzed. The accuracy was determined from the percentage of recovery.

1.4.4 Precision

a) Within run precision

Three concentrations of standard solutions (five replicates/concentration), covering the specified linearity range, were prepared and analyzed in the same run. The precision of each concentration was determined from the percentage of coefficient of variation (%CV).

b) Between run precision

Three concentrations of standard solutions, covering the specified linearity range, were prepared and analyzed in five different runs. The precision of each concentration was determined from the percentage of coefficient of variation (%CV).

2. UV-Visible spectrophotometric method

The conditions for UV-VIS spectroemetric analysis was modified from El-Samaligy, Afifi and Mahmoud, 2005. The sample were measured at maximum absorption wavelength in 40% ethanol in phosphate buffer saline pH 7.4 (329 nm).

2.1.Standard solution

Silymarin was accurately weighed and dissolved in ethanol. This stock solution was further diluted with 40% ethanol in phosphate buffer saline pH 7.4 to obtain standard solutions with the final silymarin concentrations in range of 5-17.5 μg/ml.

2.2.Sample solution

Microemulsion preparation was accurately weighed and dissolved with ethanol. This solution was further diluted with 40% ethanol in phosphate buffer saline pH 7.4 to obtain solution with the final silymarin concentration in range of 5-17.5 μg/ml.

2.3. Verification for UV-VIS spectrophotometric method (ICH topic Q2 (R1), 2005)

UV-VIS spectrophotometric method was validated with typical parameters, which are specificity, linearity, accuracy, and precision.

2.1.1. Specificity

The specificity of UV-VIS spectrophotometric method was determined by comparing the assay results of silymarin microemulsions with the standard solution. The test was aimed to ensure that the peak of silymarin was free from interference by other components in the sample.

2.1.2. Linearity

Six concentrations of standard solution were prepared and analyzed. The relation between peak areas and concentrations were plotted and least square linear regressions were calculated. The linearity was determined from the coefficient of determination (R^2). The test was done for three replications.

2.1.3. Accuracy

Three concentrations of standard solutions (five replicates/concentrations), covering the specified linearity range, were prepared and analyzed. The accuracy was determined from the percentage of recovery.

2.1.4. Precision

a) Within run precision

Three concentrations of standard solutions (five replicates/concentrations), covering the specified linearity range, were prepared and analyzed in the same run. The precision of each concentration was determined from the percentage of coefficient of variation (%CV).

b) Between run precision

Three concentrations of standard solutions, covering the specified linearity range, were prepared and analyzed in five different runs. The precision of each concentration was determined from the percentage of coefficient of variation (%CV)

CHAPTER IV

RESULTS AND DISCUSSIONS

A. Pseudo-ternary phase diagrams and the selected microemulsions

The constructed pseudo-ternary phase diagrams are showed in Figures 10-12.

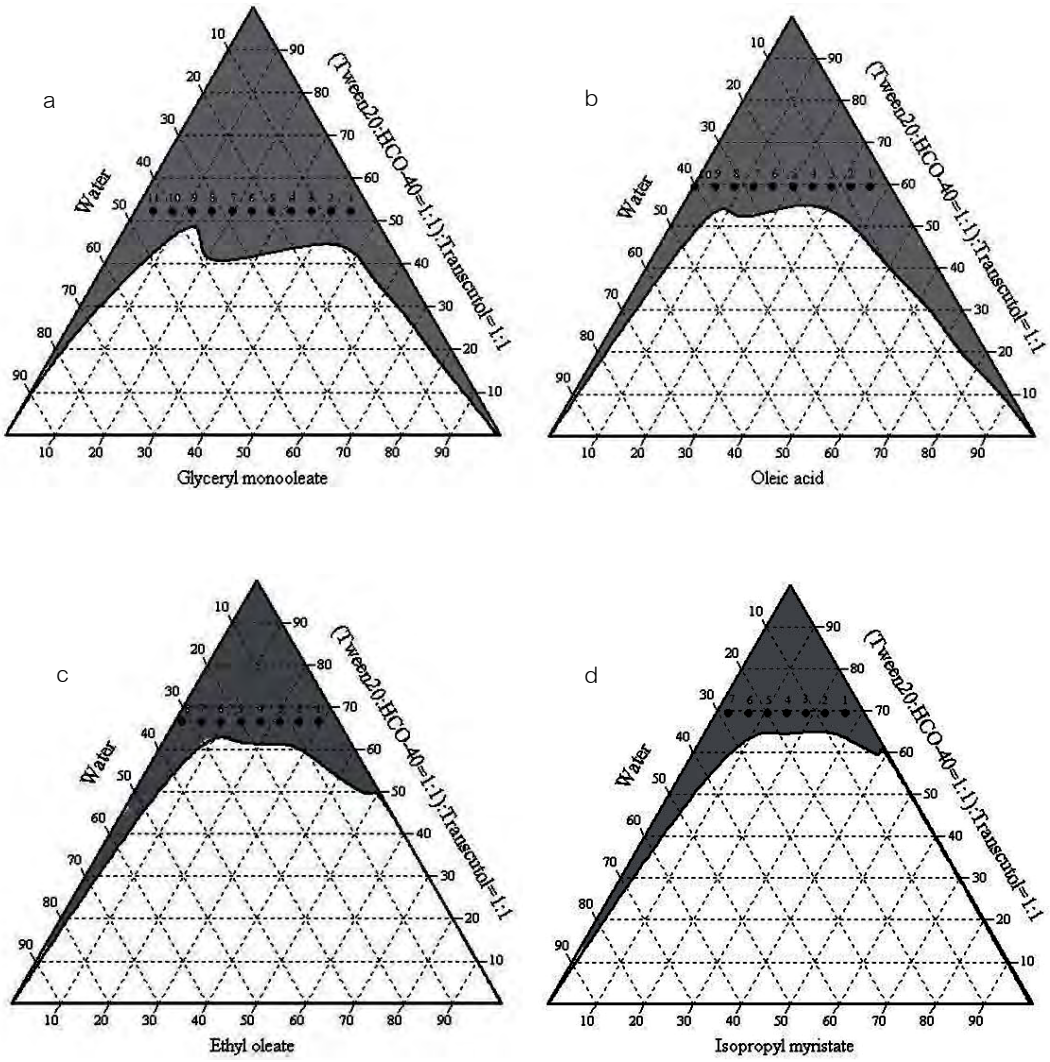

Figure 10: The microemulsions existence regions (the shaded area) of water (w)/ [(Tween 20® : HCO-40® =1:1) : Transcutol® = 1:1] (Smix) : oil [(a) glyceryl monooleate, (b) oleic acid, (c) ethyl oleate, and (d) isopropyl myristate] (O) presented in each pseudo-ternary phase diagram.

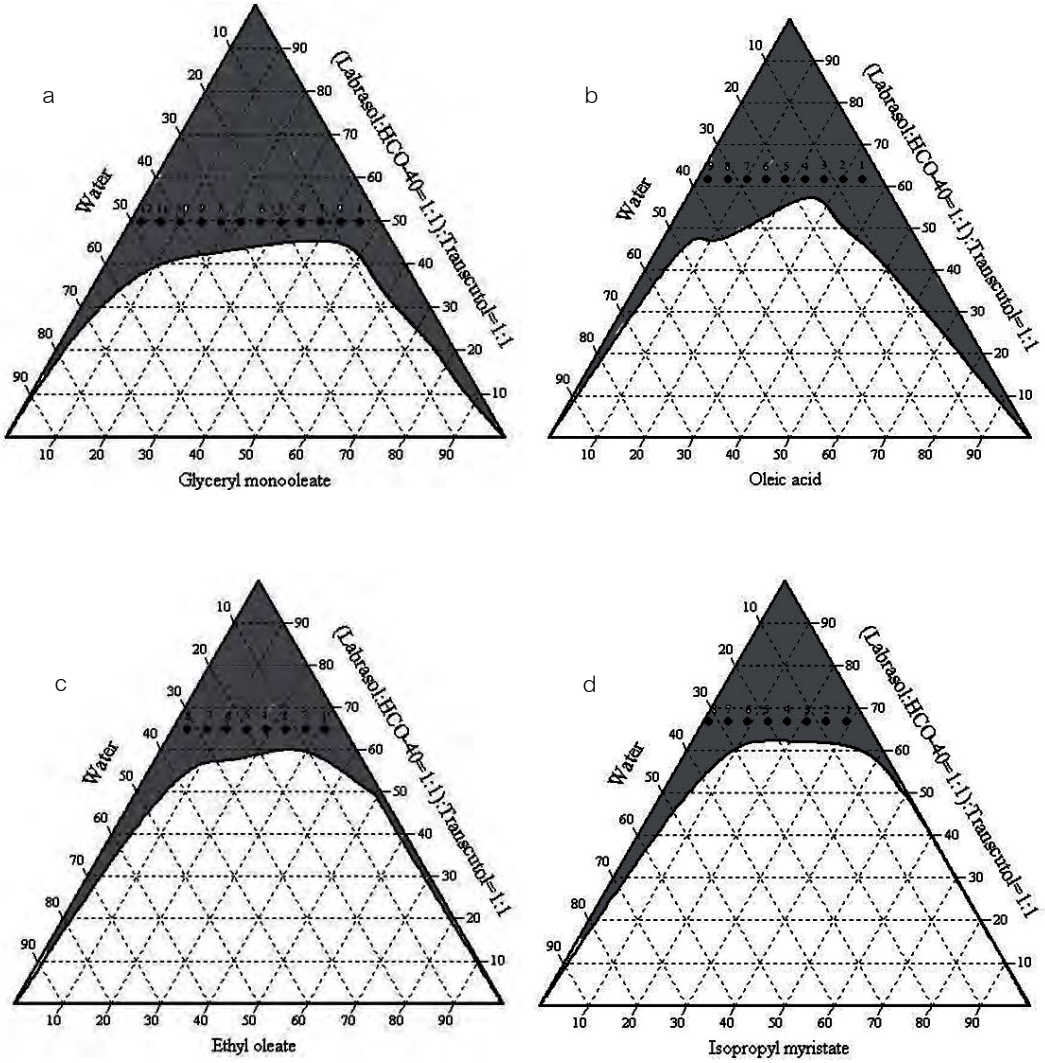

Figure 11: The microemulsions existence regions (the shaded area) of water (w)/ [(Labrasol® : HCO-40® =1:1) : Transcutol® = 1:1] (Smix) : oil [(a) glyceryl monooleate, (b) oleic acid, (c) ethyl oleate, and (d) isopropyl myristate] (O) presented in each pseudo-ternary phase diagram.

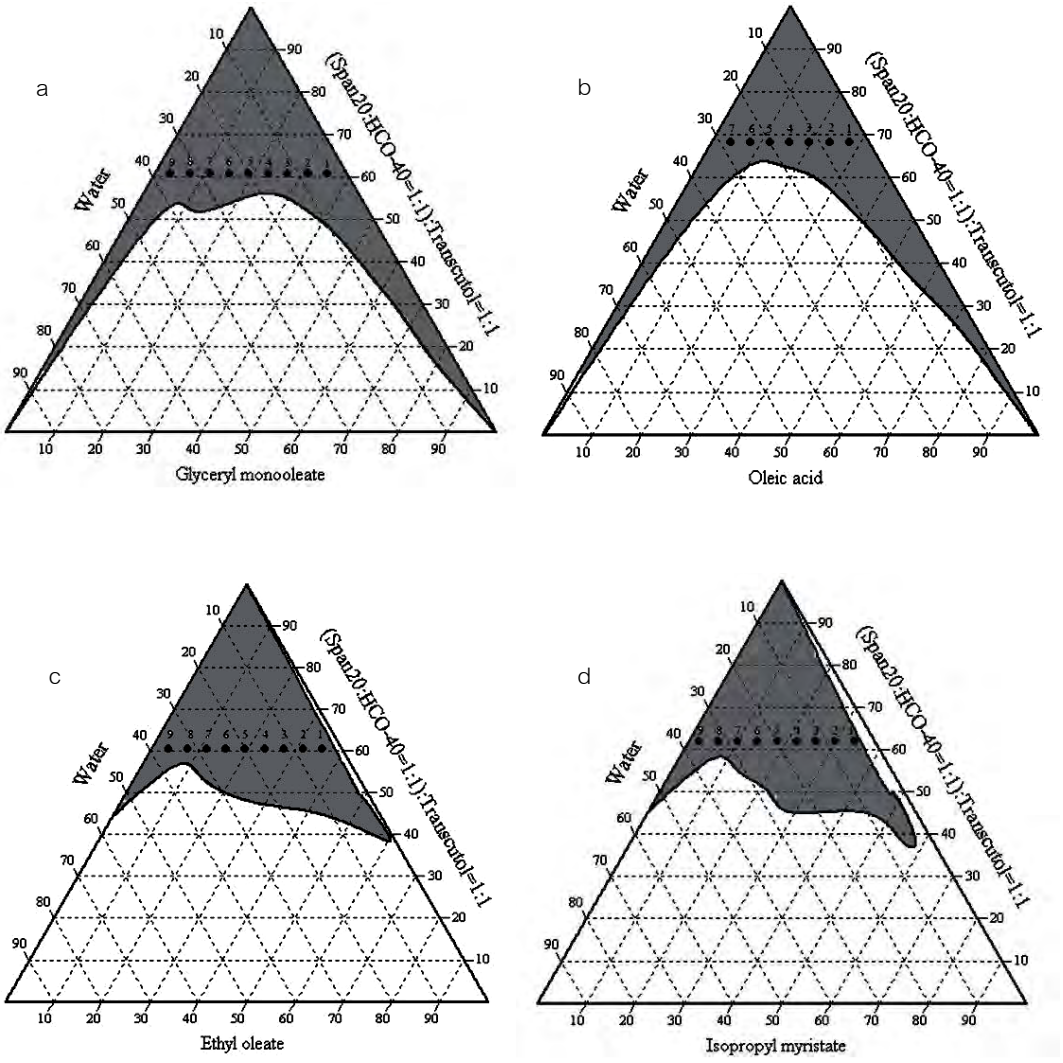

Figure 12: The microemulsions existence region (the shaded area) of water (w)/ [(Span 20® : HCO-40® =1:1) : Transcutol® = 1:1] (Smix) : oil [(a) glyceryl monooleate, (b) oleic acid, (c) ethyl oleate, and (d) isopropyl myristate] (O) presented in each pseudo-ternary phase diagram.

The surfactant monolayers at the interface of water and oil domains inside microemulsions are related to the solubilization of water and oil. The solubilization power of the surfactant could be increased when hydrophile-lipophile property of a surfactant mixture balances for water and the given oil (Shinoda et al., 1984). The miscibility of water, oil, surfactant or mixed surfactants, and cosurfactant is a composition dependent variable. In this present work when using glyceryl monooleate or oleic acid with high HLB surfactant mixtures (e.g. Tween 20® : HCO-40® or Labrasol® : HCO-40® in the 1:1 ratio) showed higher solubilizing power than low HLB surfactant mixture (e.g. Span 20® : HCO-40® in the 1:1 ratio) by comparing the isotropic region of each pseudo-ternary phase diagram.

In the contrary, the compositions using ethyl oleate or isopropyl myristate with low HLB surfactant mixture showed higher solubilizing power than high HLB surfactant mixtures. The formation of microemulsion may be used to explain the results; it seems to be important for surfactant being able to migrate into the oil-water interface to depress interfacial tension to a lower level. Since the HLB values relatively represent the polarity of the surfactants and may also indicate the extent of preference for surfactant migrating into the interface between water and oil phase (Ho et al., 1996). The high HLB surfactant mixture may prefer to localize at the interface of high polar oil while the low HLB surfactant mixture might prefer to migrate into the interface of less polar or non-polar oil. As Glyceryl monooleate and oleic acid are very polar owing to the hydroxyl and carboxyl group, respectively in its structure while the ester groups of ethyl oleate and isopropyl myristate are less polar. Thus, in case of glyceryl monooleate or oleic acid, the solubilizing power of high HLB surfactant mixtures were higher than low HLB surfactant mixture while an opposite results were found when used ethyl oleate or isopropyl myristate.

Another reason might be due to the penetration tendency of the oils into the surfactant palisade layer. Polar oils (e.g. triglycerides, fatty acids, fatty acid esters) could reduce the interfacial tension between the water and the surfactant tails if they locate themselves close to the micelle-water interface (Szekeres, et al., 2006). So, glyceryl monooleate and oleic acid may penetrate into the surfactant palisade layer of high HLB surfactant mixtures in a greater extent than the low HLB surfactant mixture. The reverse affects were expected for ethyl oleate and isopropyl myristate.

After pseudo-ternary phase diagrams were constructed, microemulsion formulations were chosen by kept the surfactant concentration constant and varied the water and oil contents. The selected microemulsions from each pseudo-ternary phase diagaram were depicted as dots presented in Figures 10-12.

B. Characterization of microemulsions

1. Visual inspection

All selected microemulsions were transparent liquids without phase separation.

2. Viscosity and conductivity

Generally, the w/o microemulsion can be formed at low water content and the oil is continuous. With increasing water-to-oil ratio, some structural transition occurs by the w/o microemulsion inverts to an o/w microemulsion. The inversion may gradually change through a bicontinuous structure without any phase separation where the system remains isotropic (Mo, Zhong, and Zhong, 2000). Macroscopic changes of microemulsions such as viscosity and electrical conductivity are obviously related to the microstructure of the solution. Viscosity represents fluidity or interactions between different microstructure, while electrical conductivity measures the ability of ions to move in the aqueous phase of the microemulsion and depends on the local viscosity (Georges and Chen, 1986).

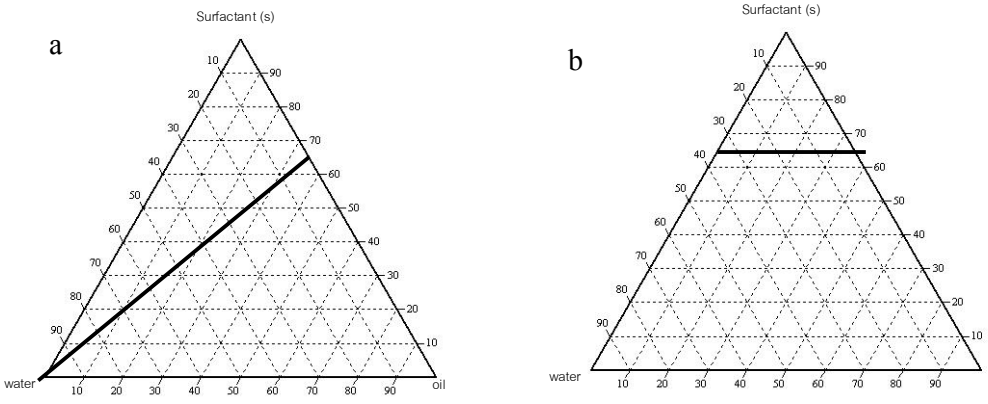

Figure 13 : The lines in which the microemulsions were selected to study

In previous studies, the structural evaluations of microemulsions by conductivity and viscosity measurements were performed along the water dilution line (Figure 13a) (Djordjevic et al., 2004; Alany et al., 2001; Sintov, and Shapiro, 2004), or the line which the surfactant concentration was kept constant and the water to oil ratios was varied (Figure 13b) (Boonme et al., 2006; Podlogar et al., 2004; Liu et al., 2006). For the present study, conductivity and viscosity were measured along the fixed minimum surfactant content as presented in Figure 13b. The conductivity and viscosity profiles are shown in Figures 14-25.

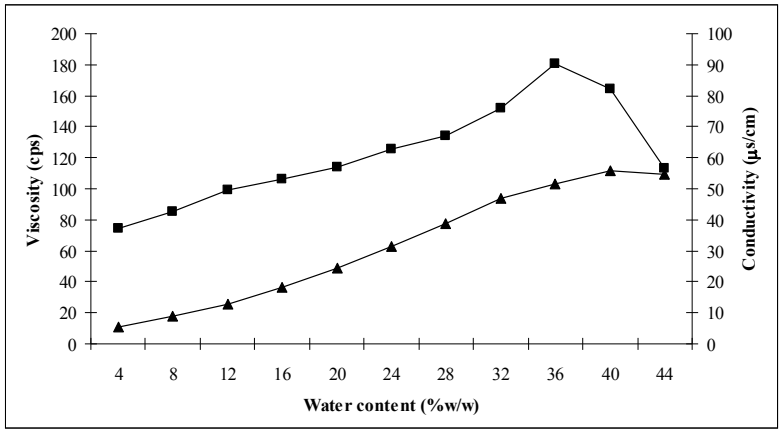

Figure 14: Conductivity (▲) and viscosity (■) of microemulsions, which used glyceryl monooleate as an oil phase, Tween 20® and HCO-40® (1:1) as a surfactant, and transcutol® as a cosurfactant (S/CoS ratio = 1:1)

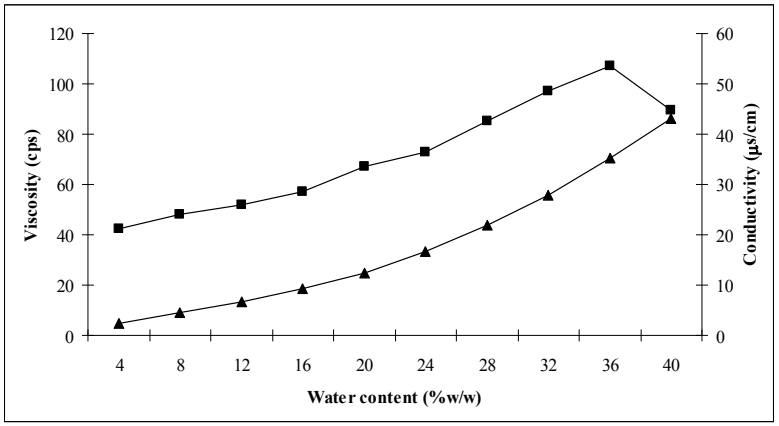

Figure 15: Conductivity (▲) and viscosity (■) of microemulsions, which used oleic acid as an oil phase, Tween 20® and HCO-40® (1:1) as a surfactant, and transcutol® as a cosurfactant (S/CoS ratio = 1:1)

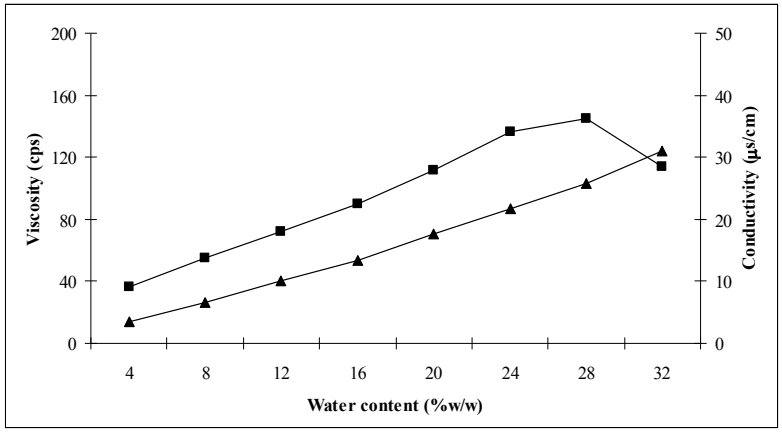

Figure 16: Conductivity (▲) and viscosity (■) of microemulsions, which used ethyl oleate as an oil phase, Tween 20® and HCO-40® (1:1) as a surfactant, and transcutol® as a cosurfactant (S/CoS ratio = 1:1)

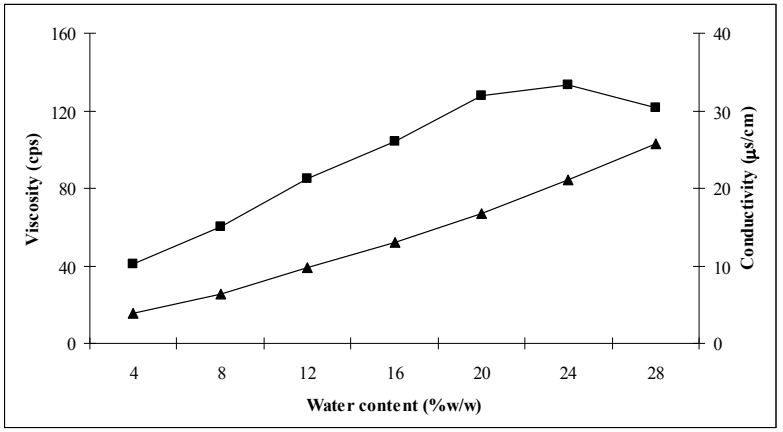

Figure 17: Conductivity (▲) and viscosity (■) of microemulsions, which used isopropyl myristate as an oil phase, Tween 20® and HCO-40® (1:1) as a surfactant, and transcutol® as a cosurfactant (S/CoS ratio = 1:1)

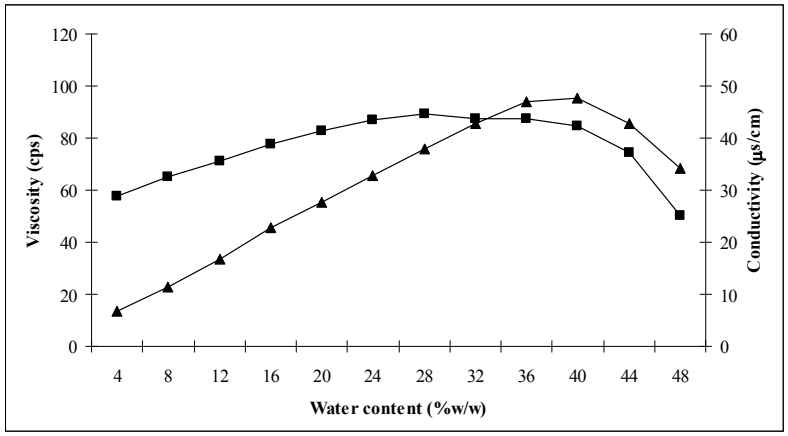

Figure 18: Conductivity (▲) and viscosity (■) of microemulsions, which used glyceryl monooleate as an oil phase, Labrasol® and HCO-40® (1:1) as a surfactant, and transcutol® as a cosurfactant (S/CoS ratio = 1:1)

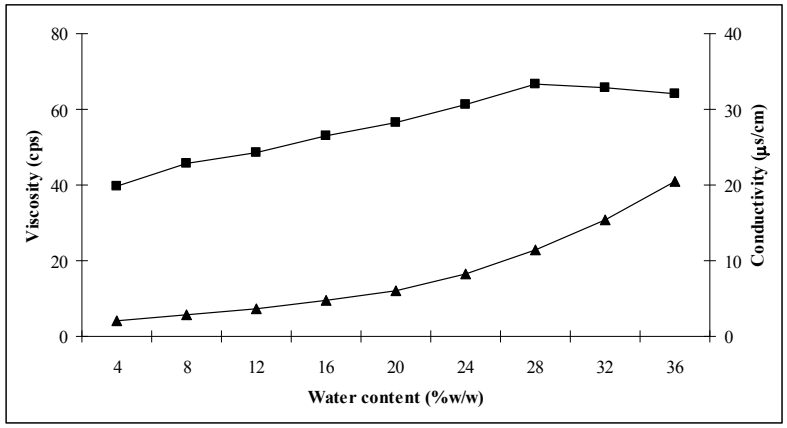

Figure 19: Conductivity (▲) and viscosity (■) of microemulsions, which used oleic acid as an oil phase, Labrasol® and HCO-40® (1:1) as a surfactant, and transcutol® as a cosurfactant (S/CoS ratio = 1:1)

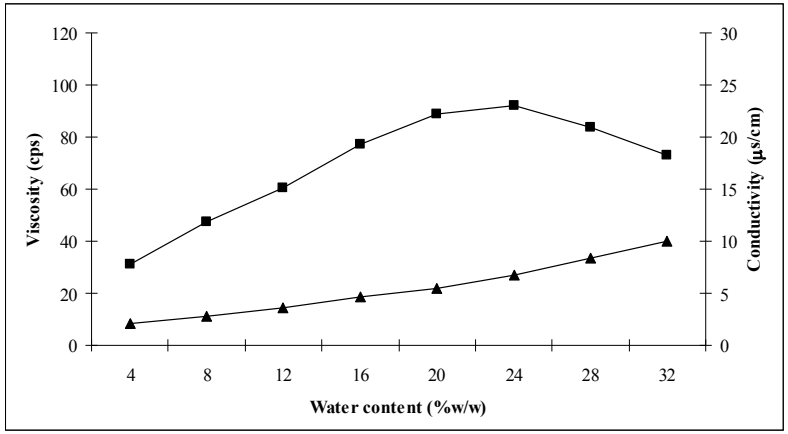

Figure 20: Conductivity (▲) and viscosity (■) of microemulsions, which used ethyl oleate as an oil phase, Labrasol® and HCO-40® (1:1) as a surfactant, and transcutol® as a cosurfactant (S/CoS ratio = 1:1)

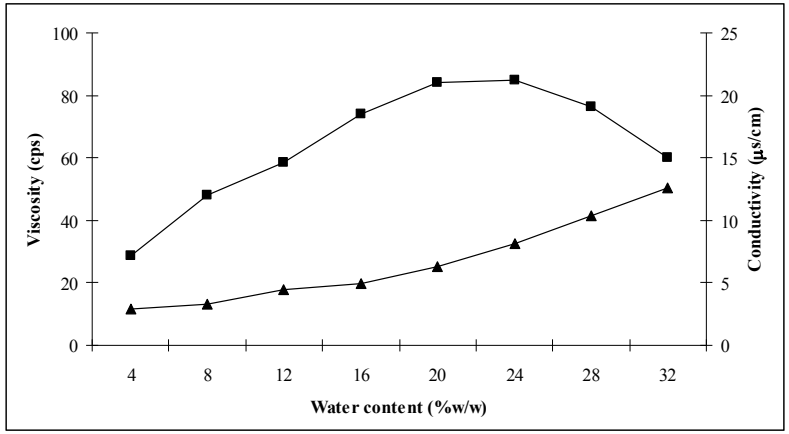

Figure 21: Conductivity (▲) and viscosity (■) of microemulsions, which used isopropyl myristate as an oil phase, Labrasol® and HCO-40® (1:1) as a surfactant, and transcutol® as a cosurfactant (S/CoS ratio = 1:1)

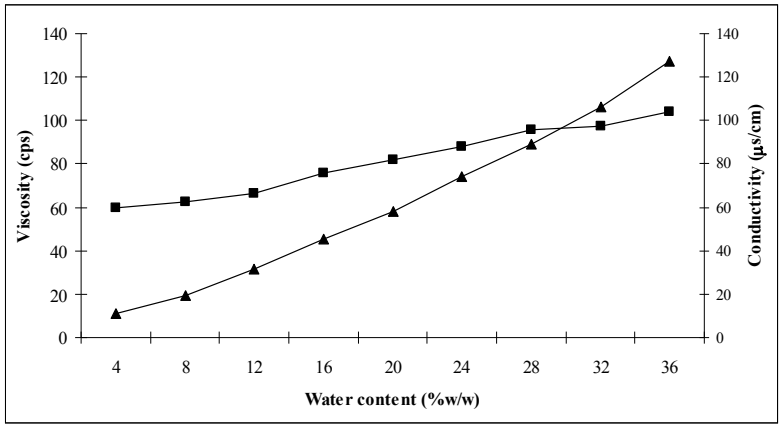

Figure 22: Conductivity (▲) and viscosity (■) of microemulsions, which used glyceryl monooleate as an oil phase, Span 20® and HCO-40® (1:1) as a surfactant, and transcutol® as a cosurfactant (S/CoS ratio = 1:1)

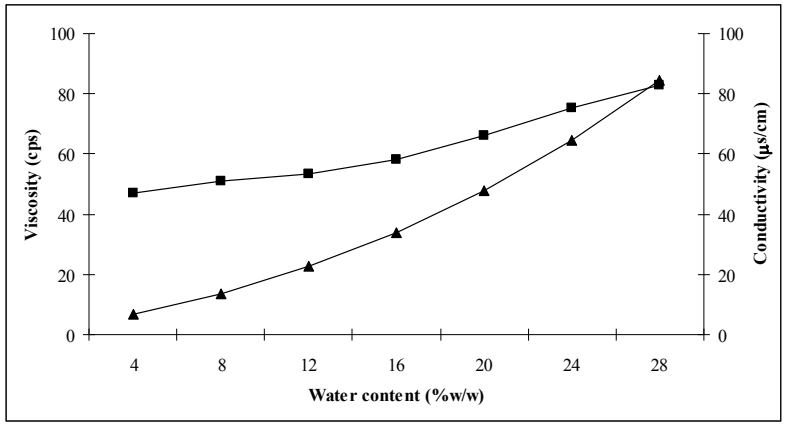

Figure 23: Conductivity (▲) and viscosity (■) of microemulsions, which used oleic acid as an oil phase, Span 20® and HCO-40® (1:1) as a surfactant, and transcutol® as a cosurfactant (S/CoS ratio = 1:1)

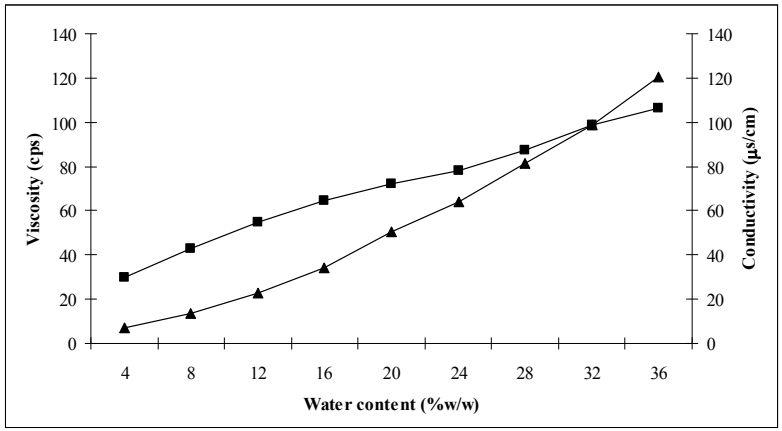

Figure 24: Conductivity (▲) and viscosity (■) of microemulsions, which used ethyl oleate as an oil phase, Span 20® and HCO-40® (1:1) as a surfactant, and transcutol® as a cosurfactant (S/CoS ratio = 1:1)

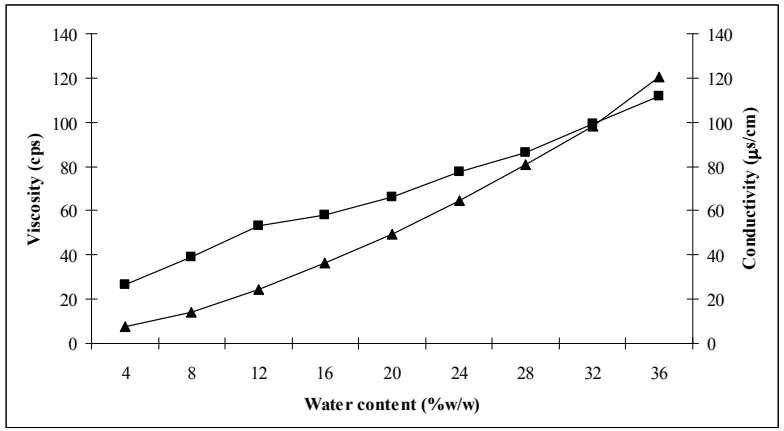

Figure 25: Conductivity (▲) and viscosity (■) of microemulsions, which used isopropyl myristate as an oil phase, Span 20® and HCO-40® (1:1) as a surfactant, and transcutol® as a cosurfactant (S/CoS ratio = 1:1)

An increase in the dispersed phase of microemulsion is known to increase in the viscosity and droplet size. The rise in the viscosity with water addition has been ascribed to the increasing diameter of water filled conduits in the bicontinuous structure. The peak point in the viscosity-water content profile denoted that transition point of the w/o system to the o/w type as seen in Figure 26a (Lee et al., 2005; Moulik and Paul, 1998). In this study, the peak points of viscosity-water profiles (Figures 14-25) were only found in microemulsion systems using high HLB surfactants (Tween 20® : HCO-40® = 1:1; Figures 14-17 and Labrasol® : HCO-40® = 1:1; Figures 18-21) which may indicate the type transformation of the microemulsion systems. However, the peak points were not found in the microemulsion systems using low HLB surfactant (Span 20® : HCO-40® = 1:1; Figures 22-25), which may imply in two cases, one is that no transformation occurred or another type transformation may occur but could not be detected with viscosity changes.

The electrical conductivities of o/w, w/o, and bicontinuous microemulsions can be dramatically different. The conductivity is almost like a normal aqueous medium in o/w microemulsions, very low in w/o microemulsions and significantly high in bicontinuous condition. The water content is the controlling factor for the magnitude of conductance, so the phenomenon of percolation may arise (Moulik and Paul, 1998). The electrical conductivity (σ) as a function of water phase volume fraction is showed in Figure 26b. While the water volume fraction (Φ_w) increases, the conductivity of the microemulsion system slightly increases as well until the critical Φ_w (Φ_c) is reached when a sudden increase in conductivity is observed. This phenomenon is known as “percolation” and the Φ_c at which it occurs is known as percolation threshold. In the region of low water content, a w/o microemulsions are formed. Beyond the percolation threshold, the conductivity increases sharply deviating from the former line up to a maximum. This may result from a progressive aqueous droplet interlinking and clustering process to form bicontinuous structure. After the maximum, conductivity of the system was slightly decreased by the further addition of water phase which decreased the concentration of dispersed oil phase (Djordjevic et al., 2004; Mo et al., 2000).

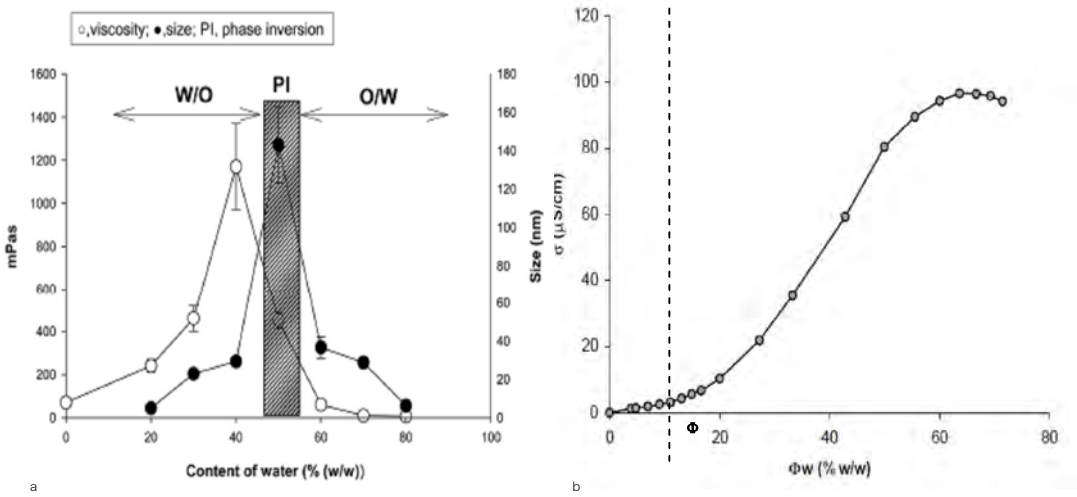

Figure 26: The droplet size and viscosity (a), and electrical conductivity (b) as a function of water phase volume fraction (Lee et al., 2005; Djordjevic, 2004)

In all systems, the conductivities increase together with the water content. A drastic increase in conductivity could not be observed, although the peak points are found in some viscosity-water content profiles which may be used to indicate the transformation of the microemulsion systems. As these two properties seem not to be sufficient to identify microemulsion type especially bicontinuous one, the dilution technique is also conducted to gain additional information.

3. Dilution test

Microemulsion types determined by dilution test and reported as water content of the microemulsion systems are shown in Table 2. The microemulsions which had ability to dilute with water were defined as o/w type. In contrast, the micreomulsions had miscibility with oil were defined as w/o type. In addition, microemulsions, which became turbid either when diluted with oil or water, were uncharacterized and may be assumed bicontinuous structure. As seen in Table 2 (System i and l), all microemulsions using ethyl oleate or isopropyl myristate with low HLB surfactant mixture (Span 20® : HCO-40® in the 1:1 ratio) were w/o type which may due to the hydrophobicity of the surfactant mixtures with low HLB. Different findings were found when using polar oils (e.g., glyceryl monooleate, or oleic acid) where glyceryl monooleate and oleic acid can penetrate into the surfactant palisade layer of the surfactant mixture, and can change the property of

the surfactant layer to be more hydrophilic. So, o/w microemulsions could be formed.

Table 2: Microemulsion types referred to dilution test (presented as water content)

Systems	Water content (%w/w)		
	w/o	uncharacterized	o/w
a) water (w)/ (Tween 20® : HCO-40® = 1:1) : Transcutol® = 1:1 (Smix) : gylceryl monooleate (O)	<16 (point 1-3)	16-36 (point 4-9)	>36 (point 10-11)
b) water (w)/ (Labrasol® : HCO-40® = 1:1) : Transcutol® = 1:1 (Smix) : gylceryl monooleate (O)	<20 (point 1-4)	20-40 (point 5-10)	>40 (point 11-12)
c) water (w)/ (Span 20® : HCO-40® = 1:1) : Transcutol® = 1:1 (Smix) : gylceryl monooleate (O)	<24 (point 1-5)	24 (point 6)	>24 (point 7-9)
d) water (w)/ (Tween 20® : HCO-40® = 1:1) : Transcutol® = 1:1 (Smix) : oleic acid (O)	<20 (point 1-4)	20 (point 5)	>20 (point 6-10)
e) water (w)/ (Labrasol® : HCO-40® = 1:1) : Transcutol® = 1:1 (Smix) : oleic acid (O)	<20 (point 1-4)	20 (point 5)	>20 (point 6-9)
f) water (w)/ (Span 20® : HCO-40® = 1:1) : Transcutol® = 1:1 (Smix) : oleic acid (O)	≤20 (point 1-5)	-	≥ 24 (point 6-7)
g) water (w)/ (Tween 20® : HCO-40® = 1:1) : Transcutol® = 1:1 (Smix) : ethyl oleate (O)	<20 (point 1-4)	20 (point 5)	>20 (point 6-8)
h) water (w)/ (Labrasol® : HCO-40® = 1:1) : Transcutol® = 1:1 (Smix) : ethyl oleate (O)	<12 (point 1-2)	12-16 (point 3-4)	>16 (point 5-8)
i) water (w)/ (Span 20® : HCO-40® = 1:1) : Transcutol® = 1:1 (Smix) : ethyl oleate (O)	All (point 1-9)	-	-
j) water (w)/ (Tween 20® : HCO-40® = 1:1) : Transcutol® = 1:1 (Smix) : isopropyl myristate (O)	<16 (point 1-3)	16-20 (point 4-5)	>20 (point 6-7)
k) water (w)/ (Labrasol® : HCO-40® = 1:1) : Transcutol® = 1:1 (Smix) : isopropyl myristate (O)	<20 (point 1-4)	20 (point 5)	>20 (point 6-8)
l) water (w)/ (Span 20® : HCO-40® = 1:1) : Transcutol® = 1:1 (Smix) : isopropyl myristate (O)	All (point 1-9)	-	-

Points referred to the selected microemulsions, which depicted as dot in the pseudo-termary phase diagrams (Figures 10-12), dash sign (-) indicated that this microemulsion type was not found.

C. Prepared silymarin microemulsion formulations

To develop silymarin microemulsion(s) for dermal delivery, o/w microemulsions was selected from each pseudo-ternary phase diagram. Free water from o/w microemulsions could hydrate skin and caused the stratum corneum to swell, and then made drug channels widen resulting in drug permeation improvement which made o/w microemulsions more suitable for topical delivery than w/o type (Yuan et al., 2006). In addition, the oil droplets of the o/w type might penetrate into the epidermis easier than the water droplets of the w/o type at the same surfactant concentration owing to the lipophilic nature of stratum corneum (Junyaprasert et al., 2007). Furthermore, high content of surfactant and oil in microemulsions may affect drug permeability and skin irritancy of the formulation. In this study, the surfactant mixtures were chosen at minimum percentages (5% above the highest boundary point) which ensure the achievement of microemulsions and oil contents were chosen in the range of 5-8%. Table 3 shows the o/w microemulsions chosen from many pseudo-ternary phase diagrams.

Table 3: The composition of the selected oil-in-water microemulsions (%w/w)

Formulation	GT10	GL11	GS8	OT9	OL8	OS6	ET7	EL7	IT6	IL7
GMO	8	6	7							
Oleic acid				5	6	8				
Ethyl oleate							6	7		
Isopropyl myristate									7	6
Tween 20® : HCO-40® (1:1)	26			29.5			33		34.5	
Labrasol® : HCO-40® (1:1)		25			31			32.5		34
Span 20® : HCO-40® (1:1)			30.5			34				
Transcutol®	26	25	30.5	29.5	31	34	33	32.5	34.5	34
Water	40	44	32	36	32	24	28	28	24	28

2% w/w silymarin was incorporated into the selected o/w microemulsions. Referring to Nield and Ippersiel (Open evaluation of silymarin cream in the management of facila redness associated with rosacea, Online) study, the 0.7% silymarin face cream when applied twice daily could reduce the facial erythema associated with rosacea - a chronic inflammatory disorder characterized by sequential or simultaneous occurrence of flushing, erythema, telangiectasia, papules and pustules

particularly in the center of the face. Bonne and Sincholle (1988) proposed that topical compositions containing from 0.01 to 1% and especially 0.1 to 0.5% by weight of the extract of fruits of *Silybum marianum* can oppose the degrading effects of free radicals which are partly responsible for skin aging. Moreover, topical application of silymarin to mouse skin at a dose of 9 mg per application inhibited UV-caused sunburn and skin edema in short term and reduced tumor formation in long term. So, 2% w/w (20 mg/g) silymarin in microemulsions might be sufficient to reduce various skin disorders.

After prepared silymarin microemulsions were stored at room temperature for 3 days, they remained transparent, phase separation or drug precipitation were not observed. The viscosities, conductivities, and microemulsion types resulted from dilution test are shown in Table 4.

Table 4: The viscosities, conductivities, and microemulsion types (ME) of blank microemulsions and silymarin-loaded microemulsions

Formulation	Viscosity (cps)		Conductivity (μs/cm)		Microemulsion type	
	Blank ME	Silymarin ME	Blank ME	Silymarin ME	Blank ME	Silymarin ME
GT10	164.37	178.87	55.8	64.2	o/w	o/w
GL11	74.28	74.50	42.8	55.5	o/w	o/w
GS8	97.61	104.42	106.0	111.0	o/w	o/w
OT9	107.37	109.16	35.2	43.6	o/w	o/w
OL8	65.78	63.44	15.5	19.3	o/w	o/w
OS6	75.2	86.60	64.4	64.2	o/w	o/w
ET7	144.59	159.90	25.9	29.1	o/w	o/w
EL7	83.88	98.21	8.4	14.7	o/w	o/w
IT6	133.03	145.52	21.1	22.7	o/w	o/w
IL7	76.46	80.99	10.4	15.6	o/w	o/w

As seen in Table 4, the viscosities and conductivities of silymarin microemulsions were slightly higher than blank microemulsions. However, the microemulsion types were unchanged due to the drug incorporation.

D. Stability of silymarin microemulsions

1. Physical stability

After six heating-cooling cycles, physical appearances of silymarin microemulsions were unchanged in terms of transparency and phase separation. Moreover, silymarin precipitation was also not detected. The studied silymarin microemulsions were considerably physical stable.

2. Chemical stability

The percentages of silybin remaining in microemulsions versus time plots are shown in Figure 27. Silybin in all formulations decreased with time when stored in acceleration condition (40°C) for 6 months. Since silymarin is a potent antioxidant, silymarin instability may due to its oxidative degradation. Moreover, the location of antioxidant substances in microemulsion may significantly influenced its stability toward oxidation. Similar finding was founded with other antioxidants like ascorbyl palmitate (Špiclin, Gašperlin, and Kmetec, 2001). Owing to its hydrophilic property, ascorbyl palmitate is higher stable in w/o microemulsion where drug deposited in the internal phase (water), and external phase (oil) acts as a barrier of the diffusion of oxygen to the internal phase. Moreover, Garti et al. (2005) compared the oxidative stability of lipophilic lycopene dissolved in acetone with lycopene solubilized in o/w microemulsions and found that the lycopene is higher stable in o/w microemulsions. In addition, the results from Xu et al. (1999) show higher lycopene stable in micelle than tetrahydrofuran (THF), thus it was also indicated that the solubilization of lycopene in the amphiphilic film protects it from oxidative degradation.

In this study, silymarin was solubilized in o/w microemulsions. Due to its low water solubility, silymarin may localize in oil and/or surfactant layer (a log octanol/water partition coefficient of silybin is 1.7 (Yang et al., 2001)). Lui et al. (2007) and Woo et al. (2007) determined the solubilities of silymarin and silybin in many oils and surfactants (as shown in Table 5 and 6, respectively), and found that silybin and silymarin were preferably dissolved in the surfactant phase.

Table 5: The solubility of silymarin in various vehicles (n=3), (Lui et al., 2007)

Vehicle		Solubility (mg/ml)
Oils	Ethyl oleate	0.583±0.05
	Olive oil	0.045±0.04
Surfactant	Cremophor EL®	41.24±4.61
	Tween 80®	35.4±3.35
	Labrasol®	79.83±6.24

Table 6: The solubility of silybin in various vehicles (n=3), Woo et al. (2007)

Vehicle		Solubility (mg/ml)
Oils	Glyceryl monooleate	33.2±2.8
	Castor oil	7.1±1.2
Surfactant	Tween 20®	131.3±6.3
Cosurfactant	Transcutol C	350.0±10.4

Thus, silymarin may be protected from oxidation by solubilizing in the surfactant film. If so the surfactant film influenced the stability of silymarin, the structure of surfactant may also be an important factor. As seen in Figure 27, the percentages of silybin remaining were sequenced in the order of Labrasol® > Tween 20® > Span 20® (as HCO-40® and Transcutol® were used in every formulations). The oxyethylene group of surfactants, which has ability to form hydrogen bond with phenol group of silybin may play a role in drug stability. Span 20® has no oxyethylene group in its structure, but has only three ester groups that can be a hydrogen bond acceptor (Appendix I). While Tween 20® and Labrasol® have 20 and 8 oxyethylene group, respectively. Since the number of moles is related to the chemical interaction, moles of Tween 20, Labrasol, and Span 20 were calculated (Table 7).

Table 7: Moles of Tween 20, Labrasol, and Span 20 in 1 g of microemulsions

Formulation	Tween 20® (mM)	Labrasol® (mM)	Span 20® (mM)
GT10	0.1161	-	-
GL11	-	0.3100	-
GS8	-	-	0.4393
OT9	0.1321	-	-
OL8	-	0.3850	-
OS6	-	-	0.4913
ET7	0.1472	-	-
EL7	-	0.4050	-
IT6	0.1534	-	-
IL7	-	0.4175	-

The number of moles of Tween 20® in microemulsions was one third of Labrasol®; however, Tween 20® has more oxyethylene groups than Labrasol® (20 and 8, respectively). Thus, total oxyethylene groups of Tween 20® and Labrasol® are comparable. Therefore, sorbitan ring of Tween 20® may cause steric hindrance against silybin to form hydrogen bonding, and then silybin prefers to localize in Labrasol® resulting in superior stability from being oxidized than others. The schematic illustrations of possible packing of silybin in o/w microemulsions are showed in Figures 28 and 29.

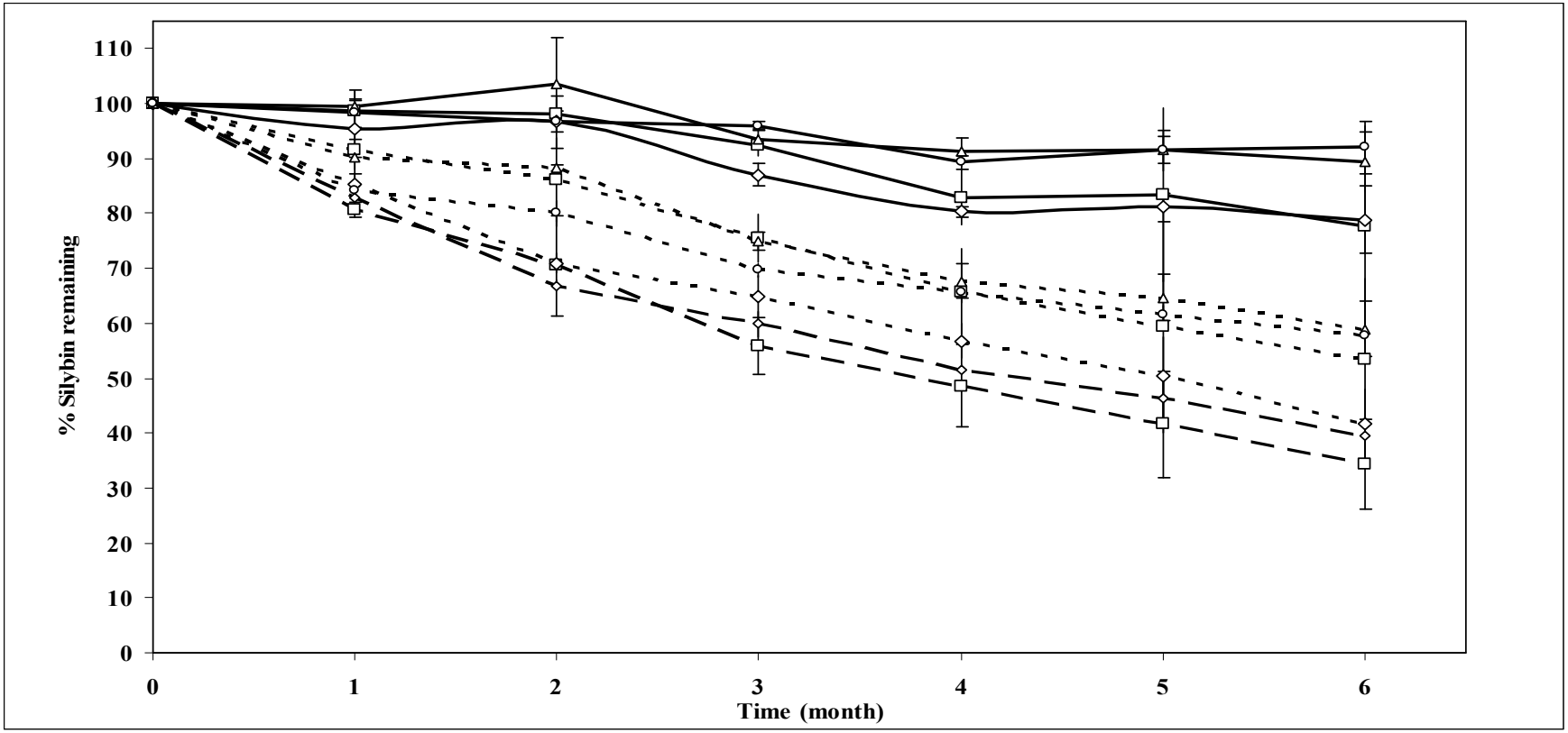

Figure 27: Stability of silymarin in o/w microemulsions (n=3); GT10 (- -□- -), GL11 (—□—), GS8 (—□ —), OT9 (- -◇- -), OL8 (—◇—), OS6 (—◇ —), ET7 (- -△- -), EL7 (—△—), IT6 (- -◇- -), and IL7 (—◇—)

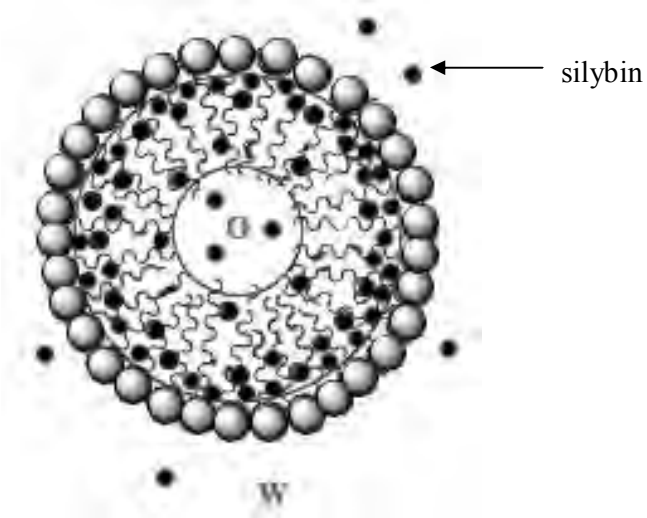

Figure 28: Schematic illustration of possible packing of silybin in o/w microemulsion (This figure was modified from Mehta et al., 2009)

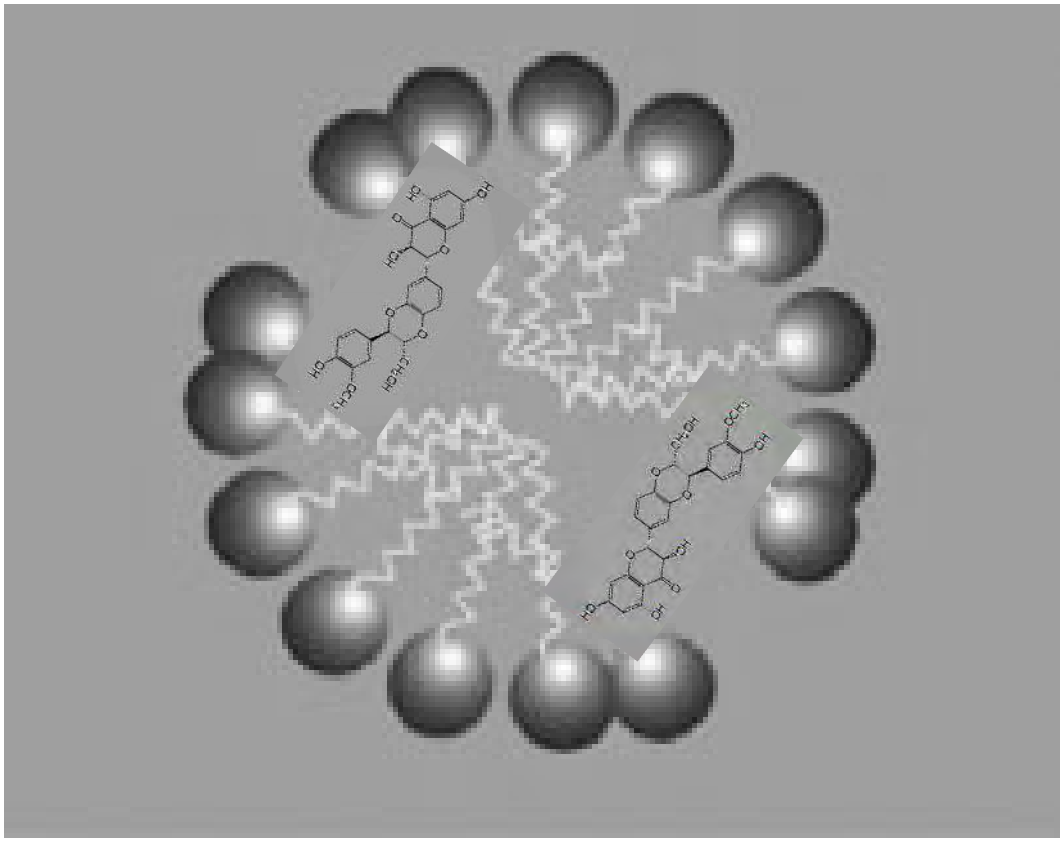

Figure 29 : Schematic illustration showed that silybin is possible preferably localized in surfactant phase near the hydrophilic group of the micelles to form hydrogen bond (This figure was modified from Kogan, Aserin, and Garti, 2007)

E. In vitro release study of silymarin microemulsions

In vitro release studies can be used for understanding the physicochemical structure of the delivery system and the drug-release mechanism, which the data can be used in prediction the likely behavior of the system in vivo (Yang and Washinton, 2006). In this study, the 24 hour release patterns of silymarin microemulsions were evaluated by using modified Franz diffusion cell with cellulose membrane. The silymarin amount was analyzed by UV spectrophotometry since there is good correlation (data not shown here) between silymarin amount analyzed by UV and silybin analyzed by HPLC. Moreover, expected silymarin release is much higher than silybin in skin, with this range silymarin could be accurately quantified by UV within shorter time. The sink condition of the receiver compartment was maintained by using 40% ethanol in phosphate buffer saline pH 7.4 (Appendix C). Silymarin solution, using 40% ethanol in phosphate buffer saline pH 7.4 as a vehicle, at the same thermodynamic activity as the microemulsions was used as a control. Since 2%w/w silymarin in microemulsions were calculated to be about 40% saturation, the same % saturation was used as a concentration of silymarin in solution (Appenidix B). The release profiles presented as the plot between % cumulative amount of silymarin versus time of silymarin microemulsions and solution are shown in Figure 30. Silymarin microemulsions showed the prolong release when compared to its solution. Kumar and Mital (1999) suggested that the microemulsions can reach prolong release if the interactions between drug and surfactants and/or partitioning of the drug between oil and water phases strongly affects the drug release.

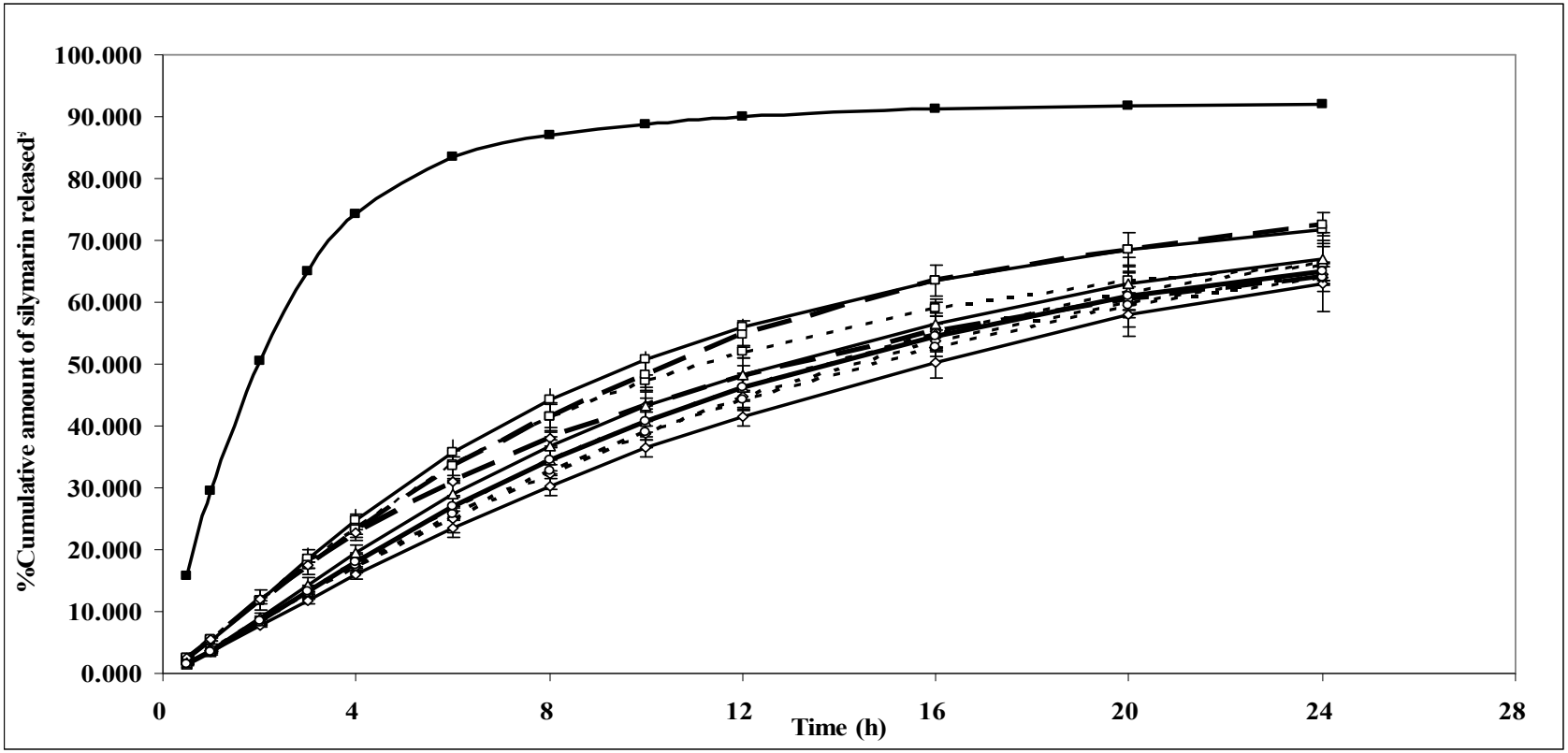

Figure 30: Release profiles of silymarin microemulsions (n=3); GT10 (- -□- -), GL11 (—□—), GS8 (—□ —), OT9 (- -◇- -), OL8 (—◇—), OS6 (—◇ —), ET7 (- -△- -), EL7 (—△—), IT6 (- -◇- -), IL7 (—◇—) and solution (—■—)

Several mathematical models were attempted to fit the drug release profile. Trotta (1999) and Montenegro et al. (2006) used the model that considers the rate of release be limited by an interfacial barrier which was developed by Guy et al. (1982). The release rate constants (k) of the drug between oil droplets and the release medium were calculated by Equation 5.

$$\ln\left(1-\frac{M_t}{M_0}\right)=\frac{-3\,k\,t}{r^2} \qquad \text{Equation 5}$$

where M_t/M_0 is the fraction of released drug at time t and r is the droplet radius. Plotting the natural logarithm of the fraction of remaining drug against time, release curves whose slope was $-3k/r^2$ were obtained.

Špiclin et al. (2003) fitted the release profiles of sodium ascorbyl phosphate from non-thickened and thickened microemulsions to different order kinetic equations including zero-order, first-order, and Higuchi kinetic (Equations 6, 7, 8, respectively) and found that the best fit were Higuchi kinetic.

$$M_t = M_0 + k_0\,t \qquad \text{Equation 6}$$

$$\ln M_t = \ln M_0 + k_1\,t \qquad \text{Equation 7}$$

$$M_t = k_H\,t^{1/2} \qquad \text{Equation 8}$$

where M_t is the cumulative amount of drug released at time t, M_0 is the initial amount of drug in the formulation, k_0, k_1, k_H are the zero order, first order, and Higuchi release rate constant.

Thus, in present study, the silymarin release profiles were fitted with Guy's model and Higuchi kinetics; and the coefficient of determination values are listed in Table 8.

Table 8: Coefficient of determination values for Guy's model and Higuchi kinetics

Formulation	Guy's model	Higuchi
GT10	0.9609	0.9815
GL11	0.9726	0.9828
GS8	0.9856	0.9900
OT9	0.9940	0.9934
OL8	0.9978	0.9935
OS6	0.9753	0.9915
ET7	0.9936	0.9940
EL7	0.9878	0.9925
IT6	0.9932	0.9947
IL7	0.9889	0.9928

In all cases, the best fits were found with Higuchi kinetics. These results were agreed with Špiclin et al. (2003). Based on this equation, the rate-limiting step for silymarin release from microemulsions may be the diffusion of silymarin from oil droplet. Table 9 shows the Higuchi rate constants of silymarin from microemulsions.

Table 9: The release rate constants of silymarin from microemulsions (n=3)

Formulation	Higuchi release rate constant ($\mu gcm^{-2}h^{-1/2}$)
GT10	347.7500 ± 20.6479
GL11	370.8533 ± 10.2149
GS8	371.0467 ± 25.2239
OT9	330.9867 ± 9.7643
OL8	321.5067 ± 8.6468
OS6	309.7933 ± 31.5862*,**
ET7	339.1100 ± 15.4755
EL7	350.6433 ± 16.0899
IT6	325.8467 ± 5.6388
IL7	338.7067 ± 10.2268

Statistical analysis was performed by one-way ANOVA followed by Tukey HSD's test.
*, ** Statistically significant different when compared to GL11 and GS 8, respectively ($p<0.05$)

As seen in Table 9, the release rate constants of silymarin from microemulsions were not significantly different. However, silymarin release seemed slightly higher from the o/w microemulsions using glyceryl monooleate as an internal oil phase compared with the others (e.g., oleic acid, ethyl oleate, or isopropyl myristate) with the same surfactant mixtures. Thus, silymarin microemulsions using glyceryl monooleate (GT10, GL11, GS8) were chosen for further permeation study. Moreover, silymarin microemulsions using Labrasol® (GL11, OL8, EL7, IL7) as a

surfactant previously showed higher chemical stability and were also chosen for permeation study.

F. In vitro skin permeation study of silymarin microemulsions

The skin permeation study of silymarin microemulsions was performed for 24 hours using modified Franz diffusion cell and excised newborn pig skin as a membrane. The newborn pig skin is suitable to use as an alternative to human epidermis because its stratum corneum is similar to human stratum corneum in terms of lipid composition and also the thickness, which considerably thinner then adult pig skin (Cilurzo, Minghetti, and Sinico, 2007; Hammond et al, 2000).

In this study, it was found that silybin, which is the active component of silymarin, could not be detected in the concentrated receiver fluid. The percentages of silybin remainings in donors and skin extracts are shown in Table 10.

Table 10: The percentage of silybin remaining in donor and skin extract (n=6)

% silybin remaining	Donor	Skin extract
GT10	94.73±3.92	0.0389±0.0320
GL11	96.50±1.06	0.0513±0.0319
GS8	96.36±1.45	0.0271±0.0114
OL8	96.86±1.17	0.0275±0.0115
EL7	93.44±4.68	0.0234±0.0166
IL7	97.41±1.97	0.0203±0.0083
40% Ethanol in PBS pH 7.4	98.59±0.52	0.2550±0.1194*

Statistical analysis was performed by one-way ANOVA followed by Tukey HSD's test.
*Statistically significant different when compared to silymarin microemulsions ($p<0.05$).

Drug present in the receiver phase represents its percutaneous delivery; however, no drug presented in the receiver but few presented in the skin which may indicate the superfacial skin penetration and not to forget to mention the drug remained after the incomplete washing. As in Vicentini et al. (2008), quercetin in w/o microemulsions showed the efficacy in vivo against UVB damage-induced by decreasing of glutathione levels and increasing of cutaneous proteinase secretion/ activity; however, quercetin could not also be detected in receptor phase in vitro. Furthermore, they also suggested that it is an advantage because the aim is the topical not transdermal delivery in their case.

As seen in Table 10, the percentage of silybin remainings in skin extracts from silymarin microemulsions were not significantly different, except for the solution (40% ethanol in phosphate buffer saline pH 7.4) which was significantly higher than microemulsions. Commonly known that ethanolic solutions can damage the skin and resulting in more drug penetrates into skin. Furthermore, the differences in drug amount found in the skin extracts may result from the supersaturation state while ethanol evaporated. Alcohol solutions are still not suitable for skin delivery due to their skin irritation. For further studies, the permeation study in occlusive condition should be performed comparing to this non-occlusive condition, as well as in vivo studies of efficacy and skin irritation of silymarin microemulsions.

G. Verification of analytical methods for silymarin

The objective of verification of an analytical procedure is to demonstrate that it is suitable for its intended analytical applications (ICH topic Q2 (R1), 2005). In this study, the HPLC (USP 30, 2007) and the UV-VIS spectroscopic (El-Samaligy, Afifi and Mahmoud, 2005) method had been validated.

1. High Performance Liquid Chromatographic (HPLC) Method

Since silymarin is an extract which composed of many flavonolignans, silybin which is the main component in silymarin was quantified by the HPLC method.

1.1 Specificity

Specificity is the ability of an analytical method to differentiate and quantify the analyte in the presence of other components in the sample.

The typical chromatograms of 30% ethanol in phosphate buffer saline pH 7.4 which was used as the dilution solvent for final solution before HPLC injection, silybin standard solution, silymarin solution, blank microemulsions, blank skin extract, blank receiver fluid sample and other chromatograms are shown in Figures 31-38. All chromatograms are shown under the same attenuation and scale.

There was no interference from other components in the chromatograms including the solvent peak of solvent system, the related substances (other flavonolignans in silymarin), oils and surfactants in microemulsions, and other

substances in skin extract and receiver fluid. Thus, the HPLC method was acceptable for specificity.

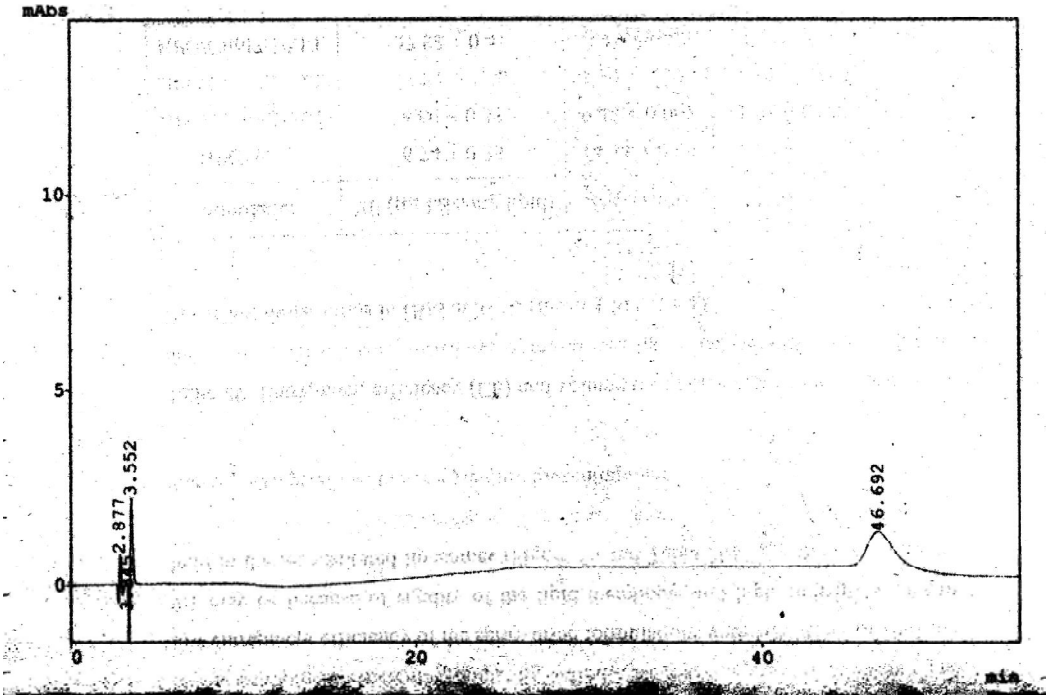

Figure 31: HPLC chromatogram of 30% ethanol in phosphate buffer saline pH 7.4

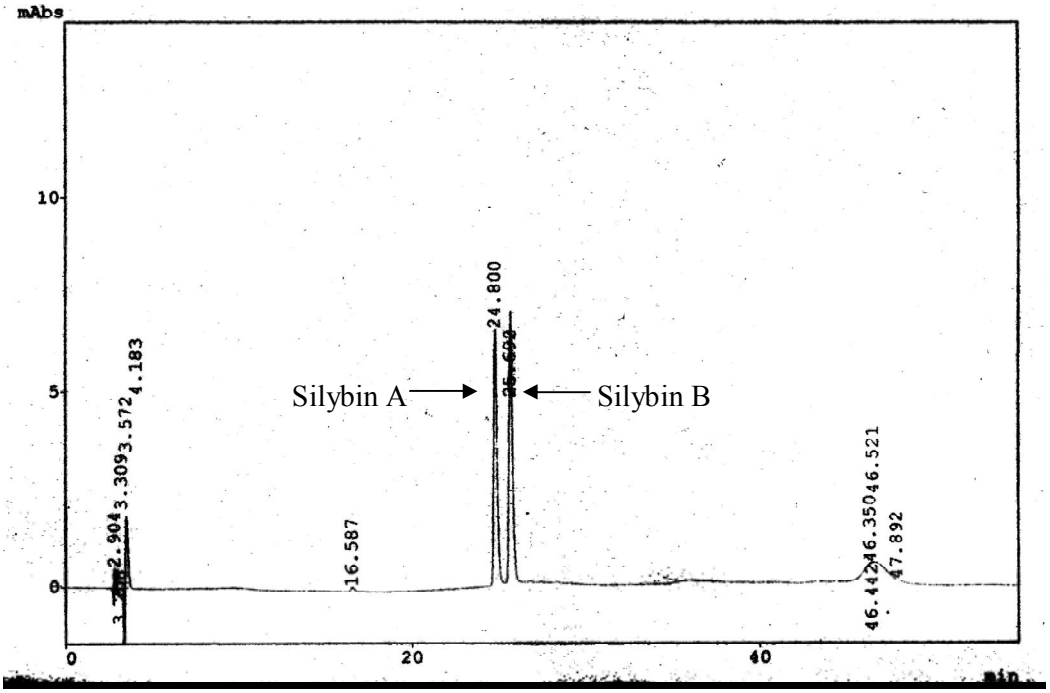

Figure 32: HPLC chromatogram of silybin standard solution

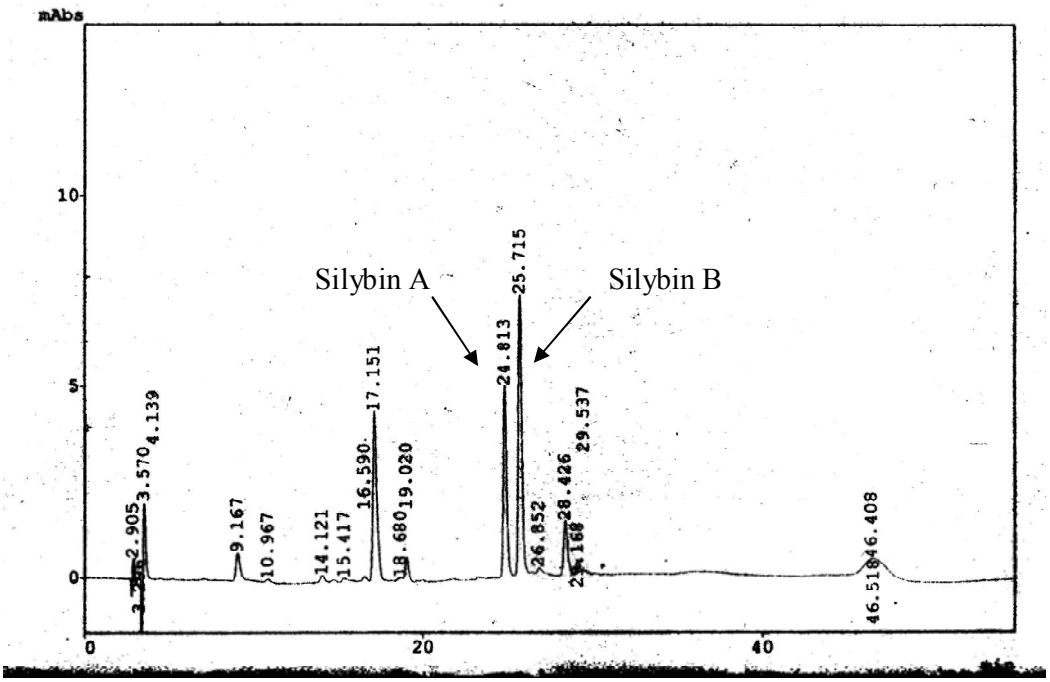

Figure 33: HPLC chromatogram of silymarin solution

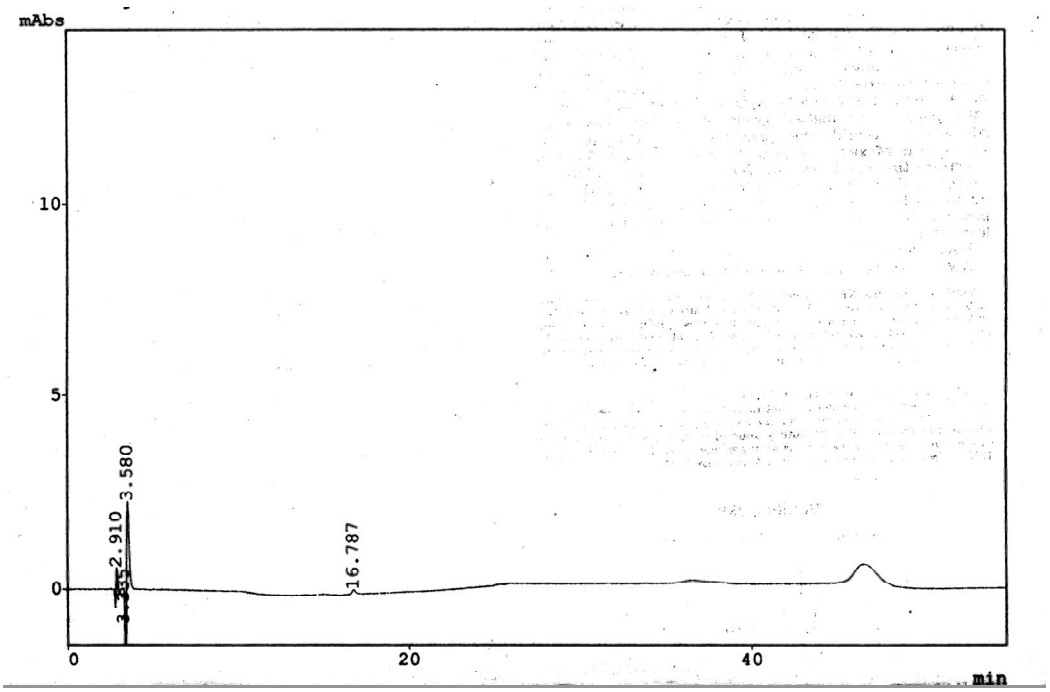

Figure 34: HPLC chromatogram of blank microemulsion (GT10)

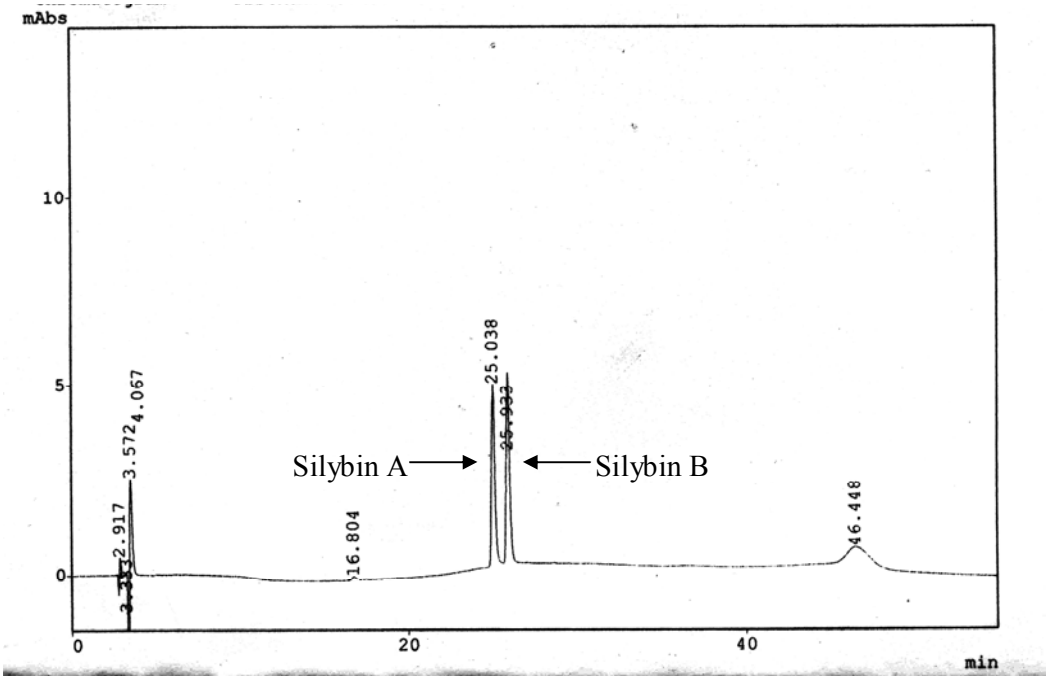

Figure 35: HPLC chromatogram of silybin in microemulsion (GT10)

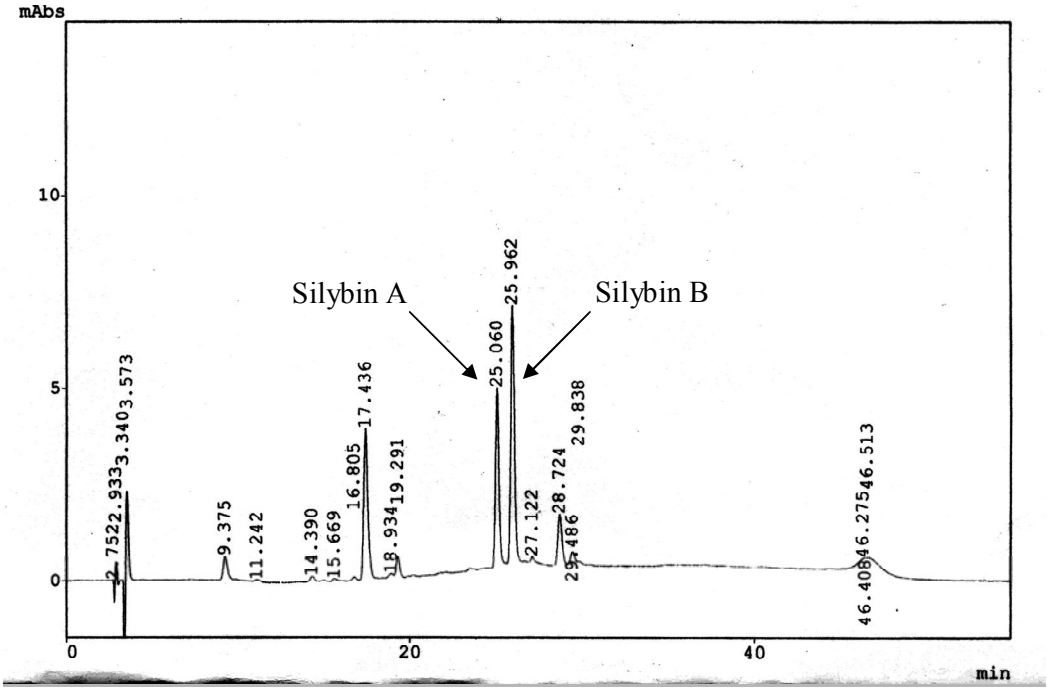

Figure 36: HPLC chromatogram of silymarin in microemulsion (GT10)

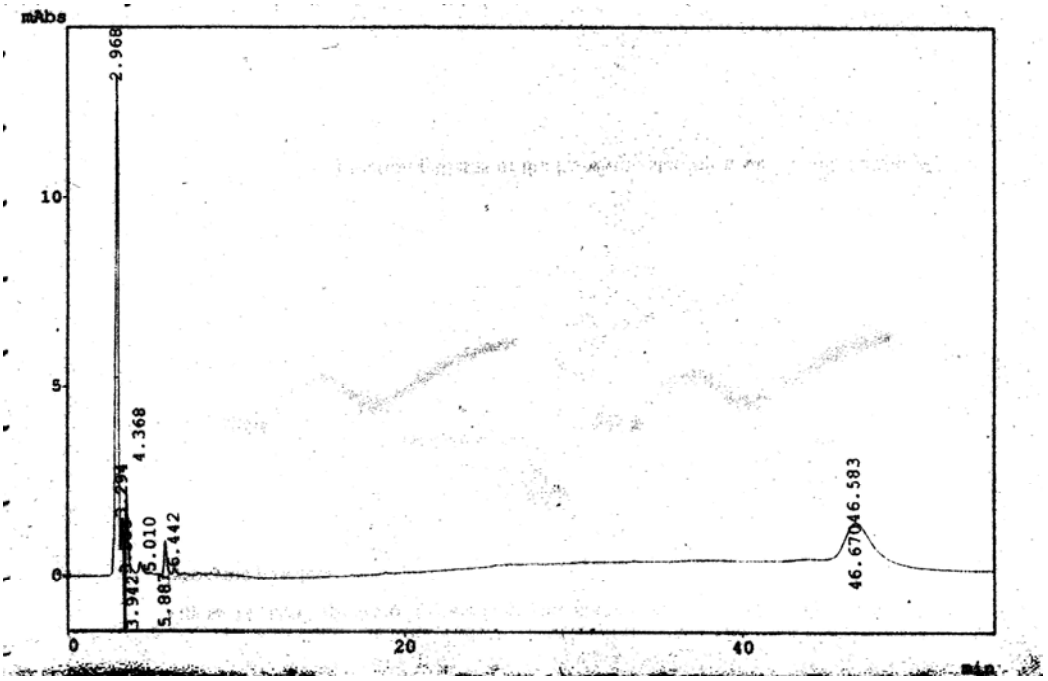

Figure 37: HPLC chromatogram of blank skin extract

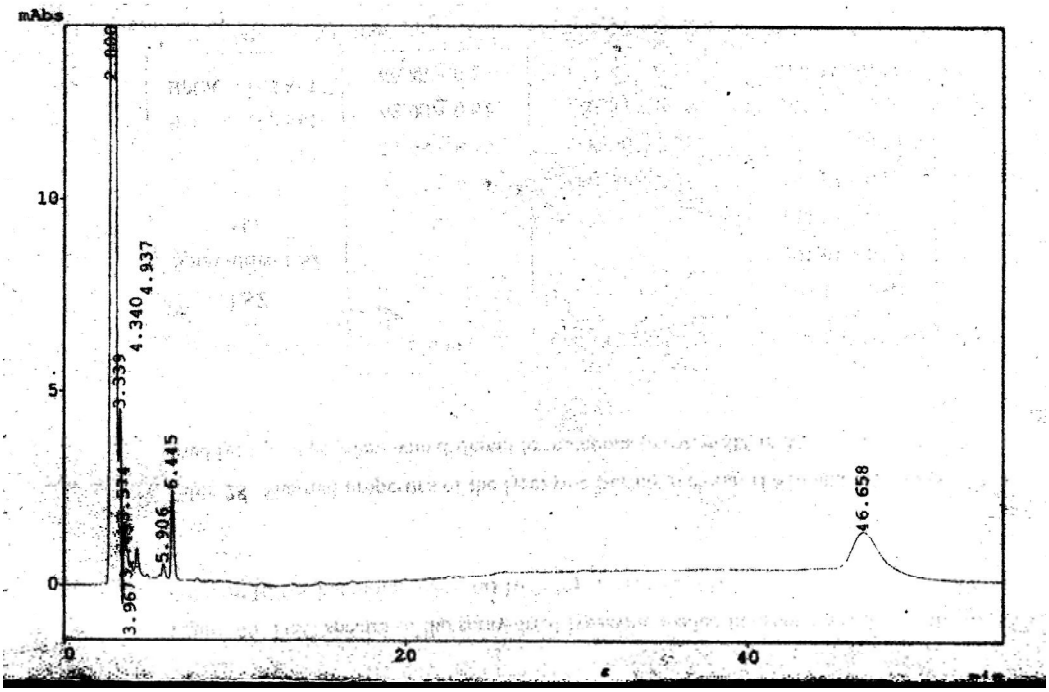

Figure 38: HPLC chromatogram of blank receiver fluid

1.2 Linearity

Linearity of an analytical method is its ability, within a given range, to obtain test results which are directly, or by a mathematical transformation, proportional to the concentration of analyte in the sample.

The representative calibration curve data of silybin standard solutions are shown in Table 11. The plot of silybin concentrations versus the peak area of silybin (Figure 39) displayed the linear correlation in the concentration rage of 4-20 µg/mL. The coefficient of determination (R^2) was 0.9996. These results indicated that the HPLC method was acceptable for quantitative analysis of silybin in the studied range.

Table 11: The calibration curve data of silybin by HPLC method

Concentration	Sum of silybin A and B peak area					
(µg/mL)	Set 1	Set 2	Set 3	Mean	SD	%CV
4	86605	88879	88654	88103.3552	1253.1516	1.4233
8	185313	179852	184108	183090.7937	2868.8700	1.5669
12	269800	269299	268207	269102.0791	814.2417	0.3026
14	323851	323201	316263	321536.7365	4205.6188	1.3097
16	371265	374854	362097	369405.2697	6578.7445	1.7809
20	463749	462507	461655	462643.3908	1053.2248	0.2277

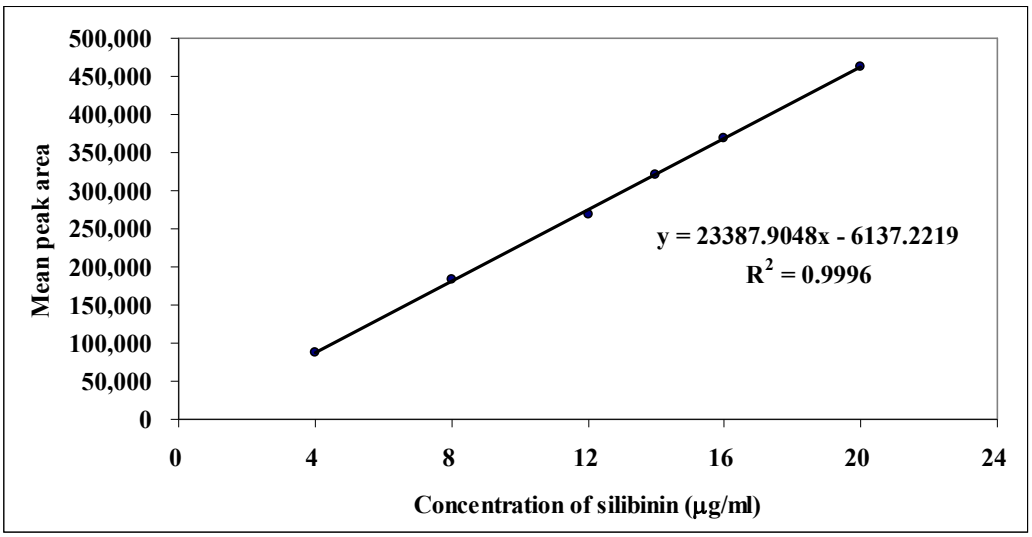

Figure 39: Calibration curve of silybin by HPLC method

1.3 Accuracy

The accuracy of an analytical method expresses the closeness of agreement between the value which is accepted either as a conventional true value or an accepted reference value and the value found. The accuracy assesses using 3 concentration levels covering the specified range.

The percentages of analytical recovery were in the rage of 99.45-101.95% (Table 12), indicated that this HPLC method could be used for silybin analysis in the studied range with a high accuracy.

Table 12: The percentage of analytical recovery of silybin by HPLC method

Concentration (µg/mL)	%Analytical recovery					Mean ± SD
	Set 1	Set 2	Set 3	Set 4	Set 5	
6	100.23	101.28	101.72	100.78	101.64	101.13±0.63
10	100.64	99.58	101.03	101.45	101.95	100.93±0.90
18	100.49	100.07	99.79	99.45	101.62	100.29±0.84

1.4 Precision

The precision of an analytical method expresses the closeness of agreement between a series of measurements obtained from multiple sampling of the same homogeneous sample under the prescribed conditions. The precision assesses using 3 concentration levels covering the specified range.

The precision were determined both within run and between run, which were expressed as the coefficient of variation (%CV) in Tables 13 and 14. The coefficient of variation values of within run and between run were in range of 0.62-0.89% and 0.85-1.37%, respectively. This indicated that this HPLC method was precise for silybin analysis in the studied range.

Table 13: Data of within run precision by HPLC method

Concentration (µg/mL)	Inversely estimated concentration (µg/mL)					Mean	SD	%CV
	Set 1	Set 2	Set 3	Set 4	Set 5			
6	6.0136	6.0766	6.1033	6.0466	6.0982	6.0676	0.0376	0.6198
10	10.0656	9.9596	10.1038	10.1460	10.1960	10.0942	0.0896	0.8874
18	18.0900	18.0145	17.9640	17.9028	18.2922	18.0527	0.1504	0.8333

Table 14: Data for between run precision by HPLC method

Concentration (µg/mL)	Inversely estimated concentration (µg/mL)					Mean	SD	%CV
	Set 1	Set 2	Set 3	Set 4	Set 5			
6	5.9767	5.8987	5.9851	5.8842	6.0572	5.9604	0.0705	1.1820
10	0.1195	10.2366	10.1807	10.0244	10.0635	10.1249	0.0859	0.8480
18	17.8759	18.3178	18.1303	17.6815	17.9096	17.9830	0.2457	1.3665

2. UV-VIS spectroscopic method

The UV-VIS spectroscopy was used to analyze silymarin content for the release study instead of time-consuming HPLC.

2.1 Specificity

The UV absorption spectrum of silymarin standard solution is shown in Figure 40. The amount of silymarin was determined from its maximum absorption at 329 nm.

The spectra of blank microemulsion and silymarin in microemulsion are shown in Figures 41-42. All spectra are shown under the same scale.

There was no interference from microemulsion components in the spectra at 329 nm. Thus, the UV-VIS spectroscopic method was acceptable for specificity.

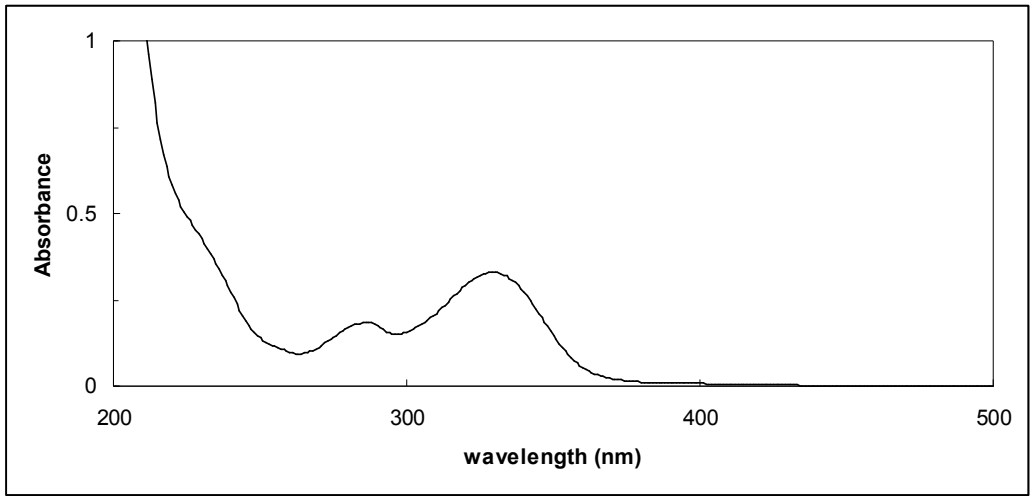

Figure 40: UV spectrum of silymarin standard solution

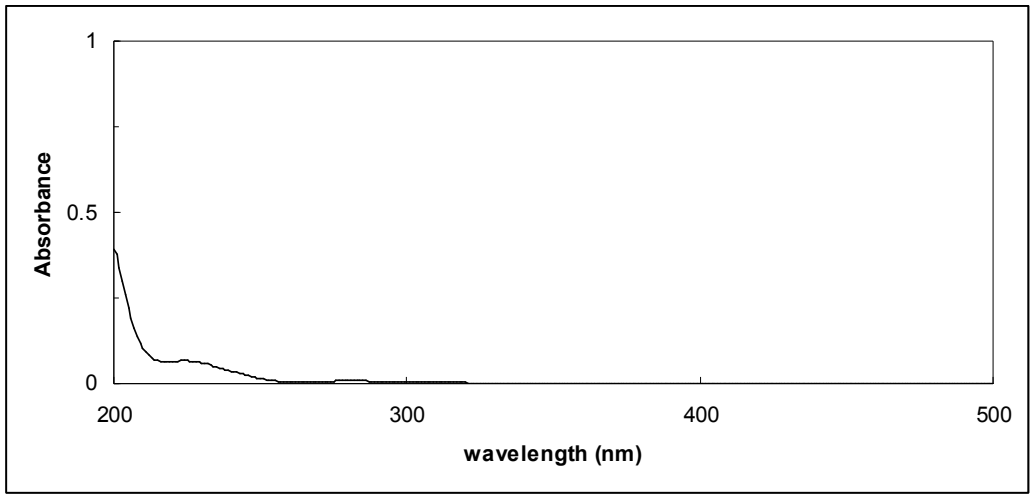

Figure 41: UV spectrum of blank microemulsion (GT10)

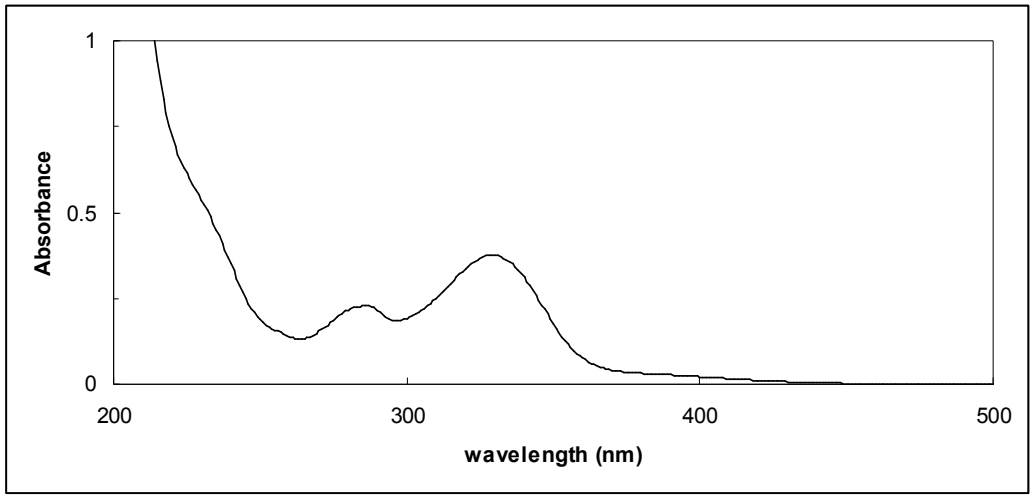

Figure 42: UV spectrum of silymarin in microemulsion (GT10)

2.2 Linearity

The representative calibration curve data of silymarin standard solutions are shown in Table 15. The plot of silymarin concentrations versus the absorbance (Figure 43) displayed the linear correlation in the concentration range of 5-17.5 μg/mL. The coefficient of determination (R^2) was 0.9997. These results indicated that the UV-VIS spectroscopic method was acceptable for quantitative analysis of silymarin in the study range.

Table 15: The calibration curve data of silymarin by UV-VIS spectroscopic method

Concentration (μg/mL)	Absorbance			Mean	SD	%CV
	Set 1	Set 2	Set 3			
5	0.2123	0.2124	0.2140	0.2129	0.0010	0.4517
7.5	0.3247	0.3207	0.3227	0.3227	0.0020	0.6258
10	0.4386	0.4314	0.4349	0.4350	0.0036	0.8347
12.5	0.5485	0.5413	0.5477	0.5459	0.0039	0.7222
15	0.6546	0.6503	0.6629	0.6559	0.0064	0.9768
17.5	0.7686	0.7654	0.7637	0.7659	0.0025	0.3277

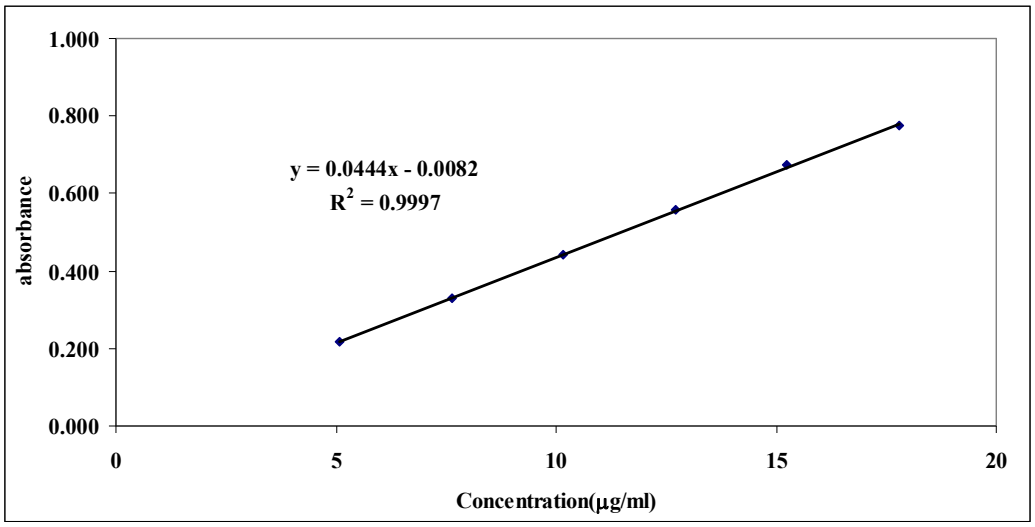

Figure 43: Calibration curve of siymarin by UV-VIS spectroscopic method

2.3 Accuracy

The percentages of analytical recovery in the range of 98.40-101.06% (Table 16), indicated that this UV-VIS spectroscopic method could be used for silymarin analysis in the range with a high accuracy.

Table 16: The percentage of analytical recovery of silymarin by UV-VIS spectroscopic method

Concentration (μg/mL)	%Analytical recovery					Mean± SD
	Set 1	Set 2	Set 3	Set 4	Set 5	
6.5	99.12	99.01	99.37	99.12	99.52	99.3355±0.2000
11.5	98.81	100.88	100.54	99.26	101.06	100.2847± 0.9293
16.5	98.70	98.15	99.92	98.40	99.66	99.3283± 0.8108

2.4 Precision

The precision were determined both within run and between run, which were expressed as the coefficient of variation (%CV) in Tables 17 and 18. The coefficient of variation values of within run and between run were in range of 0.20-0.93% and 1.11-1.73%, respectively. This indicated that this UV-VIS spectroscopic method was precise for silymarin analysis in the studied range.

Table 17: Data of within run precision by UV-VIS spectroscopic method

Concentration (μg/mL)	Inversely estimated concentration (□g/mL)					Mean	SD	%CV
	Set 1	Set 2	Set 3	Set 4	Set 5			
6.5	6.4108	6.4038	6.4271	6.4108	6.4365	6.4248	0.0130	0.2024
11.5	11.3310	11.5692	11.5295	11.3824	11.5902	11.5007	0.1069	0.9292
16.5	16.2536	16.1625	16.4544	16.2046	16.4124	16.3571	0.1338	0.8179

Table 18: Data of between run precision by UV-VIS spectroscopic method

Concentration (μg/mL)	Inversely estimated concentration (□g/mL)					Mean	SD	%CV
	Set 1	Set 2	Set 3	Set 4	Set 5			
6.5	6.4365	6.5711	6.4781	6.6051	6.4815	6.5216	0.0724	1.1100
11.5	11.5902	11.8101	11.4260	11.6962	11.5512	11.5578	0.1352	1.1701
16.5	16.4124	16.5591	16.1566	16.7221	16.3951	16.4246	0.2839	1.7285

CHAPTER V

CONCLUSIONS

This present study was aimed to develop silymarin-loaded microemulsions for skin delivery. Firstly, the pseudo-ternary phase diagrams were constructed by water titration method. Then, microemulsion formulations were characterized and o/w microemulsions were selected from each pseudo-ternary phase diagrams. These selected o/w microemulsions were loaded with 2% w/w silymarin and then the stability, the release property, and the permeability were evaluated. The results of the investigations can be concluded as follows:

1. The pseudo-ternary phase diagrams

In compositions using glyceryl monooleate or oleic acid with high HLB surfactant mixtures (e.g. Tween 20® : HCO-40® or Labrasol® : HCO-40® in the 1:1 ratio) showed higher solubilizaing power than low HLB surfactant mixture (e.g. Span 20® : HCO-40® in the 1:1 ratio). In the contrary the compositions using ethyl oleate and isopropyl myristate with low HLB surfactant mixture showed higher solubilizing power than high HLB surfactant mixtures by comparing the isotropic region of each pseudo-ternary phase diagrams.

2. Characterization of microemulsions

Microemulsion formulations along the line which kept the surfactant concentration constant and varied the water concentrations in 4% interval were transparent liquid without phase separation. In all system, the conductivities increase together with the water content. A drastic increase in conductivity could not be observed, although the peak points were found in some viscosity-water content profiles which may be used to indicate the transformation of the microemulsion systems. So, dilution technique was used to ensure the microemulsion type and o/w microemulsions were selected from each pseudo-ternary phase diagrams.

3. Stability of silymarin microemulsions

All selected o/w microemulsions which were loaded with 2% w/w silymarin presented considerably physical stable after six heating cooling cycles. However, chemical instability in terms of silybin content was discovered when stored in acceleration condition (40°C) for 6 months. Silymarin may be protected from oxidation by solubilization in the surfactant film. The percentages of silybin remainings were sequenced in the order of surfactants: Labrasol® > Tween 20® > Span 20® (as HCO-40® was used in every formulation).

4. In vitro release study of silymarin microemulsions

Silymarin microemulsions showed the prolong release when compared to its solution (40% ethanol in phosphate buffer saline pH 7.4). All silymarin release profiles showed the best fit with Higuchi kinetics which can imply that the rate-limiting step may be the diffusion of silymarin from oil droplet.

5. In vitro skin permeation study of silymarin microemulsions

In all formulations, silybin could not be detected in the concentrated receiver fluid. The percentages of silybin remainings in skin extracts from silymarin microemulsions were not significantly different, except for the solution (40% ethanol in phosphate buffer saline pH 7.4) which significantly higher than microemulsions. However, alcohol solutions are still not suitable for skin delivery due to their skin irritation.

For further studies, the permeation study in occlusive condition should be performed comparing to this non-occlusive condition, as well as in vivo studies of efficacy and skin irritation of silymarin microemulsions.

REFERENCES

Afaq, F., Adhami, V.M., Ahmad, N., and Mukhtar, H. 2002. Botanical antioxidants for chemoprevention of photocarcinogenesis. Frontiers in Bioscience. 7: 784-792.

Alany, R.G., Tucker, I.G., Davies, N.M., and Rades, T. 2001. Characterizing colloidal structures of pseudoternary phase diagrams formed by oil/water/amphiphile systems. Drug Development and Industrial Pharmacy. 27(1): 31-38.

Attwood, D. 1994. Microemulsion. In J. Kreuter (ed), Colloidal drug delivery systems, pp.31-71. New York: Marcel Dekker, INC.

Barry, B. 2002. Transdermal drug delivery. In M.E. Aulton. (ed.), Pharmaceutics – The science of dosage form design, pp. 499-533. London: Churchilll Livingstone.

Barry, B.W. 1987. Mode of action of penetration enhancers in human skin. Journal of Controlled Release. 6: 85-97.

Bonne, C., Sincholle, D. 1988. Cosmetic preparations useful for opposing skin aging containing an extract of the fruits of *Silybum marianum*. United States Patent. Patent number: 4,749,573.

Boonme, P., Krauel, K., Graf, A., Thomas, R., and Junyaprasert, V.B. 2006. Characterization of microemulsion structures in the pseudoternary phase diagram of isopropyl palmitate/water/Brij 97:1-butanol. AAPS Pharmaceutical Sciences Technology. 7(2): E1-6.

Cilurzo, F., Minghetti, P., and Sinico, C. 2007. Newborn pig skin as model membrane in In vitro drug permeation studies: a technical note. AASP Pharmaceutical Sciences Technology. 8(4): E1-4.

Date, A., Naik, B., and Nagarsenker, M. S. 2006. Novel drug delivery systems: potential in improving topical delivery of antiacne agents. Skin Pharmacology and Physiology. 19: 2–16.

Department of Environment and Conservation, Western Australian Herbarium. Florabase: the Western Australian Flora[Online]. Available from: http://florabase.calm.wa.gov.au/ browse/profile/8227[2009, August 1]

Djordjevic, L., Primorac, M., Stupar, M., and Krajisnik, D. 2004. Characterization of caprylocaproyl macrogolglycerides based microemulsion drug delivery

vehicles for an amphiphilic drug. International Journal of Pharmaceutics. 271: 11–19.

El-Samaligy, M.S., Afifi, N.N., Mahmoud, E.A. 2006. Increasing bioavailability of silymarin using a buccal liposomal delivery system: Preparation and experimental design investigation. International Journal of Pharmaceutics. 308: 140-148.

Fisher, G. J., et al. 1996. Molecular basis of sun-induced premature skin ageing and retinoid antagonism. Nature. 379: 335-339.

Flora delaterre: the plant detective[Online]. Available from: http://www.flora delaterre .com/?id=49[2009, August 1]

Flora of North America[Online]. Available from: http://www.efloras.org/florataxon.aspx?flora_id=1&taxon_id=200024549[2009, August 1]

Frank, R., de Gruijl, and Jan, C. van der Leun. 2002. Ozone depletion and ultraviolet radiation. In M. McCally. (ed), Life support – The environment and human health, pp. 135-146. Massachusetts: The MIT Press.

Garti, N., and Aserin, A. 2006. Microemulsion for solubilization and delivery of nutraceuticals and drugs. In S. Benita (ed), Microencapsulation - Methods and industrial applications, pp.345-428. New York: CRC Press.

Garti, N., Spernath, A., Aserin, A., and Lutz, R. 2005. Nano-sized self-assemblies of nonionic surfactants as solubilization reservoirs and microreactors for food systems. Soft Matter. 1: 206-218.

Georges, J., Chen, J.W. 1986. Microemulsions studies: Correlation between viscosity, electrical conductivity and electrochemical and fluorescent probe measurements. Colloid and Polymer science. 2664: 896-902.

Gupta, S., Moulik, S.P. 2008. Biocompatible microemulsions and their prospective uses in drug delivery. Journal of Pharmaceutical sciences. 97(1): 22-45.

Guy, R.H., Hadgraft, J., Kellaway, I.W., and Taylor, M.J. 1982. Calculations of drug release rates from spherical particles. International Journal of Pharmaceutics. 11: 199-207.

Hammond, S. A., Tsonis, C., Sellins, K., Rushlow, K., Scharton-Kersten, T., Colditz, I., Glenn, G.M. 2000. Transcutaneous immunization of domestic animals: opportunities and challenges. Advanced Drug Delivery Reviews. 43: 45-55.

Hire, N.N., Gudsoorkar, V.R., Bhise, K.S., Upasani, C.D., Nandgude, T.D., and Dalvi H. 2007. Microparticulate drug delivery system for topical administration of itraconazole. Asian Journal of Pharmaceutics. 1(1): 83-88.

Ho, H., Hsiao, C.,and Sheu, M. 1996. Preparation of microemulsions using polyglycerol fatty acid esters as surfactant for the delivery of protein drugs. Journal of Pharmaceutical Sciences. 85(2): 138-143.

Huang, Y.B., Lin, Y.H., Lu, T.M., Wang, R.J., Tsai, Y.H., Wu, P.C. 2008. Transdermal delivery of capsaicin derivative-sodium nonivamide acetate using microeulsions as vehicles. International Journal of Pharmaceutics. 349: 206-211.

Junyaprasert, V.B., Boonme, P., Songkro, S., Krauel, K., Rades, T. 2007. Transdermal delivery of hydrophobic and hydrophilic local anesthetics from o/w and w/o Brij 97-based microemulsions. Journal of Pharmacy and Pharmaceutical Sciences. 10(3): 288-298.

Katiyar, S.K. 2002. Treatment of silymarin, a plant flavonoid, prevents ultraviolet light-induced immune suppression and oxidative stress in mouse skin. International Journal of Oncology. 21: 1213-1222.

Katiyar, S.K., Korman, N.J., Mukhtar, H., and Agarwal, R. 1997. Protective effects of silymarin against photocarcinogenesis in a mouse skin model. Journal of the National Cancer Institute. 89(8): 556-565.

Katiyar, S.K., Meleth, S., Sharma, S.D. 2008. Silymarin, a flavonoid from milk thistle (Silybum marianum L.), inhibits UV-induced oxidative stress through targeting infiltrating CD11b(+) cells in mouse skin. Photochemistry and photobiology. 84(2): 266-271.

Kogan, A., Aserin, A., Garti, N. 2007. Improved solubilization of carbamazepine and structural transitions in nonionic microemulsions upon aqueous phase dilution. Journal of Colloid and Interface Science. 315: 637-647.

Kreilgaard, M. 2002. Influence of microemulsions on cutaneous drug delivery. Advanced Drug Delivery Reviews. 54(suppl.1): S77-S98.

Křen, V., and Walterová, D. 2005. Silybin and silymarin - new effects and applications. Biomedical papers of the Medical Faculty of the University Palacký, Olomouc, Czechoslovakia. 149(1): 29-41.

Kumar, P., Mital, K.L. 1999. Handbook of Microemulsion- Science and technology. New York: Marcel Dekker.

Lawrence, M.J., and Rees, G.D. 2000. Microemulsion-based media as novel drug delivery systems. Advanced Drug Delivery Reviews. 45: 89-121.

Lee, J., Lee, Y., Kim, J., Yoon, M., and Choi, Y.W. 2005. Formulation of microemulsion systems for transdermal delivery of aceclofenac. Archives of Pharmacal Research. 28(9): 1097-1102.

Liu, H., Li, S., Wang, Y., Han, F., and Dong, Y. 2006. Bicontinuous water-AOT/Tween 85-isopropyl myristate microemulsion: a new vehicle for transdral delivery of cyclosporin A. Drug Development and Industrial Pharmacy. 32: 549-557.

Lui, L., Pang. X., Zhang, W., and Wang, S. 2007. Formulation design and in vitro evaluation of silymarin-loaded self-microemulsifying drug deliver systems. Asian Journal of Pharmaceutical Sciences. 2(4): 150-160.

Malmsten, M. 2002. Surfactants and polymers in drug delivery. New York: Marcel Dekker, INC.

Meeran, S.M., Katiyar, S., Elmets, C.A. and Katiyar, S.K. 2006. Silymarin inhibits UV radiation-induced immunosuppression through augmentation of interleukin-12 in mice. Molecular cancer therapeutics. 5(7): 1660-1668.

Mehta, S.K., Kaur, G., Mutneja, R., Bhasin, K.K. 2009. Solublization, microstructure, and thermodynamics of fully dilutable U-type Brij microemulsion. Journal of Colloid and Interface Science. 338: 542-549.

Mo, C., Zhong, M., Zhong, Q. 2000. Investigation of structure and structural transition in microemulsion systems of sodium dodecyl sulfonate + n-heptane + n-butanol + water by cyclic voltammetric and electrical conductivity measurements. Journal of Electroanalytical Chemistry. 493: 100-107.

Montenegro, L., Carbone, C., Condorelli, G., Drago, R. and Puglisi, G. 2006. Effect of oil phase lipophilicity on in vitro drug release from o/w microemulsions with low surfactant content. Drug Delvelopment and Industrial Pharmacy. 32: 539-548.

Moulik, S.P., and Paul, B.K. 1998. Structure, dynamics and transport properties of microemulsions. Advances in Colloid and Interface Science. 78: 95-195.

Nield, G.L., Ippersiel, R. Open evaluation of silymarin cream in the management of facila redness associated with rosacea[Online]. Available form: http://www.canderm.com/files/Canderm/aRosacure_Dr_Nield_paper.pdf [2009, August 1]

Pietta, P. 2000. Flavonoids as antioxidants. Journal of Natural Products. 63: 1035-1042.

Pinnell, S.R. 2003. Cutaneous photodamage, oxidative stress, and topical antioxidant protection. Journal of the American Academy of Dermatology. 48(1): 1-19.

Podlogar, F., Gašperlin, M., Tomšič, M., Jamnik, A., and Rogač, M.B. 2004. Structural characterization of water-Tween 40®/ Imwitor 308®-isopropyl myristate microemulsions using different experimental methods. International Journal of Pharmaceutics 276: 115-128.

Saller, R., Melzer, J., Reichling, J., Brignoli, R., and Meier, R. 2007. An updated systematic review of the pharmacology of silymarin. Forsch Komplementärmed. 14: 70–80.

Santos, P., Watkinson, A.C., Hadgraft, J., and Lane, M.E. 2008. Application of microemulsions in dermal and transdermal drug delivery. Skin Pharmacology and Physiology. 21: 246-259.

Shinoda, K., Kunieda, H., Arai, T., and Saijo, H. 1984. Principles of attaining very large solubilization (microemulsion): inclusive understanding of the solubilization of oil and water in aqueous and hydrocarbon media. The Journal of Physical Chemistry. 88: 5126-5129.

Sintov, A.C., Shapiro, L. 2004. New microemulsion vehicle facilitates percutaneous penetration in vitro and cutaneous drug bioavialbility in vivo. Journal of Controlled Release. 95: 173-183.

Špiclin, P., Gašperlin, M., Kmetec, V. 2001. Stability of ascorbyl palmitate in topical microemulsions. Internal Journal of Pharmaceutics. 222: 271-279.

Špiclin, P., Homar, M. Zupančič-Valant, A., and Gašperlin, M. 2003. Sodium ascorbyl phosphate in topical microemulsions. International Journal of Pharmaceutics. 256: 65-73.

Svobodová, A., et al. 2007a. Attenuation of UVA-induced damage to human keratinocytes by silymarin. Journal of Dermatological Science. 46: 21-30.

Svobodová, A., Walterová, D., and Psotová, J. 2006. Influence of silymarin and its falvonolignans on H_2O_2-induced oxidative stress in human keratinocytes and mouse fibroblasts. Burns. 32: 973-979.

Svobodová, A., Zdařilová, A., Walterová, D., and Vostálova, J. 2007b. Flavonolignans from *Silybum marianum* moderate UVA-induced oxidative

damage to HaCaT keratinocytes. Journal of Dermatological Science. 48: 213-224.

Swarbrick, J., and Boylan, J.C. 1994. Encyclopedia of pharmaceutical technology vol. 9, New York: Marcel Dekker, INC.

Szekeres, E., Acosta, E., Sabatini, D.A., Harwell, J.H. 2006. Modeling solubilization of oil mixtures in anionic microemulsions II. Mixtures of polar and non-polar oils. Journal of Colloid and Interface Science. 294: 222-233.

The European agency for the evaluation of medicinal products, Human medicines evaluation unit. ICH Topic Q 1 A (R2) - Stability testing guidelines: stability testing of new drug substances and products[Online]. Available from: http://www.ich.org/cache/compo/363-272-1.html[2009, August 1].

The European agency for the evaluation of medicinal products, Human medicines evaluation unit. ICH Topic Q 2 (R1) – Validation of analytical procedures: text and methodology[Online]. Available from: http://www.ich.org/cache/compo/363-272-1.html[2009, August 1]

The United States Pharmacopeia 30 and the National Formulary 25. 2007. Washington D.C.: The United States Pharmacopeia Convention.

Thevenin, M.A., Grossiord, J.L., Poelman, M.C. 1996. Sucrose esters/cosurfactant microemulsion systems for transdermal delivery: assessment of bicontinuous structures. International Journal of Pharmaceutics. 137: 177-186.

Trotta, M. 1999. Influence of phase transformation on indomethacin release from microemulsions. Journal of Controlled Release. 60: 399-405.

United States Department of Agriculture, Agricultural Research Service, Beltsville Area. GRIN Taxonomy of Plants[Online]. Available from: http://www.ars-grin.gov/cgi-bin/npgs/html/taxon.pl?33952[2009, August 1]

Vicentini, F.T.M.C., Simi, T.R.M., Del Ciampo, J.O., Wolga, N.O., Pitol, D.L., Iyomasa, M.M., Bentley, M.V.L.B., Fonseca, M.J.V. 2008. Quercetin in w/o microemulsion: in vitro and in vivo skin penetration and efficacy against UVB-induced skin damages evaluation in vivo. European Journal of Pharmaceutics and Biopharmaceutics. 69: 948-957.

William, A. 2003. Transdermal and topical drug delivery. London: Pharmaceutical press.

Woo, J.S., Kim, T., Park, J., Chi, S. 2007. Formulation and biopharmaceutical evaluation of silymarin Using SMEDDS. Archives of Pharmacal Research. 30(1): 82-89.

Written findings of the state noxious weed control board – class A weed[Online]. Available from: http://www.nwcb.wa.gov/weed_info/Written_findings/Silybum_marianum.html[2009, August 1]

Wynn, S.G. *Silibum marianum*: Milk thistle[Online]. Available from: http://talkoftheinternet.com/etvma2/milk-thistle.pdf[2009, August 1]

Xu, X., Wang, Y., Constantinou, A.I., Stacewicz-Sapuntzakis, M., Bowen, P.E., and van Breemen, R.B. 1999. Solubilization and stabilization of carotenoids using micelles: delivery of lycopene to cells in culture. Lipid. 34(10): 1031-1036.

Yang, B., Kotani, A., Arai, K., Kusu, F. 2001. Estimation of the antioxidant activities of flavonoids from their oxidation potentials. Analytical Sciences. 17: 599-604.

Yang, S., Washington, C. 2006. Drug release from microparticulate systems. In S. Benita (ed), Microencapsulation - Methods and industrial applications, pp.183-212. New York: CRC Press.

Yuan, Y., Li, S., Mo, F., Zhong, D. 2006. Investigation of microemulsion system for transdermal delivery of meloxicam. International Journal of Pharmaceutics. 321: 117-123.

Zhao, J., Lahiri-Chatterjee, M., Sharma, Y., Agarwal, R. 2000. Inhibitory effect of a flavonoid antioxidant silymarin on benzoyl peroxide-induced tumor promotion, oxidative stress, and inflammatory responses in SENCAR mouse skin. Carcinogenesis. 21(4): 811-816.

APPENDICES

APPENDIX A

Descriptions of chemicals used in microemulsion formulation

Oleic acid

Synonyms: Oleic acid (USPNF, BP), Acidum oleicum (PhEur), Elaic acid, Oleinic acid

Chemical name: (Z)-9-Octadecenoic acid

Empicial formula: $C_{18}H_{34}O_2$ **Molecular weight**: 282.47

Structure formula:

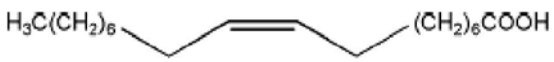

Appearance: Oleic acid occurs as a yellowish to pale brown, oily liquid with a characteristic lard-like odor and taste.

Typical properties:

Density: 0.895 g/cm^3

Reflective index: 1.4585

Solubility: Miscible with benzene, chloroform, ethanol (95%), ether, hexane, and fixed and volatile oils; practically insoluble in water.

Functional category: Emulsifying agent, skin penetrant.

Safety: Oleic acid is used in oral and topical pharmaceutical formulations. *In vitro* tests have shown that oleic acid causes rupture of red blood cells (hemolysis), and intravenous injection or ingestion of a large quantity of oleic acid can therefore be harmful. Oleic acid is a moderate skin irritant; it should not be used in eye preparation.

Glyceryl monooleate

Synonyms: Glyceryl monooleate (USPNF), Glycerol mono-oleates (BP), Glyceroli mono-oleates (PhEur), Glycerol-1-oleate, Monoolein

Chemical name: (Z)-9-Octadecenoic acid, monoester with 1,2,3-propanetriol

Empirical formula: $C_{21}H_{40}O_4$ **Molecular weight**: 356.55

Structural formula:

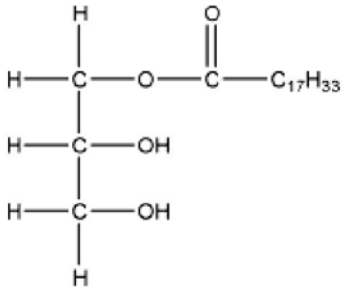

Appearance: Glyceryl monooleates occur as amber oily liquids, which may be partially solidified at room temperature and have a characteristic odor.

Typical properties:

Density: 0.942 g/cm^3

Refractive index: 1.4626

Solubility: Soluble in chloroform, ethanol (95%), ether, mineral oil and vegetable oils; practically insoluble in water.

Functional category: Bioadhesive, emollient, emulsifying agent, emulsion stabilizer.

Safety: Glyceryl monooleate is used in oral and topical pharmaceutical formulations and is generally regarded as a relatively non irritant and nontoxic excipient.

Ethyl oleate

Synonym: Ethyl oleate (BP, USPNF), Ethylis oleas (PhEur).

Chemical name: (Z)-9-Octadecenoic acid, ethyl ester

Empirical formula: $C_{20}H_{38}O_2$ **Molecular weight**: 310.51

Structural formula:

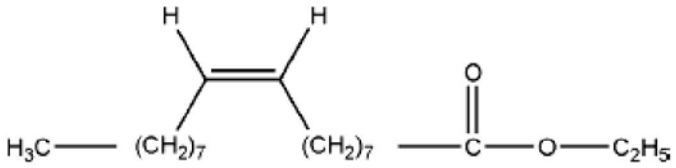

Appearance: Ethyl oleate occurs as pale yellow to almost colorless, mobile, oily liquid with a taste resembling that of olive oil and a slight, but not rancid odor.

Typical properties:

Density: 0.87 g/cm^3

Refractive index: 1.451

Solubility: Miscible with chloroform, ethanol (95%), ether, fixed oils, liquid paraffin, and most other organic solvents; practically insoluble in water.

Functional category: Oleaginous vehicle, solvent.

Safety: Ethyl oleate is generally considered to be of low toxicity but ingestion should be avoided. Ethyl oleate has been found to cause minimal tissue irritation.

Isopropyl myristate

Synonym: Isopropyl myristate (BP, USPNF), Isopropylis myristas (PhEur)

Chemical name: 1-Methylethyl tetradecanoate

Empirical formula: $C_{17}H_{34}O_2$ **Molecular weight**: 270.5

Structural formula:

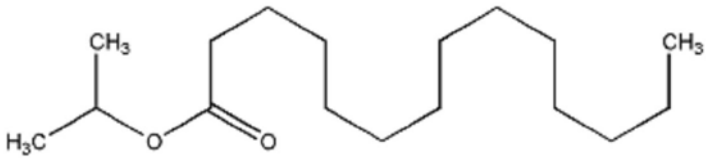

Appearance: Isopropyl myristate is a clear, colorless, practically odorless liquid.

Typical properties:

Density: 0.85 g/cm^3

Refractive index: 1.434

Solubility: Soluble in acetone, chloroform, ethanol (95%), ethyl acetate, fats, fatty alcohol, fixed oils, liquid hydrocarbons, toluene, and waxes; practically insoluble in glycerin, glycols, and water.

Functional category: Emollient, oleaginous vehicle, skin penetrant, solvent

Safety: Isopropyl myristate is widely used in cosmetics and topical pharmaceutical formulations and is generally regarded as a nontoxic and nonirritant material.

Diethylene glycol monoethyl ether (Transcutol® CG)

Synonym: Diethylene glycol monoethyl ether (USPNF), 2-(2-ethoxyethoxy) ethanol, ethyldiglycol ether, ethoxydiglycol

Empirical formula: $C_6H_{14}O_3$ **Molecular weight**: 134.18

Structural formula:

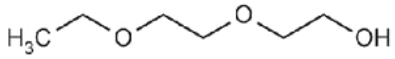

Appearance: Diethylene glycol monoethyl ether is a clear, transparent liquid with a light odor.

Typical properties:

Density: 0.989 g/cm^3

Refractive index: 1.425 – 1.429

Solubility: Soluble in water, ethanol, hexylene glycol, and propylene glycol; practically soluble in vegetable oils; insoluble in mineral oils.

Functional category: solubilizing agent, penetrant

Safety: Diethylene glycol monoethyl ether is a safe material. It has been using in a wide variety of skin care products and topical drug delivery systems.

Polyoxyl 40 hydrogenated castor oil (HCO-40®)

Synonym: Polyoxyl 40 hydrogenated castor oil (USPNF), Hydrogenated polyoxyl castor oil (BP), Macrogolglyceroli hydroxysteras (PhEur), POE-40 hydrogenated castor oil, PEG-40 hydrogenated castor oil

Empirical formula: Polyoxyethylene castor oil derivatives are complex mixtures of various hydrophobic and hydrophilic components. Members within each range have different degrees of ethoxylation (moles)/ PEG units as indicated by their numerical suffix (n). The chemical structures of the polyethoxylated hydrogenated castor oils are analogues to polyethoxylated castor oils with the exception that the double bond in the fatty acid chain has been saturated by hydrogenation.

Polyoxyl 40 hydrogenated castor oil; approximately 75% of the components of mixture are hydrophobic. These comprise mainly fatty acid esters of glycerol polyethylene glycol and fatty acid esters of polyethylene glycol. The hydrophilic portion consists of polyethylene glycols and glycerol ethoxylates.

Appearance: Polyoxyl 40 hydrogenated castor oil occurs as a white to yellowish, semisolid paste at 20°C that liquefied at 30°C. It has a very faint characteristic odor and almost tasteless in aqueous solution.

Typical properties:

Density: -

Refractive index: 1.453 – 1.457

HLB: 12.5

Solubility: Soluble in water, ethanol, 2-propanol, n-propanol, ethyl acetate, chloroform, fatty acids, and fatty alcohol, olive oil; insoluble in mineral oil.

Functional category: Emulsifying agent, solubilizing agent, wetting agent.

Safety: Polyoxyethylene castor oil derivatives are used in a variety of oral, topical, and parenteral pharmaceutical formulations. Acute and chronic toxicity tests in animals have shown polyoxyethylene castor oil derivatives to be essentially nontoxic and nonirritant material. However, several serious anaphylactic reactions, cardiotoxicity, nephrotoxicity, neurotoxicity, and pulmonary toxicity have also been observed in humans and animals following parenteral administration of formulation containint polyoxyethylene castor oil derivative. The precise mechanism of the reaction is not known.

Caprylocaproyl polyoxylglycerides (Labrasol®)

Synonym: Caprylocaproyl polyoxylglycerides (USPNF), Caprylocaproyl macroglycerides (PhEur), PEG-8 caprylocaproyl glycerides

Empical structure: Caprylocaproly polyoxylglycerides are mixtures of monoesters, diesters, and triesters of glycerol and monoesters and diesters of polyethylene glycols with a mean relative molecular weight between 200 and 400. The main fatty acids are caprylic and capric acids.

A: PEG monocaprylate

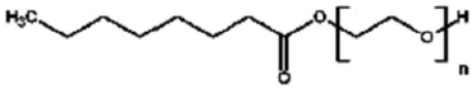

n = 8

B: PEG dicaprylate

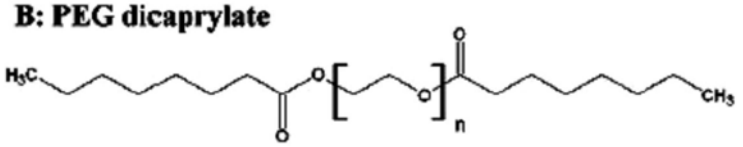

Appearance: Caprylocaproyl polyoxylglycerides occur as a pale-yellow oily liquid, with a characteristic odor.

Typical properties:

Density: about 1.0

Refractive index: about 1.4

HLB: 14

Solubility: Dispersible in hot water, freely soluble in methylene chloride.

Functional category: Solubilizing agent, penetrant, emulsifiying agent

Safety: Labrasol is a novel low irritant surfactant which has been demonstrated to form microemulsions with several non-alcohol cosurfactant. This diminished the risk of cutaneous toxicological reaction by application of topical microemulsion. The ocular irritation studies showed that labrasol at a concentration of 0.5-3.0% v/v was non-irritant, while labrasol produced slight irritation at a conceontration of 5% v/v.

Polysorbate 20 (Tween 20®)

Synonym: Polysorbate 20 (USPNF, BP), Polysorbatum 20 (PhEur)

Chemical name: Polyoxyethylene 20 sorbitan monolaurate

Empirical formula: $C_{58}H_{114}O_{26}$ **Molecular weight**: 1128

Structural formula:

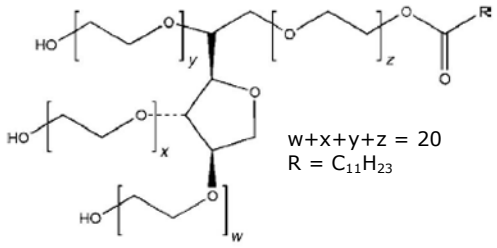

Appearance: Polysorbate 20 occur as a yellow oily liquid, with a characteristic odor.

Typical properties:

Density: 1.11 g/cm^3

Refractive index: 1.468

HLB: 16.7

Solubility: Soluble in water and ethanol; insoluble in vegetable oil and mineral oil.

Functional category: Emulsifying agent, solubilizing agent, wetting agent.

Safety: Polysorbates are widely used in cosmetics, food products, and oral, parenteral, and topical pharmaceutical formulations and are generally regarded as nontoxic and nonirritant materials. However, there have been occasional reports of hypersensitiviy of polysorbates following their topical and intramuscular use. Polysorbates have also been associated with serious adverse effects, including some deaths, in low-birthweight infants intravenously administered a vitamin E preparation containing a mixture of polysorbate 20 and 80. When heated to decomposition, the polysorbates emit acrid smoke and irritating fumes.

Sorbitant monolaurate (Span 20®)

Synonym: Sorbitan monolaurate (USPNF), sorbitan laurate (BP), Sorbitani lauras (PhEur)

Chemical name: Sorbitan monododecanoate

Empirical formula: $C_{18}H_{34}O_6$ Molecular weight: 346

Structural formula:

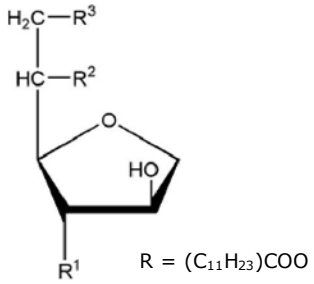

Appearance: Sorbitan monolaurate occur as a yellow viscous liquid, with a distinctive odor and taste.

Typical properties:

Density: 1.01 g/cm^3

Refractive index: 1.474

HLB value: 8.6

Solubility: Generally soluble or dispersible in oils, also soluble in most organic solvents; insoluble in water, but generally dispersible.

Functional category: Emulsifying agent, solubilizing agent, wetting agent

Safety: Sorbitan esters are widely used in cosmetics, food products, and oral and topical pharmaceutical formulations and are generally regarded as nontoxic and nonirritant materials. However, there have been occasional reports of hypersensitive skin reactions following the topical application of products containing sorbitan esters. When heated to decomposition, the sorbitan ester emit acrid smoke and irritating fumes.

APPENDIX B

Saturation solubilities of silymarin in microemulsions

An excess amount of silymarin was added to each microemulsion formulations and shaken using suspension mixture at controlled temperature, 30°C for 6 days. The suspensions were centrifuged at 5,000 rpm for 30 minutes, and then filtered through 0.45 μm membrane filter. Silybin saturated solubility in each microemulsion formulations was determined using an HPLC method and silymarin concentration were then back calculation from silybin content in used silymarin raw material (35.62 ± 0.15%). Three replicates of each experiment were performed.

In case of 40% ethanol in phosphate buffer saline pH 7.4, which use as a solution vehicle for silymarin, the saturation solubility of silymarin in this solution was performed in the same process of microemulsions.

The solubilities of silybin in microemulsions and solution are shown in Table B.1 and the estimated solubility of silymarin in these vehicles are shown in Table B.2.

For release and permeation study, silymarin solution, which had the same thermodynamic activity as silymarin microemulsion, was used. Thus, the percentage of silymarin saturation in microemulsion-loaded 2%w/w was calculated and showed in Table B.3.

Table B.1: The solubility of silybin in microemulsions and solution

Silybin solubility (mg/g)	
GT10	21.22±1.61
GL11	17.57±0.58
GS8	19.07±0.42
OT9	25.11±0.71
OL8	26.30±0.67
OS6	23.99±1.52
ET7	36.31±1.74
EL7	34.51±0.96
IT6	38.06±0.71
IL7	38.43±1.17
40% Ethanol in PBS pH 7.4	13.98±0.9

Table B.2: The estimated solubility of silymarin in microemulsions and solution

Silymarin solubility (mg/g)	
GT10	59.57±4.51
GL11	49.32±1.64
GS8	53.55±1.18
OT9	70.49±1.99
OL8	73.83±1.89
OS6	67.35±4.26
ET7	101.93±4.87
EL7	96.88±2.71
IT6	106.86±1.99
IL7	107.89±3.29
40% Ethanol in PBS pH 7.4	39.24±0.25

Table B.3: Calculated percentage of silymarin saturation in microemulsion-loaded 2%w/w silymarin

% saturation of 2% silymarin in each microemulsion formulation	
GT10	33.57
GL11	40.55
GS8	37.35
OT9	28.37
OL8	27.09
OS6	29.70
ET7	19.62
EL7	20.64
IT6	18.72
IL7	18.54

APPENDIX C

Saturation solubilities of silymarin in ethanolic solutions

An excess amount of silymarin was added to 40%, 30%, 20%, 10%, and 0% ethanol in phosphate buffer saline pH 7.4 and shaken using suspension mixture at room temperature for 24 hours. The suspensions were centrifuged at 5,000 rpm for 30 min, and then filtered through 0.45 μm membrane filter. Silymarin saturation solubility in each solution was determined using a spectroscopic method. Three replicates of each experiment were performed.

The solubilities of silymarin in ethanolic solutions are shown in Table C.1. This experiment was performed to provide the choices of receiver fluid in release study.

Table C.1. The solubility of silymarin in ethanolic solutions

Silymarin solubility (mg/ml)	
40% Ethanol in PBS pH 7.4	35.229±1.109
30% Ethanol in PBS pH 7.4	12.745±0.784
20% Ethanol in PBS pH 7.4	2.871±0.492
10% Ethanol in PBS pH 7.4	2.228±0.058
0% Ethanol in PBS pH 7.4	1.764±0.131

APPENDIX D

Fitted models of silymarin release from o/w microemulsions

D1. Guy's model

$$\ln\left(1-\frac{M_t}{M_0}\right)=\frac{-3\,k\,t}{r^2}$$

where M_t is the cumulative amount of drug released at time t, M_0 is the initial amount of drug in the formulation, k is the release rate constant, and r is the droplet radius.

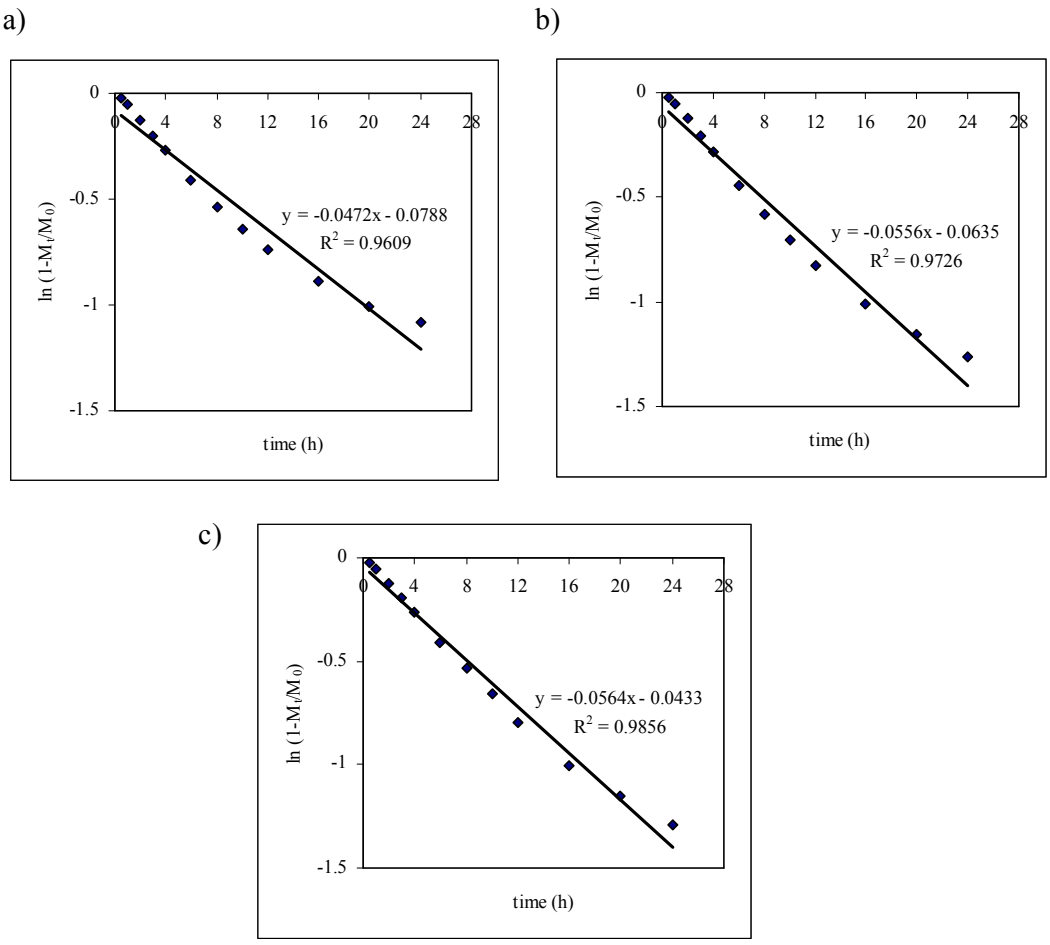

Figure D1.1: Guy's model plot of silymarin release profile (mean, n=3) from o/w microemulsions using glyceryl monooleate as an oil phase; a) GT10, b) GL11, c) GS8

a)

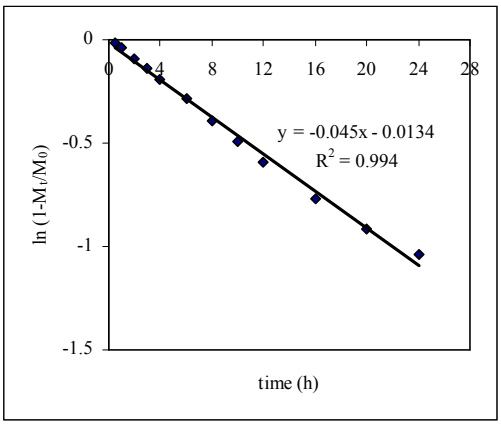

b)

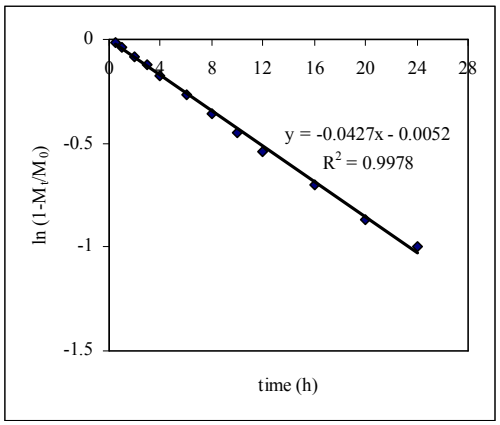

c)

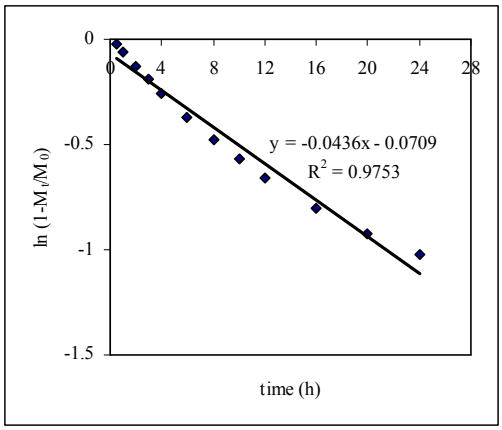

Figure D1.2: Guy's model plot of silymarin release profile (mean, n=3) from o/w microemulsions using oleic acid as an oil phase; a) OT9, b) OL8, c) OS6

a)

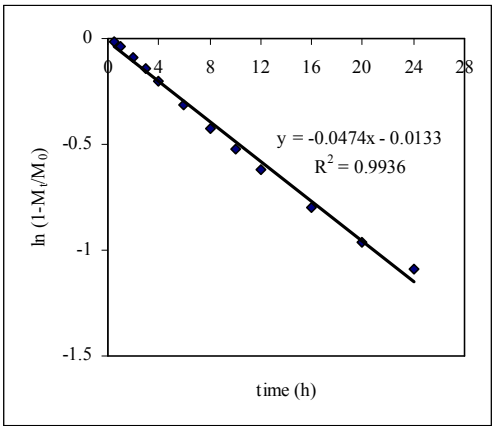

b)

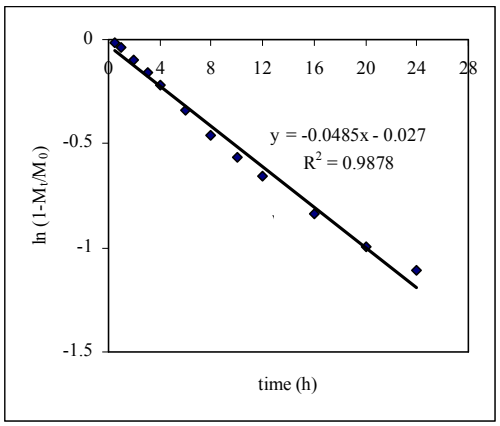

Figure D1.3: Guy's model plot of silymarin release profile (mean, n=3) from o/w microemulsions using ethyl oleate as an oil phase; a) ET7, b) EL7

a) b)

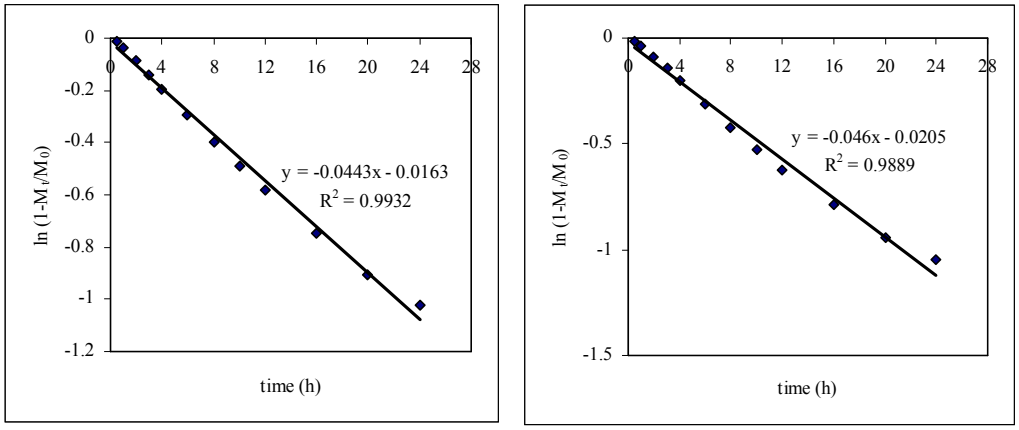

Figure D1.4: Guy's model plot of silymarin release profile (mean, n=3) from o/w microemulsions using isopropyl myristate as an oil phase; a) IT6, b) IL7

D2. Higuchi kinetic

$$M_t = k_H t^{1/2}$$

where M_t is the cumulative amount of drug released at time t, k_H is the Higuchi release rate constant

a)

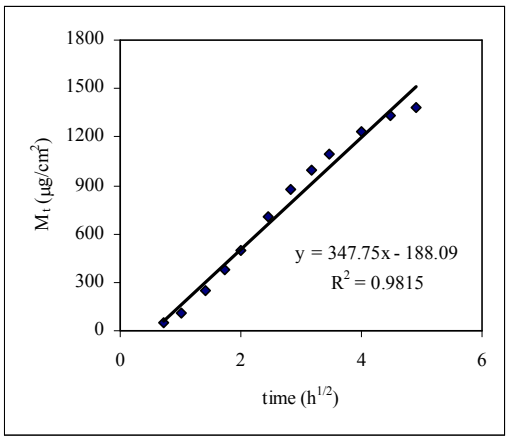

b)

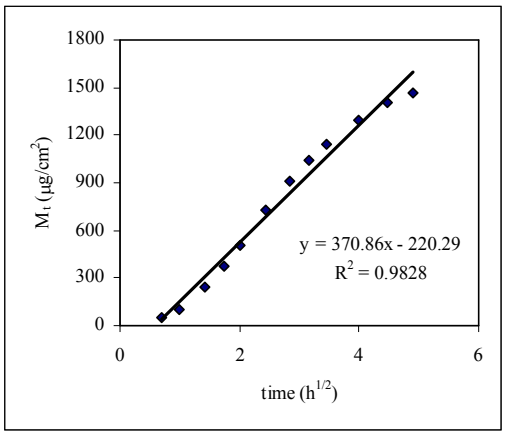

c)

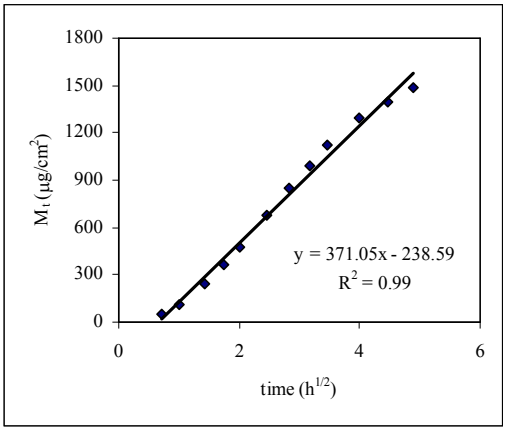

Figure D2.1: Higuchi plot of silymarin release profile (mean, n=3) from o/w microemulsions using glyceryl monooleate as an oil phase; a) GT10, b) GL11, c) GS8

a) b)

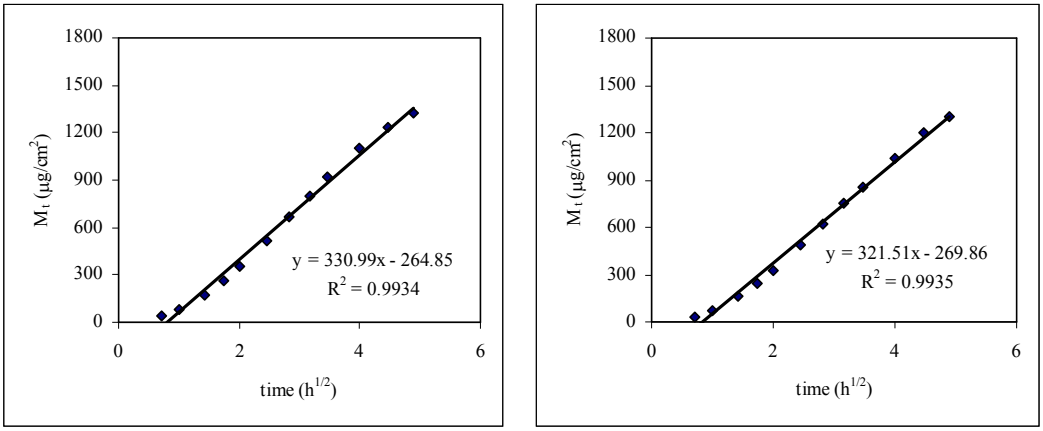

c)

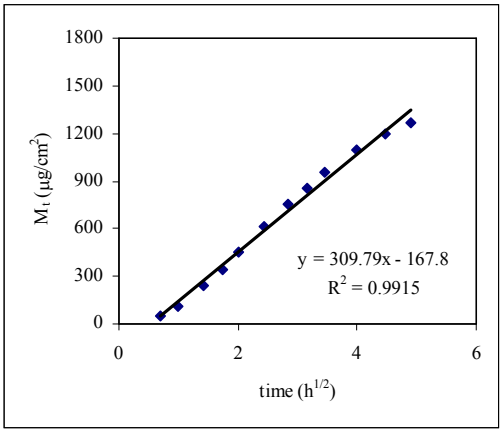

Figure D2.2: Higuchi plot of silymarin release profile (mean, n=3) from o/w microemulsions using oleic acid as an oil phase; a) OT9, b) OL8, c) OS6

a) b)

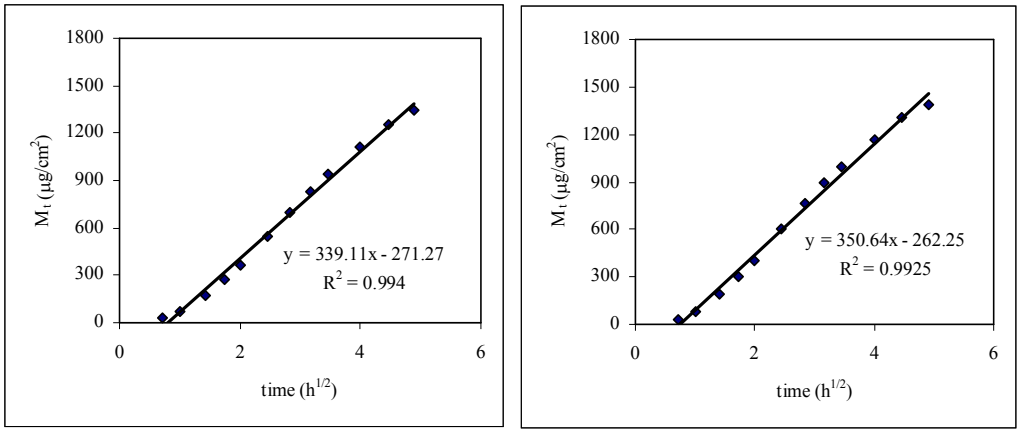

Figure D2.3: Higuchi plot of silymarin release profile (mean, n=3) from o/w microemulsions using ethyl oleate as an oil phase; a) ET7, b) EL7

a) b)

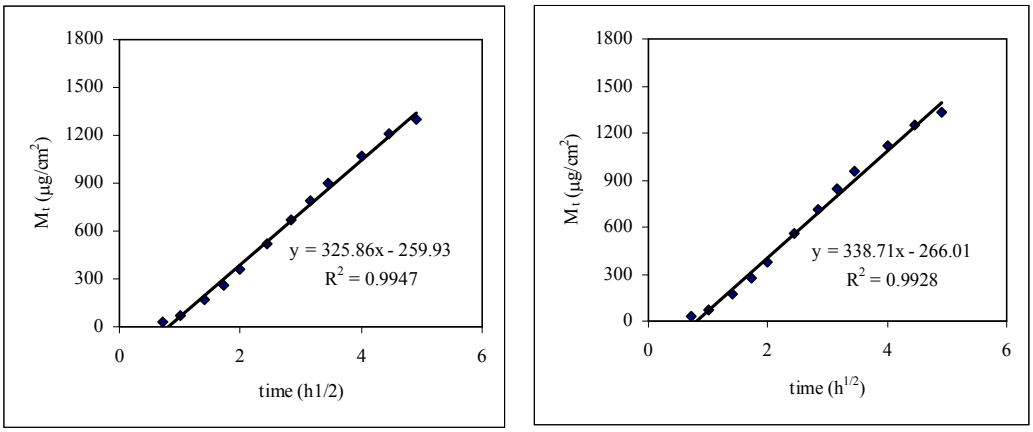

Figure D2.4: Higuchi plot of silymarin release profile (mean, n=3) from o/w microemulsions using isopropyl myristate as an oil phase; a) IT6, b) IL7

VITA

Miss Sawitree Charoensri was born on September 4, 1981 in Nakornpathom, Thailand. She received the bachelor's degree of science in pharmacy from Chulalongkorn University in 2004. Since graduation, she has worked at the Medicinal Plant Research Institute, Department of Medical Sciences, Nonthaburi. She entered the master's degree program in pharmacy at Chulalongkorn University in 2006.